Fetoplacental-derived extracellular vesicles: a mechanism of feto-maternal communication in pregnancy

by

Juliana Schneider Powell

B.S. Biology, Dickinson College, 2015

Submitted to the Graduate Faculty of the

School of Medicine in partial fulfillment

of the requirements for the degree of

Doctor of Philosophy

University of Pittsburgh

2023

UNIVERSITY OF PITTSBURGH

SCHOOL OF MEDICINE

This dissertation was presented

by

Juliana Schneider Powell

It was defended on

April 14, 2023

and approved by

Dr. Arjumand Ghazi, Associate Professor, Department of Pediatrics

Dr. Jacqueline Ho, Associate Professor, Department of Pediatrics

Dr. Yaacov Barak, Associate Professor, Department of Obstetrics, Gynecology, and Reproductive Science

Dissertation Directors: Dr. Yoel Sadovsky, Distinguished Professor, Department of Obstetrics, Gynecology, and Reproductive Science
and
Dr. Adrian E. Morelli, Professor, Department of Surgery and Immunology

Fetoplacental-derived extracellular vesicles: a mechanism of feto-maternal communication in pregnancy

Juliana Schneider Powell

University of Pittsburgh, 2023

Pregnancy is associated with highly complex changes in a woman's physiology, requiring multiple developmental, metabolic, endocrine, and immunological pathways to function in a synchronized and highly regulated manner in order to achieve successful birth. When any of these mechanisms are disrupted, diseases such as preeclampsia (PE) may result. PE is a common disease of pregnancy, characterized by hypertension and proteinuria after gestational week 20. Severe PE can be fatal to both mother and baby. Extracellular vesicles (EVs) are lipid-bilayer nanovesicles released from cells. They are involved in cell-cell communication and transport of cargo molecules. The function of circulating gestational EVs, released by the placenta, remains to be explored. We focused on EVs that circulate in the maternal blood during pregnancy. We first hypothesized that EVs from pregnant women with PE play a role in regulation of vessel tone. When compared to EVs from women with uncomplicated pregnancies, *ex vivo* exposure of isolated mouse mesenteric arteries to EVs purified from plasma of pregnant women with PE led to constriction in response to intraluminal pressure. These data support the notion that circulating EVs from pregnant women play a role in the regulation of arterial tone.

Pregnancy constitutes an "immunological paradox," where despite the competent maternal immune system, the semi-allogeneic fetus evades rejection. The mechanisms at the maternal-fetal interface and mother's secondary lymphoid tissues (SLTs) that dodge the immunologic attack to the fetus, remain largely unknown. Passage of EVs is a mechanism of cell-to-cell communication that transfer antigens (Ags), regulatory mediators, and RNAs. Second, we tested whether

fetoplacental EVs could transport paternal Ags to maternal SLTs via blood, in a tolerogenic fashion.

Table of Contents

List of Tables

List of Figures

Preface

I would like to thank all of the people who supported me and made this possible. First, to my mentors, Dr. Yoel Sadovsky and Dr. Adrian Morelli for their constant support and mentorship throughout graduate school. I feel so lucky to have had two mentors with distinct styles and feel I have truly benefited from both of you. Thank you for teaching me to be a scientist. And to Bill Shufesky of the Morelli Lab and all of the members of the Sadovsky Lab, thank you for your help with procuring reagents/mice and conducting experiments. I would also like to thank my honorary third mentor, Dr. Adriana Larregina for all of her help and guidance especially during this last year of graduate school.

Thank you, especially, to my committee, Dr. Arjumand Ghazi, Dr. Jacqueline Ho, and Dr. Yaacov Barak. Every single meeting, you had constructive comments and truly helped shape my project into what it is today. And thank you to the Interdisciplinary Biomedical Graduate Program and the Molecular Genetics and Developmental Biology Program for your teaching and support during my graduate training.

Outside of the University of Pittsburgh, I would like to thank my parents, Tim and Judy Schneider, for all of their love and constant support not only through graduate school, but throughout my entire life. You pushed me to be the best I could be and always assured me that I could do anything I set my mind to. You taught me to be a strong, independent woman. My mom was an organic chemist in the 80s/90s and inspired me to become a scientist. To my mother-in-law, Mary Powell, sister-in-law Caitlin Sok (MD/PhD), brother-in-law Daniel Sok (MD), and nephew Peter, thank you for your constant words of encouragement, support, and love. My father-in-law, Daniel A. Powell passed away on March 6th, 2023. I know he knows how thankful I am

for all of his love and all of the times he made me laugh. To my sister, Jacqueline Eacret (PhD, Immunology) and brother-in-law Darrell Eacret (PhD, Neuroscience) thank you for all of your guidance and advice about navigating science and graduate school, for all of the times you visited Pittsburgh and welcomed me to Philly for fun-filled decompressing weekends, and for all of your love and support. And to my brother, Tim Schneider Jr., thank you for all of the weekend rounds of golf, fun dinners, and laughs.

Finally, I want to thank my husband, Dan (PharmD). You always pushed me and encouraged me to do whatever I set my mind to and to be the best version of myself. Even when I was doubting myself, when the imposter syndrome kicked in, you assured me I was where I was meant to be. Thank you for listening to me incessantly talk about my project and for letting me practice presentations for you. Most importantly, thank you for your unwavering support, countless laughs, and endless love.

1.0 Introduction

Pregnancy is associated with highly complex changes in a woman's physiology, requiring multiple developmental, metabolic, endocrine, and immunological pathways to function in a synchronized and highly regulated manner in order to achieve successful birth. When any of these mechanisms are disrupted, diseases such as preeclampsia (PE) may result. PE occurs after the 20th week of pregnancy, affects 3-8% of pregnant women [1, 2], and is clinically manifested by high blood pressure, proteinuria, and edema [3] with possible worsening that may lead to target organ dysfunction. The pathogenesis of PE is widely disputed, with previous studies reporting abnormal invasion of placental interstitial and endovascular trophoblasts into the decidua and uterine wall, inadequate trophoblast differentiation, placental malperfusion, oxidative placental stress, and dis-regulated innate or adaptive immune responses against the fetoplacental unit [1, 4-6]. Therefore, the underlying mechanism of the cause of PE is largely unknown.

Extracellular vesicles (EVs) are small membrane vesicles released by all eukaryote cell types analyzed thus far[7]. During pregnancy, the fetoplacental unit (i.e., conceptus), releases EVs into the maternal systemic circulation. These conceptus-derived EVs appear in the maternal peripheral blood approximately 6 weeks post-conception and remain in circulation until a few hours after giving birth [8, 9]. In humans, placenta-derived sEVs carry a group of placenta-specific micro RNAs known as the Chromosome 19 microRNA cluster (C19MC) [10]. Our laboratory found that these C19MC-containing sEVs confer resistance to infection by DNA and RNA viruses to target cells [11-13]. Other examples of potential biological effects of sEVs released by the fetoplacental unit include (i) activation or suppression maternal immune cells [14-16], (ii) miRNA

transport of labor-associated EVs [17], and (iii) contribution to the remodeling of maternal spiral arteries in the placenta [18].

As initially described by Peter Medawar, pregnancy constitutes an "immunological paradox", where despite the presence of paternal allogeneic antigens (Ags), the fetus does not elicit a maternal immunological effector response [19]. The mechanisms by which the fetus evades the maternal immune system and thereby rejection are not fully understood. Proposed mechanisms of immunological tolerance include downregulation of the uterine natural killer cell (uNK) cytolytic function, M2-polarization of decidual macrophages, retention of conventional dendritic cells (cDCs) in the decidua, increased percentage of regulatory T cells in the decidua, epigenetic silencing in decidual cells of chemokines that attract effector T cells, release of immunosuppressive cytokines and galectins by the trophoblast, and downregulation of expression of classic major histocompatibility complex (MHC) molecules by trophoblasts [7]. However, whether fetoplacental EVs are involved in induction / maintenance of peripheral tolerance / immuno-suppression against transiently expressed placental Ags or paternal Ags during pregnancy remains largely unexplored [20-22]. A better understanding of the mechanisms of feto-maternal tolerance at the placenta – maternal interface and in the maternal secondary lymphoid tissues may help to elucidate immune dysfunction underlying PE, intrauterine growth restriction (IUGR), preterm birth, and infertility.

1.1 Pregnancy and the placenta

The placenta is a temporary organ that develops during mammalian pregnancy and partially invades the uterine decidua in a highly controlled manner. Among mammals, the structure of the

placenta differs (as will be discussed below), but the functions remain similar. The placenta governs the delivery of oxygen and nutrients to the fetus, removal of CO_2 and waste metabolites, release of hormones that sustain pregnancy, and the development of immune defense to the fetus. According to a study conducted by the National Institutes of Health examining the cause of roughly 200 still births (pregnancy loss after the 20th week), 50% were a result of placental malfunction, abnormalities, or both [23]. Therefore, a fully developed and functional placenta is imperative for a healthy pregnancy.

1.1.1 Development of the human placenta during a normal pregnancy

Roughly six days after conception, the human blastocyst attaches to and invades the endometrium. During the implantation of the blastocyst, the endometrial fibroblasts differentiate into decidual cells. The decidua anchors the placenta to the uterine wall. It also contains maternal leukocytes and maternal blood vessels [24]. The placenta develops from the trophectoderm (outer layer) of the blastocyst and the inner cell mass becomes the fetus. The trophectoderm forms a syncytium within the decidua and further invades toward the myometrium. This later develops into the decidua [25]. In the lacunar or trabecular stage of placental development (from days 8-13 post-conception), a trabeculae forms from the creation of fluid-filled spaces within the endometrium, this trabeculae is made up of syncytiotrophoblasts and lamellae [26]. This area later develops into the villous trees of the human placenta [27]. The human blastocyst becomes totally embedded in the decidua by day 14 post-conception.

The chorionic villous of the human placenta is made up of different types of trophoblast cells. Cytotrophoblasts proliferate rapidly to form the primary villi. The cytotrophoblasts fuse to form the multi-nucleated syncytiotrophoblasts and separately, give rise to the extravillous

trophoblasts. The extravillous trophoblasts at the tip of the anchoring villi interact with the decidua and its blood vessels, and as endovascular trophoblasts they eventually become bathed in maternal blood [28]. Secondary villi form around day 17 post-conception by the penetration of extraembryonic mesenchymal cells through the core of the villous. The tertiary villi form about one day later from the development of fetal capillaries within the villous core [25]. The villi continue to branch from the chorionic plate, or the "fetal side" of the placenta, to eventually form a delicate network of villous branches.

The trophoblasts are responsible for carrying out the key functions of the placenta, including the transport of oxygen and nutrients across the placenta, release of hormones into maternal circulation. They also release conceptus-derived EVs into the maternal peripheral blood. The human placenta is fully developed by the end of the first trimester and continues to grow along with the fetus throughout pregnancy [29].

1.1.1.1 The Mouse Placenta

The human and mouse placentas differ anatomically; however, they are similar in hemochorial placentation, the structural formation where the fetal-derived trophoblasts are in contact with maternal blood. After the first trimester, humans have a hemo-monochorial formation, meaning that there is only one layer of trophoblasts between maternal and fetal blood, while mouse placentas are hemo-trichorial (three layers of trophoblasts separate maternal and fetal blood). Trophoblast giant cells anchor the mouse placenta to the uterine wall. The human placenta does not have trophoblast giant cells. Rather than fetal vasculature forming villi, the mouse placenta is arranged in a labyrinth formation (Figure 1). Maternal blood is encircled by trophoblast giant cells and syncytiotrohophlasts with fetal blood surrounding the other side of the syncytiotrophoblasts

[30]. The functions of the human and mouse placenta are similar including nutrient transfer, providing oxygen, removal of carbon dioxide and waste, and production of hormones.

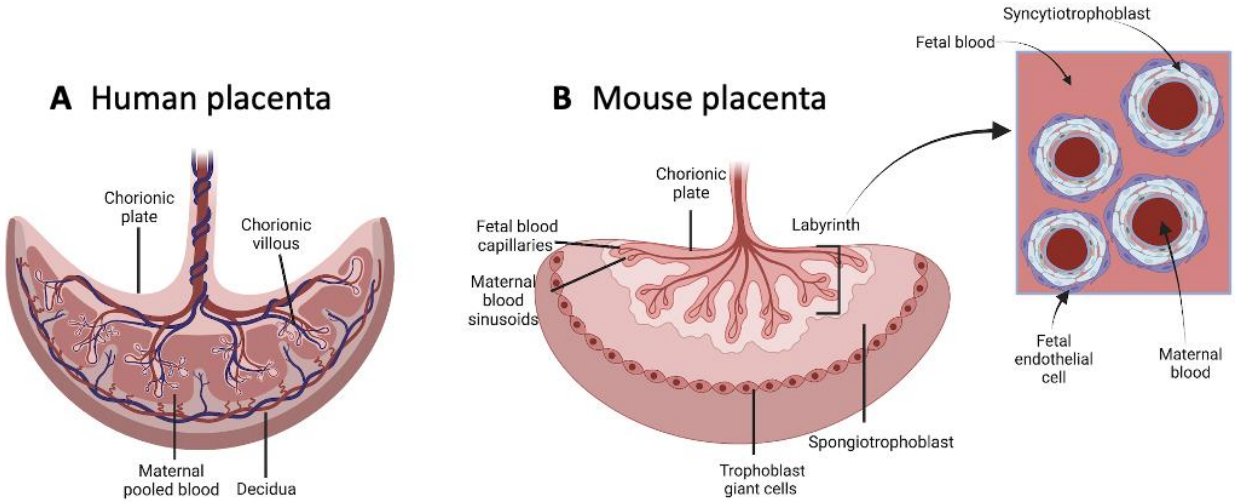

Figure 1: Diagram of the human and mouse placentas.

A) Diagram of the human placenta showing the chorionic plate, decidua, maternal blood, and placental villous. **B)** Depiction of the mouse placenta including the chorionic plate, labyrinth containing the fetal blood capillaries and maternal blood sinusoids, trophoblast giant cells, and spongiotrophoblast. A region of interest from the mouse placenta shows a detailed image of the labyrinth formation containing fetal blood, fetal endothelial cells, maternal blood, and syncytiotrophoblast. Made with BioRender.

1.1.2 Pathological pregnancy

Pregnancy is a complex and highly-regulated process in which multiple factors contribute to maintain the heath of the fetoplacental unit. Common complications of pregnancy include PE, gestational diabetes, intra-uterine growth restriction (IUGR), preterm labor, and miscarriage/still birth. PE is a serious disease manifested by high blood pressure, edema, headaches, blurred vision, and proteinuria that occurs in the second to third trimester, mainly after week 20 of pregnancy. If not treated, it can progress to eclampsia with maternal seizures and severe bleeding and can be

fatal to both the mother and fetus. PE is the leading cause of perinatal mortality [31]. It is a complication that occurs in approximately 8% of pregnancies and is responsible for roughly 15% of premature births. History of PE, age, high blood pressure, race, obesity, and multi-fetal pregnancy [32] are the most common risk factors for PE. The full cause(s) of PE is unknown, with previous studies reporting potential causes including shallow invasion of placental interstitial and endovascular trophoblasts into the decidua and uterine wall, inadequate trophoblast differentiation, placental malperfusion, oxidative placental stress, and dis-regulated innate or adaptive immune responses against the fetoplacental unit [1, 4-6]. Interestingly, numerous studies have found that peripheral blood of women with PE exhibits a higher concentration of placental-derived EVs with a different molecular cargo, compared to blood-borne EVs of women with healthy pregnancies [33]. Studies have also revealed that the concentration of EVs in plasma of women with PE increases with disease severity and progression [34].

1.2 Extracellular vesicles

The family of EVs encompasses multiple types of membrane vesicles with different biogenesis, size and composition that are released by most eukaryotic cell types studied thus far. They include microvesicles, exosomes, apoptotic cell-derived EVs, and small vesicles that have not been fully characterized [35-37]. EVs represent a mechanism of cell-to-cell communication by which cells transfer miRNAs, non-coding RNAs, small DNA fragments, proteins and metabolites [38]. EVs may also function as a mechanism of removal of unwanted products from the parent cells. Indeed, reticulocytes employ EVs to dispose of surface receptors and adhesion molecules during their differentiation into erythrocytes [39]. EVs also play critical roles in the induction of

the metastatic niche in cancer, pathogenesis of neurodegenerative and autoimmune disorders, and allorecognition of transplanted tissues / organs by the recipient's immune system [40-43]. Indirect evidence suggests that blood-borne EVs may play a role in the pathogenesis of PE [44].

1.2.1 Extracellular vesicle biology

The three main types of EVs are microvesicles, exosomes and apoptotic cell-derived EVs. Microvesicles (~ 0.1–1mm) are released via budding and pinching off of the plasma membrane (Figure 2). Exosomes (~ 50-150 nm) are generated within the endocytic compartment of the cell. They originate as intraluminal vesicles by reverse invagination of the limiting membrane of early endosomes, which then become multivesicular bodies. When multivesicular bodies fuse their limiting membrane with the plasma membrane, the intraluminal vesicles are released into the extracellular milieu or bodily fluids [35-37], where the intraluminal vesicles are termed exosomes (from now on referred to as sEVs, as the literature has moved from the term "exosomes" to "small extracellular vesicles") (Figure 2). Apoptotic cell-derived EVs include apoptotic blebs (0.1–1 μm) shed by the plasma membrane, and bigger EVs (~ 0.8-5 μm in size) that result from disintegration of the remnants of the apoptotic cell (i.e., apoptotic bodies and apoptotic cell bodies) containing fragments of the cell nucleus.

The most important criteria to differentiate the different types of EVs is their biogenesis, which cannot be conclusively determined when the EVs are harvested from bodily fluids. Bona fide exosomes originated in multivesicular bodies are highly enriched in the protein Tumor susceptibility gene 101 (Tsg101) that is involved in the exosome biogenesis and in the tetraspanins CD63 and CD81, all commonly used as exosome-associated markers. However, EVs ranging in size between ~ 50 - 120 nm and expressing Tsg101, CD63 and CD81, purified from cell culture

supernatants or bodily fluids are in general referred to as small EVs (sEVs) instead of exosomes, because (i) the biogenesis of the sEVs in the endocytic compartment cannot be conclusively determined, (ii) different types of EVs overlap in size, and (iii) there are no reliable markers for microvesicles, which is why EVs are commonly defined by both size and protein markers.

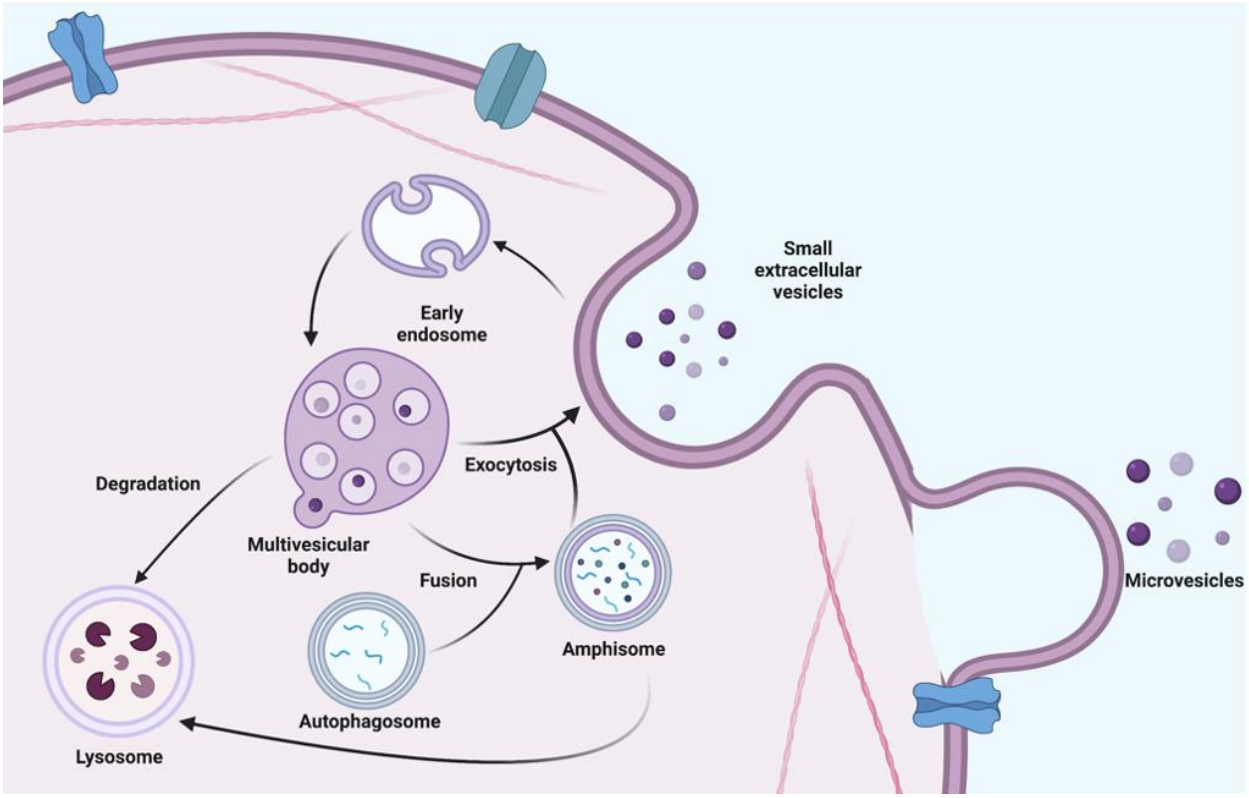

Figure 2: Diagram of small extracellular vesicle and microvesicle release.

Small extracellular vesicles form via the endocytic pathway. Reverse invagination of the early endosome limiting membrane forms intralumenal vesicles, which then become multivesicular bodies (MVB). The MVB can release the sEVs by exocytosis, be degraded by the lysosome or fuse with an autophagosome (containing dsDNA) to form an amphisome. The amphisome can release sEVs and dsDNA via exocytosis or be degraded by the lysosome. Microvesicles are released by a budding and pinching off of the plasma membrane. Made with BioRender.

1.2.2 Extracellular vesicles in pregnancy

Increasing evidence indicates that EVs play important biological roles from implantation through parturition. Indeed, embryonic stem cells of the inner cell mass release EVs that facilitate blastocyst implantation in the endometrium [8].

Placental-derived EVs, including microvesicles, sEVs and apoptotic cell-derived EVs are released into the maternal circulation during pregnancy. Placental sEVs are detected in the maternal peripheral blood roughly 6 weeks after conception and remain in circulation until a few hours after giving birth, increasing in concentration as pregnancy progresses. The source of placenta-derived sEVs can be identified by detection on the vesicles of the sEV-associated marker CD63, the trophoblast-associate marker placental alkaline phosphatase (PLAP), and marker syncytin which is also unique to the placenta. Placental sEVs have been found to carry a placenta-specific microRNA family, the C19MC [45]. Our group found that one of the functions of this microRNA family is to confer resistance to infection by DNA and RNA viruses to target cells [11]. As aforementioned, previous studies have shown that the peripheral blood of women with PE contains an increased number of EVs with an altered cargo. It has been suggested that these EVs could be used as a diagnostic or disease progression biomarker for PE [44, 46]. Previous findings also indicate that placental sEVs may be involved in the pathogenesis of PE. ***Therefore, we hypothesized that when compared to sEVs from healthy pregnancies, sEVs isolated from the plasma of women with PE increase arterial vessel tone and reduce endothelial cell-mediated vasorelaxation.***

In addition to PE, placental EVs are also involved in pregnancy-related conditions including gestational diabetes, IUGR, and preterm birth. EVs also play an important role in sperm and oocyte development [47]. In gestational diabetes, EVs are thought to modify metabolic

pathways and facilitate insulin sensitivity [16, 48]. Amnion epithelial EVs have been found to contribute to preterm labor by triggering pro-inflammatory pathways in uterine cells with the subsequent induction of labor [49, 50]. Potential roles of placental EVs in IUGR include disruption of feto-maternal tolerance by activating the protein, NF-kβ in T cells [51].

1.3 Feto-maternal immunological tolerance. Potential role of small extracellular vesicles.

Sir Peter Medawar considered pregnancy as an "immunological paradox" in which the semi-allogenic (or even fully-allogeneic) fetus evades the maternal immune system and thrive in the mother's uterus for 9 months, whereas in the absence of pharmacological immunosuppression, semi- or fully-allogenic cell, tissue or organ grafts are rapidly rejected by the recipient's immune system [19]. Such paradox even takes place when pregnancy results from a sperm and a donor oocyte, or in a surrogate pregnancy, where the fetus represents a full allograft. The three original mechanisms proposed by P. Medawar by which the conceptus is not recognized by the maternal immune system were (i) the placenta physically separates the mother from the fetus, (ii) fetal Ags are immature and unable to elicit a response in the maternal Ags, and (iii) an inactive maternal immune system during pregnancy [52]. Medawar's theory provided the foundation for the field of pregnancy immunology. More recent evidence indicates that multiple mechanisms promote immunological tolerance/immunosuppression at the maternal fetal interface. They include decrease in the uNK cytolytic function, M2-polarization of decidual macrophages, sequestration of cDCs in the decidua, increased percentage of regulatory T cells in the decidua, epigenetic silencing of chemokines that attract effector T cells to the fetoplacental interface, release of soluble immunosuppressive mediators by the trophoblast, and downregulation of the classic HLA-A and

HLA-B molecules in trophoblasts [20, 21, 53]. In mice, presentation of conceptus-derived peptides occurs in the context of maternal classic H2 class-I and -II molecules (equivalent to HLA-A/B/C and HLA-DR/DQ/DP molecules in humans), within the mother's secondary lymphoid tissues (SLTs) that drain the uterus (SLTs) [54]. During a normal mouse pregnancy, this leads to deficient activation followed by clonal deletion or anergy of maternal CD4 or CD8 T cells that recognize the paternal Ag-derived peptides, and differentiation of $CD4^{Pos}$ $FoxP3^{Pos}$ regulatory T cells specific to the paternal Ags (Tregs) [55]. Despite the biological importance of this phenomenon, the cell-free mechanism(s) by which the conceptus delivers fetoplacental (no-self) Ags to the mother's leukocytes in SLTs remains unknown. Because the placenta releases EVs into peripheral blood [9, 56], and EVs have been shown to function as carriers for horizontal transfer of proteins and Ags between cells [57], we investigated if trophoblast EVs released in the mother's peripheral blood constitute a platform in which conceptus-derived Ags are delivered intact to maternal APCs in SLTs.

At systemic level, the mechanism(s) and platform by which the fetoplacental unit delivers placental-specific Ags or paternal Ags to uterus-draining secondary lymphoid tissues (e.g. spleen and uterus-draining lymph nodes), and if fetoplacental sEVs are involved in this process is unknown (Figure 2). Similarly, whether systemic delivery of fetoplacental Ags via sEVs promotes the deficient activation followed by deletion of conceptus-specific CD4 and CD8 T cells, decrease in type 1-biased polarization of T cells, and generation of conceptus-specific $CD4^{Pos}$ $FoxP3^{Pos}$ regulatory T cells, previously described in uterus-draining secondary lymphoid tissues in mouse models, remains unexplored. Researchers in the field of feto-maternal tolerance originally hypothesized that fetal dendritic cells were released into maternal peripheral blood where they targeted maternal SLTs and were directly recognized by maternal T cells in a pro-tolerogenic

fashion. This theory has since been disproved as fetal dendritic cells have not been found during pregnancy in maternal SLT [58-60] (Figure 3). An additional previous hypothesis was that fetoplacental EVs carrying paternal Ags and MHC class I and II are released into maternal peripheral blood and target maternal SLT where they present paternal Ags on placental MHCs (cross-dressing) (Figure 3). This has also been disproved because the placenta does not contain MHC class I or class II [61].

Important for our research, the involvement of fetoplacental sEVs in induction / maintenance of tolerance against the conceptus, both locally at the feto-maternal interface and systemically within maternal secondary lymphoid tissues, remains unknown [20-22]. Therefore, we hypothesize that ***in a healthy pregnancy, conceptus-derived EVs represent one of the cell-free platforms by which paternal Ags are transported to maternal lymphoid tissues, where these Ags are presented to maternal T cells in a pro-tolerogenic fashion (Figure 3).***

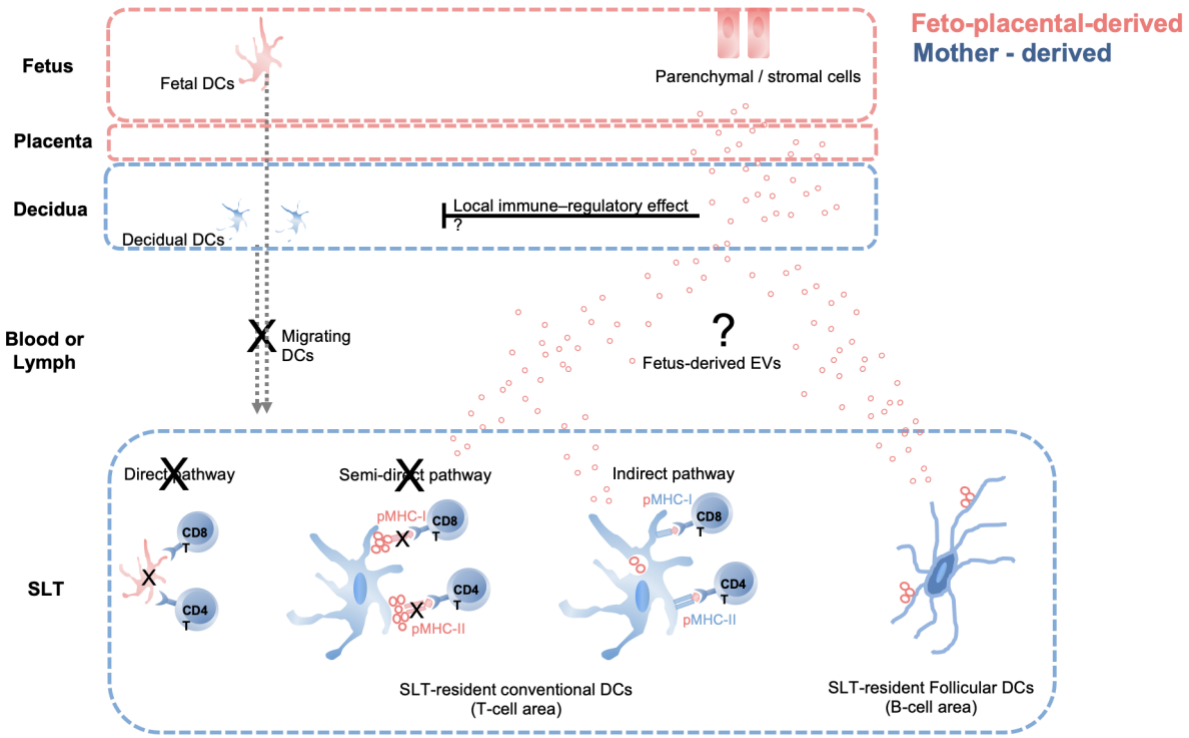

Figure 3: Fetoplacental EVs deliver paternal Ags to maternal SLT.

Fetal tissues are indicated in red, and maternal tissues in blue. Fetal DCs develop late, thus maternal T cells are unable to recognize allo-MHC molecules on fetal migrating DCs mobilized to the mother's SLTs (via the direct allorecognition pathway). Since trophoblastic EVs do not express classic MHC molecules, they are not recognized by directly alloreactive T cells on the surface of maternal APCs, when cross-dressed with the EVs (via the semi-direct allorecognition pathway). Instead, fetoplacental EVs may interact with maternal decidual uNK cells, macrophages, T cells, endothelium, and decidual stromal cells at the feto-maternal interphase, or traffic via peripheral blood or lymph to the maternal SLTs (spleen, lymph nodes), where the EVs are internalized and processed by maternal APCs. In mice, fetus-derived antigenic peptides are presented within maternal MHC molecules by maternal APCs (likely conventional DCs) to T cells via the canonical pathway (also known, in transplantation, as the indirect pathway.) Fetoplacental EVs could also be presented to maternal B cells by subcapsular sinus (SCS) macrophages in lymph nodes (or analogue macrophages in the spleen) or by follicular DCs located deep in B cell follicles.

2.0 Small extracellular vesicles from pregnant women with preeclampsia increase myogenic tone and decrease endothelium-dependent relaxation of mouse-mesenteric arteries

This article was published in *Journal of Pregnancy Hypertension*, Vol 28, **Juliana S. Powell**, Robin E. Gandley, Emily Lackner, Andrea Dolinish, Yingshi Ouyang, Robert W. Powers, Adrian E. Morelli, Carl A. Hubel, Yoel Sadovsky, Small extracellular vesicles from plasma of women with preeclampsia increase myogenic tone and decrease endothelium-dependent relaxation of mouse mesenteric arteries, Pg 66-73, Copyright Elsevier (2022)."

2.1 Introduction

Preeclampsia (PE) is a major complication of pregnancy that affects approximately 3-8% of pregnancies in the late second or third trimester [1, 2]. PE is the most common cause of perinatal mortality [31]. It is clinically characterized by new-onset high blood pressure and proteinuria and, when it worsens, can result in life-threatening damage to maternal target organs, fetal growth restriction, and death [1, 62-64]. Although the etiology of PE remains unclear, shallow invasion of placental interstitial and endovascular trophoblasts into the decidua and uterine wall seems to play an important role in early-onset disease [1, 4]. Other pathways that have been implicated in disease pathogenesis include inadequate trophoblast differentiation, placental malperfusion, oxidative stress, and abnormal immune and inflammatory responses, culminating in maternal systemic vasoconstriction and related clinical manifestations [1, 5, 6].

Extracellular vesicles (EVs) are micro- and nano-size particles that are released from most cell types. The EV family encompasses a growing number of particle subtypes [35-37]. Most studied are the larger sized (1-5 μm) apoptotic bodies, which are formed by cell disintegration during apoptotic death, the smaller (0.1-1 μm) microvesicles (MVs), which are formed by budding off from the plasma membrane, and the even smaller (30-150 nm) small extracellular vesicles (sEVs), also referred to as exosomes, formed as intraluminal vesicles within endocytic multivesicular bodies or by budding from the cell membrane [35-37]. A growing number of biological processes are linked to sEV-based cell-cell communication, such as cancer metastatic spread and cardiovascular and neurodegenerative diseases [40-43].

Several lines of evidence link sEVs to hypertension and, possibly, PE. Otani *et al*. found that intravascular injection of plasma exosomes isolated from hypertensive rats caused increased blood pressure in normotensive rats [65]. Additionally, Tong *et al*. reported that sEVs derived from first trimester human placentas can impair nitric oxide-mediated relaxation in exposed maternal arteries [66]. Women with PE have more sEVs in their blood compared to women with uncomplicated pregnancy [67, 68]. Our laboratory has previously shown that sEVs from the plasma of women with PE contain different miRNA cargo when compared to sEVs from healthy controls or from pregnancies complicated by fetal growth restriction [46]. Biro *et al.* found that levels of sEV-bound miR-210 are elevated in placentas from women with PE, implicating sEV miRNAs in PE pathology [69]. Wu *et al*. found that miR-302a expression is upregulated in tissues from PE patients, with increasing expression in more severe disease presentation [70]. Others suggested that sEVs contribute to the pathogenesis of PE by contributing to impaired angiogenesis, dysfunction of trophoblast cells, and increases in inflammation and immunological pathways [9, 71, 72]. However, the involvement of sEVs in regulation of vascular tone remains to be defined.

Placental sEVs, released from trophoblast cells, appear in the maternal circulation roughly 6 weeks post conception and remain circulating in the maternal blood several hours after birth [9, 56]. Work from our laboratory suggests a role for trophoblastic EVs in conferring viral resistance to non-trophoblastic cells [11-13]. Additionally, during pregnancy, sEVs are involved in feto-maternal communication, the inflammatory response, and parturition [73-75]. However, the role of sEVs in normal and pathological pregnancy remains to be further explored [33, 76].

Here, we surmised that plasma sEVs from women with PE interact with vascular endothelial cells and promote vessel constriction. Using an *ex vivo* system of perfused mouse mesenteric arteries, we hypothesized that, when compared to sEVs from healthy pregnancies, sEVs isolated from the plasma of women with PE increase arterial vessel tone and reduce endothelial cell-mediated vasorelaxation.

2.2 Results

2.2.1 Participants

Pregnant women in the PE group were group-matched as detailed in Materials and Methods. As expected, the mean systolic and diastolic blood pressure before delivery was higher in women with PE, and women with PE delivered earlier and had smaller newborns (Table 1).

Table 1: Clinical characteristics of participants from whom plasma samples were obtained

Clinical characteristics of participants from whom plasma samples were obtained.

	Uncomplicated pregnancy (n = 10)		Preeclampsia (n = 10)		Non-pregnant (n = 10)	
Maternal age (years)	24	(21,27)	28	(25,31)	29	(24,30)
Race (n, % Black)	2	(20%)	2	(20%)	2	(20%)
Pre-pregnancy BMI (kg/m^2)	28	(24, 34)	26	(24, 34)	25	(20, 31)
Gestational age at delivery (wks)	39.7	(39.2, 40.7)	37.3	(36.0, 41.0)	39.6	(39.0, 40.8)
Gestational age at venipuncture (wks)	37.4 ± 0.78		37.2 ± 1.1		N/A	
Third trimester, pre-delivery BP						
Systolic	122 ± 3**		148 ± 3*		108 ± 3#	
Diastolic	69 ± 3		92 ± 2*		69 ± 3#	
Infant weight (grams)	3538 ± 157		2658 ± 238*		3551 ± 109#	
Infant birth weight centile	52 ± 11		31 ± 10		59 ± 7	
Infant sex (n, % female)	4	(40%)	6	(60%)	6	(60%)
Postpartum interval (wks)	N/A		N/A		53	(46–62)
Postpartum BP (1 year)						
Systolic	N/A		N/A		108 ± 2	
Diastolic	N/A		N/A		69 ± 3	

Continuous data are given as mean ± SEM if normally distributed or median (25th percentile,75th percentile). Categorical data are given as number (percent). Groups were compared by either the Kruskal-Wallis or Holm-Sidak tests. BMI. Body mass index was prepregnancy or at study visit for nonpregnant subjects (approximately 1 year after the index uncomplicated pregnancy). *$P \leq 0.003$ Preeclampsia vs. Uncomplicated pregnancy, ** $P < 0.003$ Uncomplicated pregnancy vs Nonpregnant, # $P < 0.004$ Preeclampsia vs. Nonpregnant. N/A. Not applicable.

2.2.2 Plasma from women with PE increased myogenic tone

We exposed mouse mesenteric arteries to individual samples of whole plasma from 10 pregnant women with PE or to individual plasma samples from pregnant women with uncomplicated pregnancy. We then used pressurized arteriography to examine the myogenic

response of the arteries. We found that exposure to individual plasma samples from pregnant women with PE increased the vessel tone, when compared to arteries exposed to plasma from women with uncomplicated pregnancies. Arteries exposed to plasma from women with PE had an average peak of 30% constriction, whereas arteries exposed to plasma from women with uncomplicated pregnancies had a peak constriction of approximately 6% (Fig. 4).

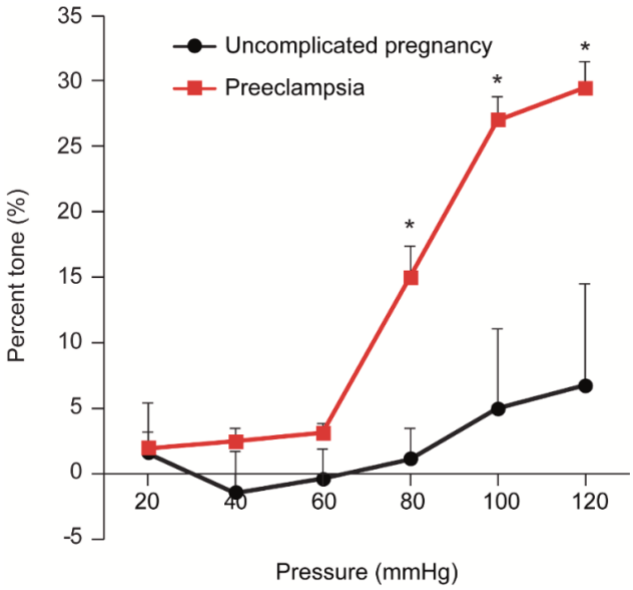

Figure 4: The myogenic response (% tone) of mesenteric arteries exposed to plasma.

The figure shows the percent tone generated (Y-axis), calculated at each pressure as [(Di–Da)/Di]x100, where Da is the steady-state arterial diameter achieved after each 20-mm Hg increase in pressure (x-axis) and Di is the passive arterial diameter measured at the same pressure steps when the smooth muscle is inactivated (detailed in Materials and Methods). The data are presented as mean ± SEM, n = 10 plasma samples from individual participants. *denotes $p < 0.0001$ for PE *vs* healthy pregnancy (control), calculated by 2-way repeated measures ANOVA with *post hoc* Tukey Test for pairwise comparisons.

2.2.3 Arterial tone is increased when exposed to sEVs from plasma of women with PE

To investigate whether isolated sEVs reproduce the effect of plasma on vessel tone, we isolated sEVs from pooled plasma of pregnant women with PE and pooled plasma from uncomplicated pregnant women or healthy women at 1 year postpartum. We found that the application of sEVs from women with PE led to an approximate 15% increase in arterial tone at the 100- and 120-mmHg pressure steps when compared to sEVs from women with uncomplicated pregnancies (Fig. 5). Interestingly, sEVs from non-pregnant women led to increased tone in a manner near that of sEVs from women with PE, suggesting a vessel tone-relaxing effect of sEVs during healthy pregnancies.

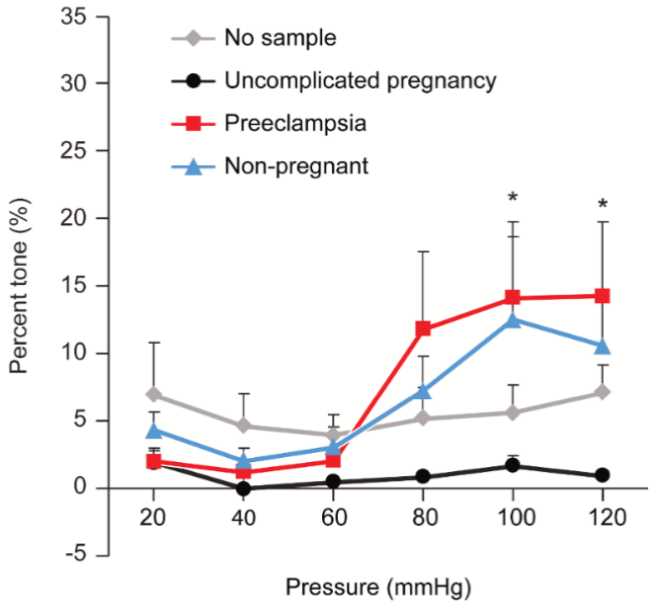

Figure 5: The myogenic response (% tone) of mesenteric arteries exposed to sEVs.

The figure shows the percent tone (Y-axis), calculated as shown in Fig. 1 and detailed in Materials and Methods. The data are presented as mean ± SEM, n = 4 replicates using sEVs from pooled plasma samples (n = 10). *denotes p <

0.05 for PE *vs* healthy pregnancy (control) or no sEVs, calculated by 2-way repeated measures ANOVA with *post hoc* Tukey Test for pairwise comparisons.

2.2.4 The effect of EV-depleted plasma or isolated MVs on vessel tone

Using plasma from women with PE or from women with uncomplicated pregnancies, we depleted all EVs as described in Materials and Methods and tested the effect of these EV- depleted plasma samples on vessel tone. Arteries exposed to EV-depleted plasma from women with PE exhibited no significant increase in tone (Fig.6A). Interestingly, EV-depleted plasma from healthy pregnancies exhibited a 15% increase in arterial tone, supporting the notion that sEVs may contribute to the myogenic tone-reducing effect of normal-pregnancy plasma. To assess whether the effect of sEVs can be recapitulated using MVs, we isolated MVs from women with PE and from plasma from healthy pregnant women. Exposure of the isolated mesenteric arteries to MVs obtained from the plasma of women with PE or from those with uncomplicated pregnancies did not significantly affect myogenic tone compared to vehicle (no treatment, Fig. 6B), suggesting the observed effect is unique to sEVs.

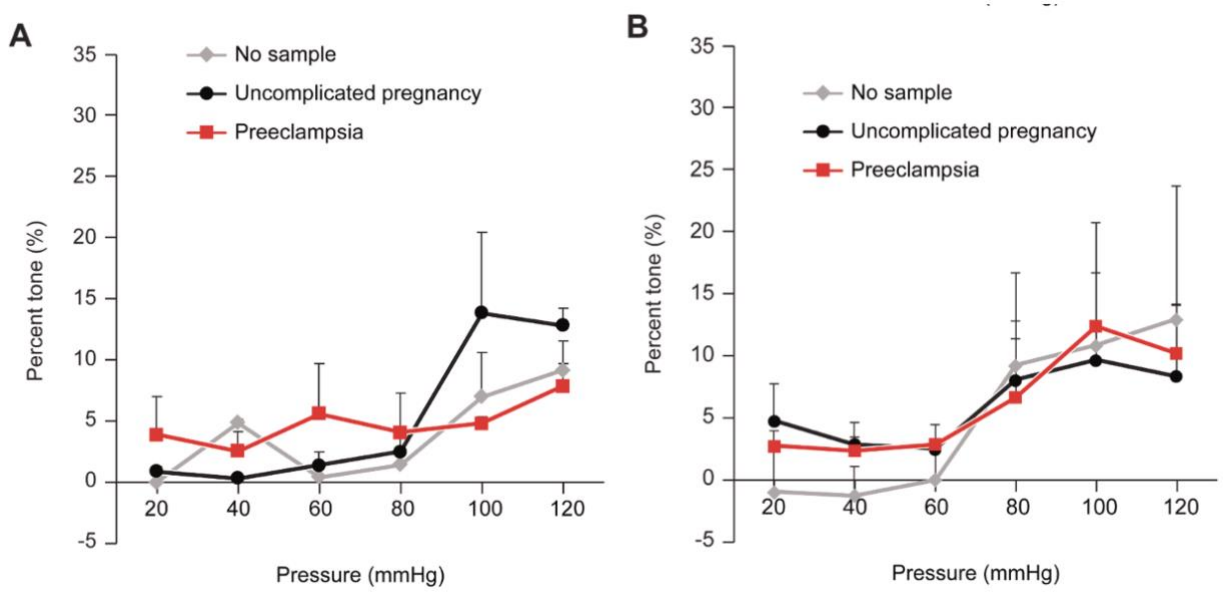

Figure 6: The myogenic responses (% tone) of mesenteric arteries exposed to plasma that was depleted of all EVs, or to MVs.

The figure shows the percent tone (Y-axis), calculated as detailed in Materials and Methods and in Fig. 1. **A)** plasma that was depleted of EVs. **B)** Exposure to MVs. The data are presented as mean ± SEM, n = 4. None of the differences were significant, calculated by 2-way repeated measures ANOVA.

2.2.5 The effect of sEVs on endothelium-mediated vessel relaxation

To provide additional support for our observations, we assessed the effect sEVs on arterial endothelium-dependent relaxation response. In these experiments, the vessels were initially constricted to 50% of their initial diameter at 60 mmHg using the alpha-adrenergic agonist phenylephrine (0.1-10 µM). We exposed the vessels to increasing concentrations of methacholine (0.001-1.0 µM) in the absence or presence of sEVs from women with PE *vs* sEVs from women with uncomplicated pregnancies. We found that exposure to sEVs from women with PE led to an impairment of methacholine-induced relaxation, with a more complete relaxation response when

exposed to sEVs from uncomplicated pregnancies (Fig. 7). These data suggest that sEVs from women with PE blunt the relaxation capacity and increase the myogenic tone generated in response to pressure stimuli.

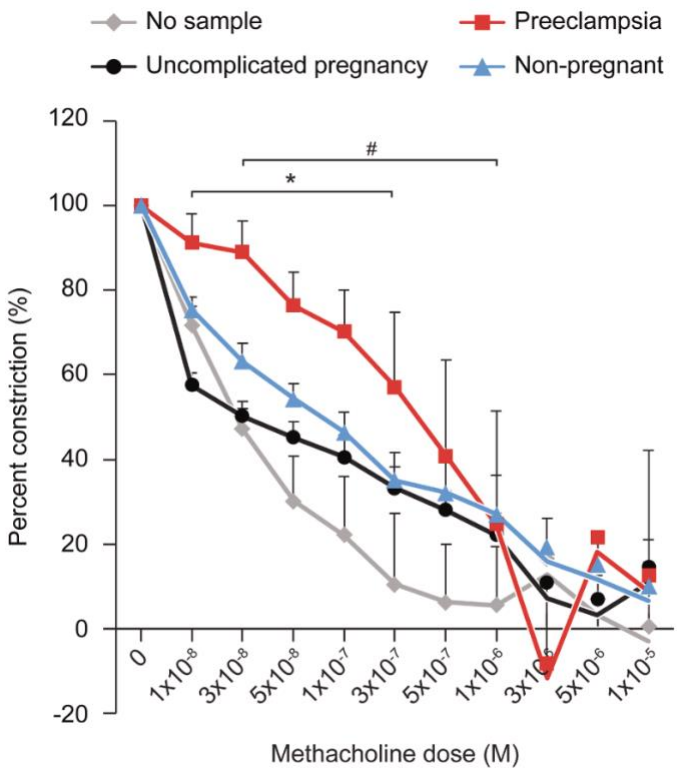

Figure 7: Endothelium-dependent methacholine-induced relaxation response (% relaxation of preconstriction) of mesenteric arteries exposed to sEVs.

See text for details. The figure shows the percent preconstriction remaining after consecutive doses of methacholine (Y-axis), calculated as detailed in Materials and Methods. The data are presented as mean ± SEM, n = 4. *denotes $p < 0.05$ for PE *vs* healthy pregnancy (control), and # denotes $p < 0.05$ for PE *vs* no EVs, calculated by 2-way repeated measures ANOVA with *post hoc* Tukey Test for pairwise comparisons.

2.2.6 Labeled sEVs localize to the endothelial cell layer of mouse mesenteric artery

To test whether trophoblast-derived sEVs interact with endothelial cells, we perfused mouse mesenteric arteries with buffer solution containing sEVs isolated from the culture supernatant of the human trophoblast cell line BeWo and labeled red with the CM-DiI dye. As shown in Fig.8, we found that perfused sEVs localized to $CD31^{+}$ endothelial cells. These results were consistent when arteries were exposed to sEVs isolated from human plasma and labeled with CM-DiI (data not shown). These data, along with the effect of sEVs on endothelial cell relaxation, suggest that sEVs can be trafficked to endothelial cells, and this may be a mechanism by which these particles affect mesenteric arterial tone.

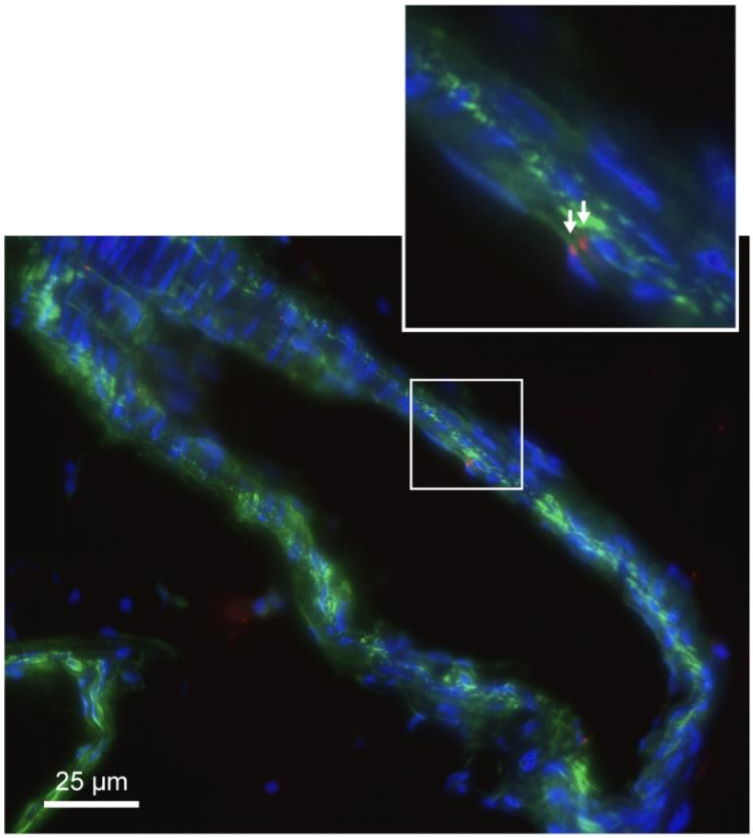

Figure 8: Localization of sEVs in mesenteric artery endothelial cells.

CM-DiI-labeled sEVs (red) are shown in CD31-labeled endothelium (green) of mesenteric artery from a 12-week-old female virgin C57Bl6J mouse. sEVS were derived from the BeWo trophoblast line. Cell nuclei are stained blue with DAPI (n = 4). White arrows point to sEVs (red) in endothelial cells.

2.3 Discussion

Using an *ex vivo* pressurized arteriography system, we found that exposing arteries to whole plasma from women with PE led to an increase in arterial vessel myogenic (pressure step-induced) tone, compared to arteries exposed to whole plasma from women with uncomplicated pregnancy, as previously shown [77]. We obtained similar results when we exposed mouse mesenteric arteries to sEVs isolated from the plasma of women with PE compared to sEVs from plasma of women with uncomplicated pregnancies. These data suggest sEVs from women with PE contribute to the vasoconstrictive effect and, thus, high blood pressure that is characteristic of PE. Supporting this notion, the vascular contractile effects of PE sEVs was lessened when we exposed vessels to EV-depleted plasma from women with PE, suggesting that sEVs are involved in the vasoconstrictive effect of plasma from women with PE. Interestingly, these vascular effects were specific to sEVs and not recapitulated in experiments with the larger MVs alone. This may be related to differences in the ability of sEVs to enter and interact with vascular endothelial cells [78, 79] or could also be related to variation in EV content. Possible differences in cargo molecules may involve RNA, including miRNA, DNA, proteins, lipids, or pro-inflammatory and anti-inflammatory cytokines [46, 70, 80-92]. Notably, our data suggest that non-EV mediated plasma signals contribute to the arterial vessel myogenic tone in our system.

Among our control samples we used sEVs that were purified from the plasma of non-pregnant women one-year postpartum. Interestingly, these sEVs also caused some increase in arterial tone, although the differences were statistically insignificant compared to sEVs from women with uncomplicated pregnancies. Such differences might point to a vasodilatory component in sEVs from the plasma of healthy pregnant women, and possibly the lack of a vasodilatory factor in sEVs from women with PE. In future studies it might be intriguing to examine the myogenic effects of sEVs from non-pregnant women, with and without hypertension, to investigate the role of sEVs in this condition [93, 94].

Previous data have shown that myometrial arteries from women with normotensive pregnancies exhibit impaired endothelium-dependent relaxation when incubated with plasma from women with PE [95-97]. Our vessel relaxation data and the immunofluorescence analysis of the arterial wall suggest that short-term exposure to plasma-derived sEVs can act directly on the arterial endothelial cell layer, leading to impaired endothelium-mediated relaxation in response to sEVs from women with preeclampsia. We recently showed that human trophoblastic sEVs enter target cells (endothelial cells, fibroblasts) through discrete endocytic pathways and are processed through early and late endosomes and lysosomes [79]. Previous studies have also shown that placental EVs containing miRNAs are taken up into arterial endothelial cells *in vitro* [79, 98]. Future experiments may allow us to detect the origin of the vasoactive circulating sEVs during pregnancy, and possibly inhibit their target cell entry, which may have therapeutic implications. Our data may also support the use of sEVs designed to carry synthetic cargo for the treatment of hypertension. Additional research into sEV cargo during disorders of pregnancy, including PE, is needed to assess this potential application.

There were several limitations to our study. First, although we observed a significant increase in arterial tone stimulated by sEVs from women with PE, these sEVs were isolated from whole plasma, and thus, their origin is not known and may include placental trophoblasts, platelets, diverse endothelial beds, and other cellular sources. Second, the sEV cargo or surface molecules contributing to these effects remain to be identified. Third, using a cross-species system (human sEVs and mouse blood vessels) may not capture the full spectrum of the phenomenon analyzed, even though an immune-based response is unlikely because of the short incubation time (2 h). In addition, the *ex vivo* artery system from *non-pregnant* mice, may not recapitulate the physiology of these vessels during pregnancy and may not resemble the response of human arterioles *in vivo*. These notions highlight the need for additional investigations into the function sEVs in uncomplicated human pregnancies or pregnancies complicated by PE.

2.4 Materials and Methods

2.4.1 Study subjects and sample collection

Clinical data and plasma samples were obtained from twenty nulliparous women, 10 with PE and 10 with uncomplicated pregnancies, enrolled in the Prenatal Exposures and Preeclampsia Prevention: Mechanisms of Preeclampsia and the Impact of Obesity (PEPP3) project, which recruited subjects either early in pregnancy or at the time of admission to labor and delivery at Magee-Women's Hospital from 2008 to 2014 [99]. All women provided written informed consent, and the study was approved by the University of Pittsburgh's Institutional Review Board (IRB

#PRO08050339). PE was defined using the criteria of the American College of Obstetricians and Gynecologists (ACOG) guidelines of 2002, and as updated in 2013 [62, 100]. Subjects were adjudicated by the PEPP3 research team through chart review. Proteinuria was defined as >300 mg per 24h urine collection, or ≥2+ (100 mg/dL) on a voided or ≥1+ (30 mg/dL) on a catheterized random urine specimen, or protein:creatinine ratio of ≥ 0.3. Women with uncomplicated pregnancies were normotensive throughout gestation, did not have proteinuria, and delivered at term. Women with PE or uncomplicated pregnancies were group-matched on the basis of age, pre-pregnancy body mass index (BMI), race, and gestational age at blood sample collection. The mean maternal age, pre-pregnancy BMI, blood pressure prior to 20-weeks gestation, and time of blood sampling among these women were not different between the groups. All women were non-smokers. Blood samples were obtained prior to labor and therapeutic intravenous administration of $MgSO_4$. Samples were also obtained from 10 non-pregnant subjects at 10-14 months after normotensive uncomplicated pregnancy (as described and adjudicated above, and who had no history of pregnancy complications) enrolled in the Glycocalyx Pathways Linking Pregnancy Profile with Microvascular Dysfunction Postpartum (the Pathways Study, IRB #PRO16030582). For all groups, patients with positive toxicology screen, chronic hypertension, renal disease, or a previous history of metabolic disorders were excluded. The plasma was separated by centrifugation within 60 min of blood collection and immediately frozen at -70^{o}C until use for isolation of sEVs.

2.4.2 Small extracellular vesicle isolation

To ensure a sufficient number of sEVs for the experiments, plasma samples (2 ml total) derived from pooled plasma samples (n=10) were centrifuged for 15 min at 2,500 g to remove

debris. Samples were then diluted with 2 mL PBS (Sigma-Aldrich, St. Louis, MO, 0.1 µm filtered) and filtered through a 0.2 µm syringe filter. Samples were diluted again to 10 mL and passed three times through gelatin-agarose columns (Sigma, G5384). PEG6000 (Sigma, 81253-250g) was added to the filtrate, and samples were incubated at room temperature (RT) for 10 min, then centrifuged at 10,000 g for 15 min at RT. The pellet was resuspended in 0.4 mL PBS. A 6-30% OptiPrep (Sigma, D1556) gradient was created using a gradient formation chamber and peristaltic pump. The sample was centrifuged for 22 h at 100,000 g at 4°C. Fractions 1-12 (1 mL each) were collected, fractions 4-6 were diluted 10-fold with PBS and concentrated using Vivaspin 20 (100 kDa cutoff) (Sigma, GE28-9323-63). Protein concentration was measured using microBCA assay (Thermo Fisher, Waltham, MA, 23235), and particle size was assessed by nanoparticle tracking analysis (NTA; Malvern Panalytical, Malvern, UK, Supplemental Fig. 2). [46]. For each vesicle type, the same number of EVs were added to each vessel.

For experiments with labeled sEVs, BeWo cells (from American Type Culture Collection) were cultured in Kaighn's modified medium F-12K (Gibco, Thermo Fisher) supplemented with 10% v/v GemCell SuperCalf Serum (Gemini Bioproducts, West Sacramento, CA), 20 mM HEPES, 1% v/v penicillin/streptomycin, then changed to EV-free F-12K medium supplemented with EV-free FBS (Thermo Fisher, A2720801) for 72 h. The medium was collected and centrifuged at 500 g for 10 min at 4°C. The supernatant was transferred to new tubes and centrifuged at 1,800 g for 20 min at 4°C to remove cells and apoptotic fragments. The supernatant was transferred to new tubes and centrifuged at 12,000 g for 30 min at 4°C to remove microvesicles, and then filtered through 0.22-µm filters (Genessee Scientific, San Diego, CA). Samples were concentrated using Vivacell 100 (100 kDa cutoff, Sartorius VC1042), and the

concentrate was diluted to 14 mL with EV-free PBS and ultracentrifuged overnight at 4°C and 100,000 g. For staining of BeWo sEVs, the pellet was resuspended in 0.5 mL PBS, and 1µg/µl of CM-DiI lipophilic dye (Invitrogen 2272596, Thermo Fisher) was added. The samples were incubated for 10 min at 37°C and 30 min at 4°C. Each sample was then processed as noted above, with removal of unbound dye during the OptiPrep gradient step. Staining of plasma sEVs was performed in a similar fashion, yet the final sEV samples were stained with CM-DiI at the end of the isolation, and the unbound dye was removed using an additional OptiPrep gradient centrifugation step.

2.4.3 MV isolation

Plasma samples (2 ml) were centrifuged for 15 min at 2,500 g to remove cell and apoptotic fragments. Supernatant was then centrifuged at 12,000 g for 15 min at 4°C to pellet MVs. MVs were washed three times by resuspending pellets in PBS and centrifuging 15 min at 12,000 g at RT.

2.4.4 Preparation of EV-depleted plasma

Plasma samples (2 ml) were first centrifuged at 2,500 g for 15 min at RT to remove apoptotic bodies. Supernatant was then centrifuged at 10,000 g for 15 min at RT to remove microvesicles. Finally, samples were centrifuged at 100,000 g for 2 h at 4°C to remove sEVs. The supernatant was retained as EV-depleted plasma. The depletion of vesicles was confirmed by NTA.

2.4.5 Establishment of the *ex vivo* mouse mesenteric artery system

Female C57Bl/6J mice, 7-12 weeks old, were obtained from Jackson Laboratory (Bar Harbor, ME) and maintained on a 12:12-hour light-dark cycle with food and water available *ad libitum*. Mice were euthanized by CO_2 asphyxiation, using cervical dislocation as a secondary method, and mesenteric arteries were immediately removed. The protocol was approved by the Magee-Women's Research Institute and University of Pittsburgh Animal Care and Use Committee protocol (IACUC #19085595).

2.4.6 Mesenteric arterial bioassay

Mesenteric arteries (inner diameter <300 μm) were used, given that vessels of this caliber constitute the major site of generation of systemic (peripheral) vascular resistance [101]. These arteries receive 30% of cardiac output and therefore contribute significantly to overall cardiovascular homeostasis. A portion of the mesenteric arcade 1 cm distal from the pylorus was placed in a HEPES buffered physiological saline solution (pH 7.4). Second order branches arising from the mesenteric arcade were dissected free, and two branches arising from the same artery were mounted in the dual chamber myograph described below. The inner diameter of these vessels at 60 mm Hg was 200-300 μm, which is consistent with the notion that approximately 50% of the flow resistance between the aorta and precapillary arterioles occurs in arteries of this diameter [101].

The vessels were transferred to a dual-chamber pressurized arteriograph (Living Systems, Burlington, VT) and mounted on two glass microcannulas suspended inside each chamber. Residual blood was flushed from the lumen. Buffer containing either 1% plasma or an EV sample

was introduced into the lumen at approximately 1.5 x 10^9 sEVs/mL of buffer. The distal cannula was occluded to prevent flow. The proximal cannula was attached to a flow-through pressure transducer and pressure servo control unit. This system allowed the intraluminal pressure to be maintained and controlled. A video dimension-analyzing system (Living Systems) processed a selected vidicon line to provide lumen diameter and wall thickness measurements. Both the pressure and dimensional parameters were calibrated at the beginning of each experiment. Further description of this system is reported elsewhere [102]. sEVs at a matched concentration were added to the bath, and this began the 2-h exposure period, during which the vessels were equilibrated at 60 mm Hg transmural pressure. A conditioning stretch [101, 103] was performed by slowly increasing the transmural pressure from 60 to 100 mm Hg (1mm Hg/sec) and decreasing back to 60 mm Hg 15 min before the end of the equilibration and exposure. After the 2-h incubation, the vessels were washed with HEPES-PSS, such that sEVs were removed from the bath but remained in the vessel lumen for the remainder of the experiment.

2.4.7 Myogenic assessment

Immediately following refreshment of HEPES-PSS in the vessel bath, intraluminal pressure was reduced to 20 mm Hg for 10 min. The arteries were then subjected to rapid (~2 s) pressure steps of 20 mm Hg every 4 min, from 20 to 120 mmHg in the absence of flow [103]. The 20 mm Hg pressure step was chosen to approximate the type of stimuli that occurs *in vivo* [104, 105]. At the end of the relaxation responsiveness experiments (described below), the smooth muscle was inactivated by a 10-min incubation in Ca^{2+}-free buffer with EGTA and 10^{-4} M papaverine, and the pressure steps were repeated, providing the passive (inactivated vascular smooth muscle) internal diameter response needed for the percent tone calculation. The percent

tone of individual arteries was calculated, at each pressure, as % tone = $[(D_r - D_{PSS})/D_r] \times 100$, where D_r is the passive internal diameter (relaxed and inactivated by Ca^{2+}-free buffer with EGTA and papaverine) and D_{PSS} is the stable internal diameter in normal HEPES-PSS [103]. Calculating tone in this manner adjusts for differences that exist in the size of individual arteries.

2.4.8 Endothelium-dependent relaxation responsiveness

The alpha-adrenergic agonist phenylephrine (0.1-10 µM, Sigma) was used to constrict arteries to 50% of their initial diameter. Relaxation response curves were generated to cumulative doses of the endothelium-dependent agonist methacholine (0.001-1.0 µM, Sigma). Vessels were washed and buffer was replaced with a calcium-free buffer to inactivate vascular smooth muscle. The rapid pressure steps were repeated to determine the maximum vessel diameter at each intraluminal pressure step, which was needed for the percent myogenic tone calculation.

2.4.9 Immunofluorescence microscopy

Following 2 h exposure of mesenteric arteries to CM-DiI-labeled sEVs (described above), the arteries were rinsed and mounted in Optimal Cutting Temperature Compound (OCT, Thermo Fisher), snap-frozen in 2 methyl-butane, pre-chilled in liquid nitrogen, and stored at -80ºC until use. Frozen tissues were sectioned (8 µm) with a cryostat and mounted on slides pre-treated with Vectabond (Vector Laboratories, Burlingame, CA). Tissue sections were fixed with 4% paraformaldehyde in PBS (15 min, RT) and blocked with 5% goat serum (G9023-10ML, Sigma) followed by the avidin/biotin blocking kit (Vector, PK-7200). Artery sections were incubated with biotin-CD31 antibody (BD Pharmingen, # 558737, BD Biosciences, San Jose, CA, 1:100) in 5%

goat serum at 4ºC overnight, followed by AF647-streptavidin (Thermo Fisher S-21374, 1:400 in 5% goat serum at RT for 45 min). The slides were washed with PBS, and then streptavidin AF647 secondary antibody (Thermo Fisher S-21374), diluted 1:400 in 5% goat serum, was added and incubated, protected from light, for 45 min at RT. The slides were washed with PBS, and cell nuclei were counterstained with DAPI (0.1µg/ul, D9542, Sigma) was added for 15 min at RT. Tissue sections were fixed again in 4% paraformaldehyde in PBS (15 min at RT). Coverslips were mounted with Gelvatol (81365, Sigma). The tissues were imaged using a Nikon E800 microscope with Zeiss Axiocam 506 camera.

2.4.10 Data analysis

Unpaired analyses were used to compare characteristics between PE and uncomplicated pregnancy groups. Continuous, normally distributed variables were compared by one-way analysis of variance (ANOVA). Clinical characteristics were compared using either the Kruskal-Wallis or Holm-Sidak test. Myogenic and relaxation responses were compared using two-way repeated measures ANOVA with *post hoc* Tukey Test for pairwise comparisons. The total sample size was estimated on the basis of previous publications demonstrating differential effects of PE *vs* normal pregnancy plasma-derived sEVs on vascular function [87] and our preliminary vascular data and estimates of the total amount of plasma required for sEV isolation and arterial bioassay experiments.

3.0 Paternal antigens and fetoplacental small extracellular vesicles traffic to maternal secondary lymphoid tissues.

3.1 Introduction

In mouse experimental models, it has been shown that maternal naive CD4 and CD8 T cells recognize paternal antigen (Ag)-derived peptides, presented or cross-presented by maternal Ag-presenting cells (APCs), including cDCs and B cells. In mice, presentation of conceptus-derived peptides occurs in the context of maternal classic H2 class-I and -II molecules (equivalent to HLA-A/B/C and HLA-DR/DQ/DP molecules in humans), within the mother's secondary lymphoid tissues (SLTs) that drain the uterus (SLTs) [54]. During a normal mouse pregnancy, this leads to deficient activation followed by clonal deletion or anergy of maternal CD4 or CD8 T cells that recognize the paternal Ag-derived peptides, and differentiation of $CD4^{Pos}$ $FoxP3^{Pos}$ regulatory T cells specific to the paternal Ags (Tregs) [55]. Despite the biological importance of this phenomenon, the cell-free mechanism(s) by which the conceptus delivers fetoplacental (no-self) Ags to the mother's leukocytes in SLTs remains unknown. Because the placenta releases EVs into peripheral blood[9, 56], and EVs have been shown to function as carriers for horizontal transfer of proteins and Ags between cells [57], we investigated if trophoblast EVs released in the mother's peripheral blood constitute a platform in which conceptus-derived Ags are delivered intact to maternal APCs in SLTs.

3.2 Results

3.2.1 Paternal antigens are found in maternal tissues during pregnancy

We first analyzed the spread of paternal Ags to immune cells within the mother's SLTs in a semi-allogeneic pregnancy model in which wild type BALB/c ($H2^d$) females were impregnated with C57Bl/6 (B6, $H2^b$) mice hemizygous for the membrane-bound chicken ovalbumin (Act-mOVA) transgene. In this model, mOVA functions as a paternal surrogate Ag that is highly expressed by the trophoblasts, in particular by the secondary trophoblast giant cell layer that surrounds the conceptus, trophoblasts of the junctional zone, and to a lesser extent by the labyrinth trophoblasts (Figure 9A). In the maternal SLTs, we confirmed by microscopy on E17.5 the accumulation of OVA Ag on maternal splenic follicular dendritic cells (FDCs, as previously reported in a different female strain combination [53] (Figure 9B and C). This finding was indicative of spread of conceptus-derived OVA via maternal peripheral blood because the spleen lacks afferent lymphatics [106]. On E17.5, OVA Ag was also detected on FDCs of uterus-draining and non-draining lymph nodes (Figure 9C). Analysis of sections of the maternal spleen (E17.5) by super-resolution stimulated emission depletion (STED) microscopy revealed that the OVA associated to the splenic FDCs, is concentrated in small foci compatible with sEVs (Figure 9D).

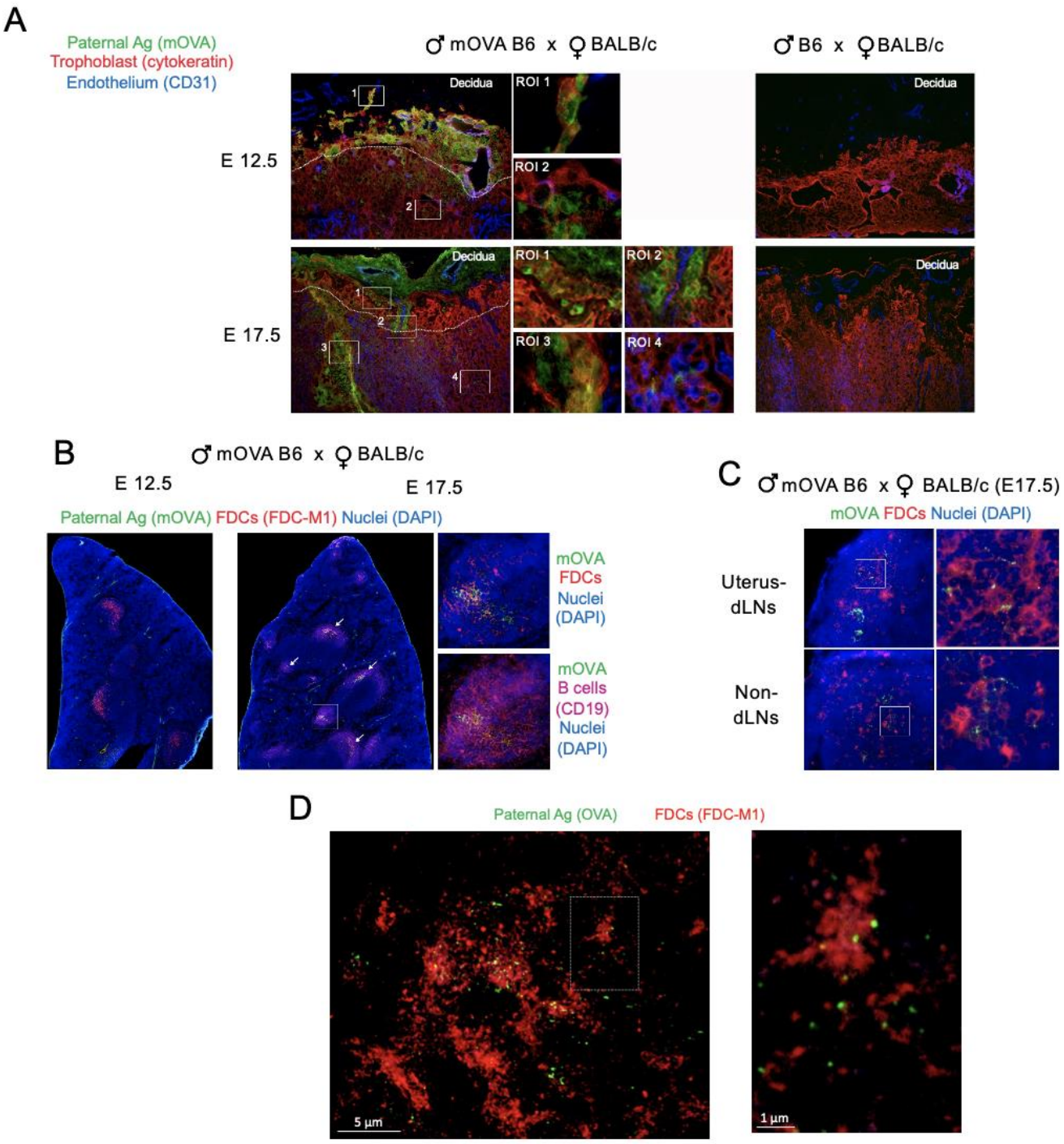

Figure 9: OVA Ag is detected in placenta and maternal SLT.

A) Detection by fluorescence microscopy on tissue sections of the surrogate paternal Ag OVA (green) in the trophoblast (in red) of BALB/c females mated with Act-mOVA B6 males, analyzed at E12.5 and E17.5. OVA Ag was undetectable in placentas of control BALB/c pregnant females mated with WT B6 males. **B and C)** Detection of OVA

(green) in a punctate pattern on FDCs (red) located in the maternal spleen, draining, and non-draining LN on E17.5. **D)** Image by super-resolution stimulated emission depletion (STED) microscopy STED image of OVA content (green) on FDCs (red) in the spleen of spleen of BALB/c females mated with Act-mOVA B6 males, analyzed at E17.5.

3.2.2 Conceptus-generated small extracellular vesicles reach maternal cells in secondary lymphoid tissues.

We next investigated if sEVs released by the fetoplacental unit are transferred locally to maternal cells at the fetal-maternal interphase, and systemically to maternal immune cells in the mother's lymphoid organs. We used a novel mouse model, MT124 B6 mice encoding a floxed STOP cassette containing tdTomato, followed by the sEV-associated marker CD81 linked to mNeonGreen, driven by the ubiquitous CAG promoter (Figure 10). Upon mating homozygous MT124 B6 males with homozygous CMV-Cre B6 females, the stop cassette is removed, which is confirmed by the lack of tdTomato expression in the conceptus, leading to the generation of sEVs carrying CD81-mNeonGreen on their membrane, exclusively in EVs that originate in fetal-placental tissues. As negative controls without Cre, homozygous MT124 B6 males were mated with WT B6 females.

Analysis by microscopy of immuno-labelled cryosections of E17.5 placentas revealed the presence of CD81-mNeonGreen scattered, in a dotted pattern, in trophoblast cells lining the vascular canals of the placenta and in trophoblast cells at the interphase between the junctional zone and decidua (Figure 11A). CD81-mNeonGreen was also detected in the decidua (a maternal tissue), in close apposition or within stromal cells and blood vessel endothelial cells (Figure 11C-D), and in decidua-infiltrating leukocytes (Figure 11E). We did not detect CD81-mNeonGreen^{Pos} material in placentas from MT124 males mated with WT females (Supplemental Figure 3B).

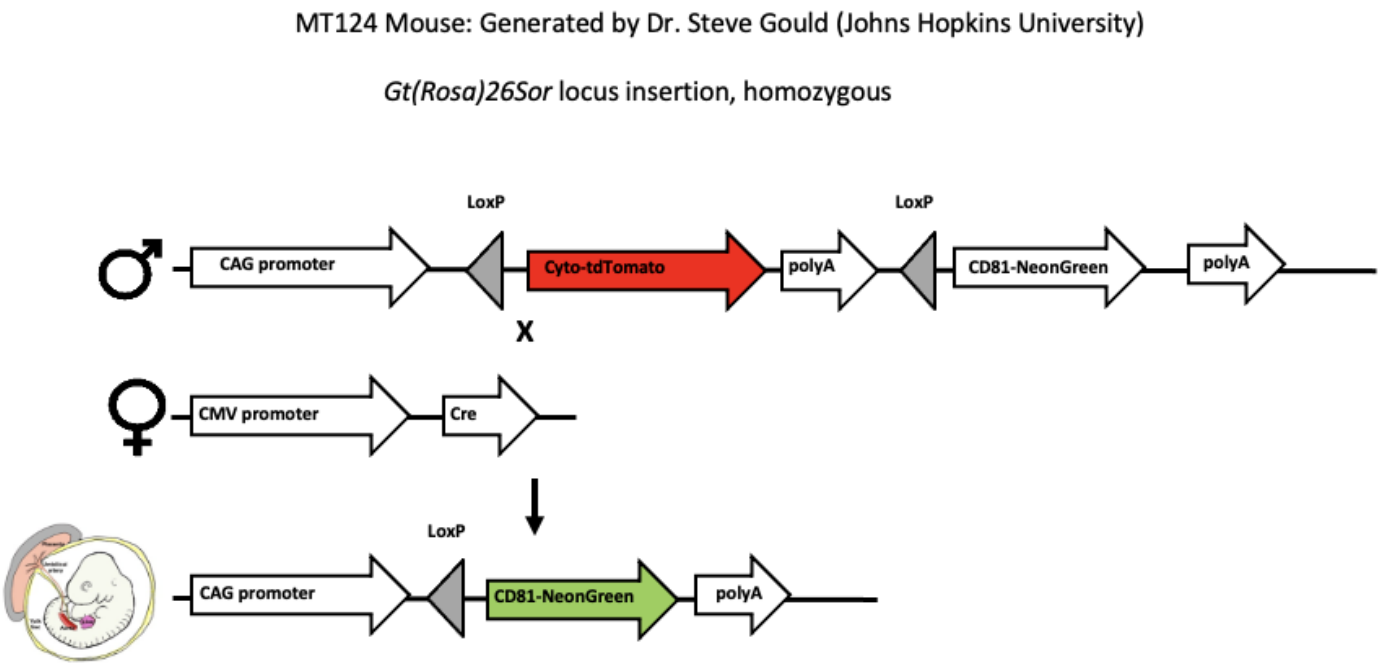

Figure 10: MT124 B6 mouse model.

MT124 B6 mice encode Cyto-TdTomato cDNA driven by the CAG promoter upstream of a PolyA tail, resulting in cytoplasmic expression of tdTomato in the absence of Cre. In the presence of Cre, recombination of the LoxP sites flanking the Cyto-tdTomato-polyA leads to its excision and transcription of CD81-NeonGreen cDNA located downstream. The CD81-NeonGreen protein is then sorted into the fetoplacental-derived sEVs, which become green.

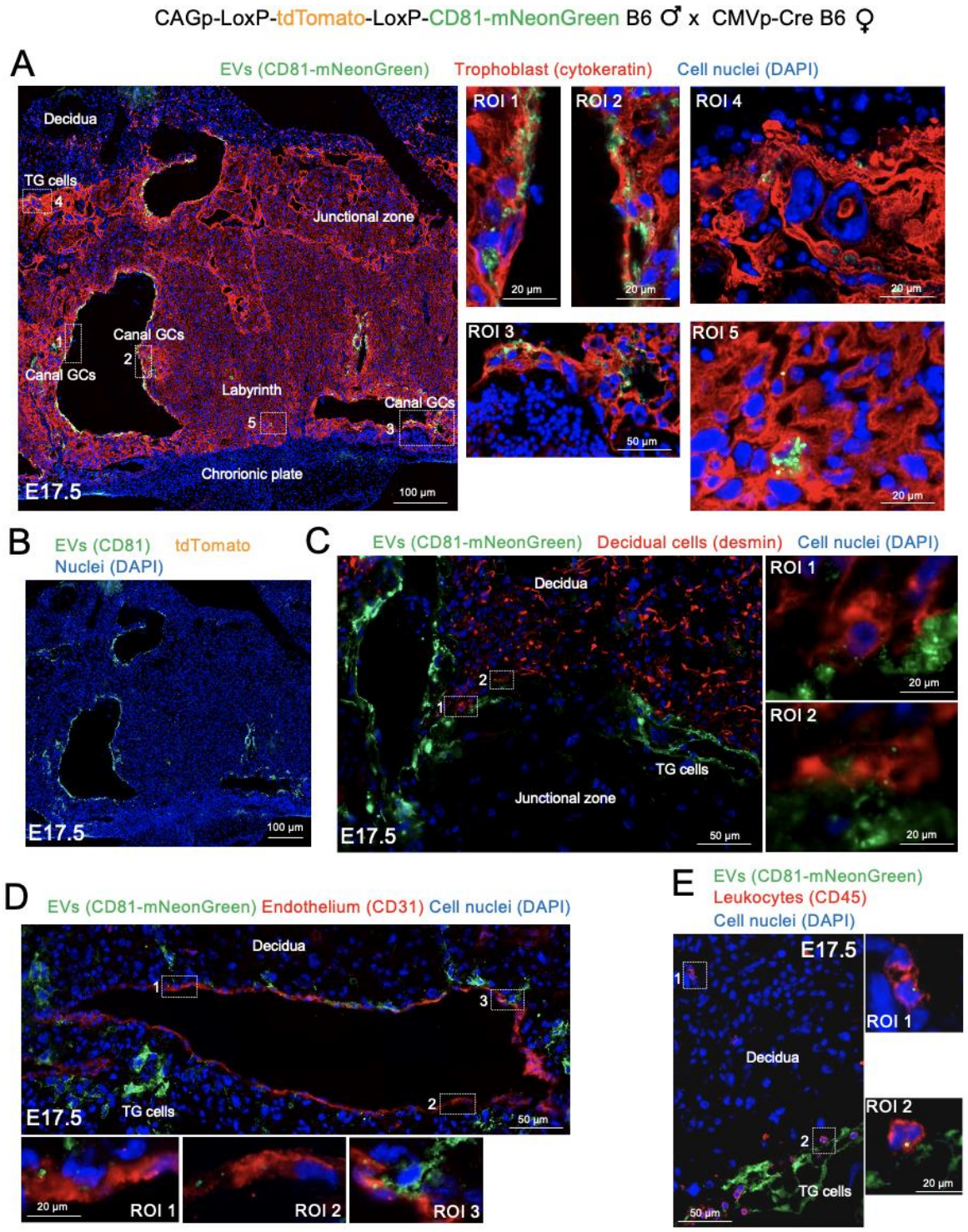

Figure 11: CD81-mNeonGreen^{Pos} content in E17.5 placenta.

A and B) Detection by fluorescence microscopy on tissue sections of CD81-mNeonGreen (A) in junctional zone trophoblast cells, trophoblast giant cells and canal giant cells (red) and lack of tdTomato expression (B) in placentas from CMV-Cre B6 females mated with MT124 B6 males, analyzed at E12.5 and E17.5 **C)** Detection by fluorescence

microscopy of CD81-mNeonGreen in decidual cells (red) at the interphase between the junctional zone and the decidua. **D and E)** Maternal blood vessel endothelium and infiltrating leukocytes with CD81-mNeonGreen^{Pos} content in the decidua. ROI: region of interest.

On E17.5, in the mother's SLTs, CD81-mNeonGreen^{Pos} content was detected, concentrated in punctate areas in FDCs within B cell follicles, B cells, marginal zone CD169^{Pos} macrophages, red pulp F4/80^{Pos} macrophages, and cDCs (CD11c^{Pos}) in T cell areas (Figure 12A-D). Importantly, the CD81-mNeonGreen^{Pos} foci detected in immune cells in the mother's spleen were not the result of capture of small fragments of detached trophoblast released systemically, since they were negative for pan-cytokeratin (Figure 13A). CD81-mNeonGreen was undetectable in maternal SLTs in the absence of Cre when control WT B6 females were impregnated by homozygous MT124 B6 males (Figure 13B).

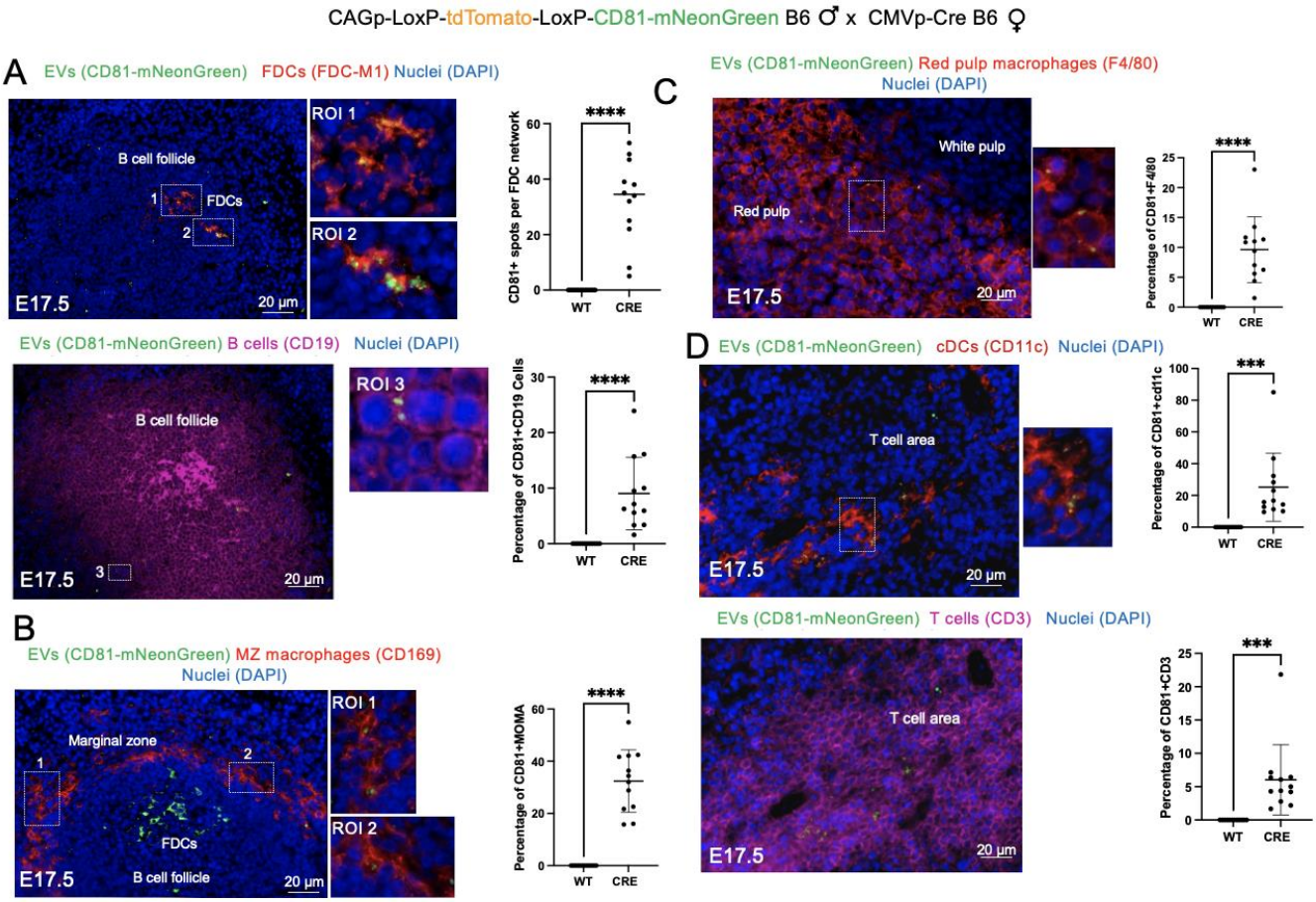

Figure 12: Fetoplacental sEVs traffic to maternal SLT.

A) Detection and quantification by fluorescence microscopy of tissue sections of CD81-mNeonGreen^{pos} content in FDCs (red) and B cells in the spleen of CMV-Cre B6 females mated with MT124 B6 males, analyzed on E17.5 ($p<000.1$). **B and C)** CD81-mNeonGreen^{Pos} foci associated with CD169 macrophages and F4/80 macrophages ($p<000.1$). **D)** CD81-mNeonGreen^{Pos} material in cDCs (red) and T cells (pink) in T cell area of the spleen. Dot plots: quantification of CD81-mNeonGreen^{Pos} content in substes of immune cells in the maternal spleen, by microscopy on tissue sections. Each dot in the dot plots represents one tissue section.

3.3 Discussion

Using OVA as a surrogate paternal Ag in a semi-allogeneic mouse pregnancy model, we confirmed the presence of paternal Ags in maternal SLTs during normal pregnancy. The OVA Ag was detected in primary B cell follicles of the maternal spleen and colocalized with FDCs that reside within the B cell follicles. This suggests that the OVA Ag is captured and retained by FDCs whose function is to present soluble intact Ags to B cells. The OVA Ag was also detected in FDCs resident in maternal uterine-draining and non-draining lymph nodes. Previous studies in non-pregnancy models in mice, have shown that FDCs avidly capture, concentrate and retain for weeks or months soluble Ags in the form of immuno-complexes, or soluble Ags coated with complement factors, which bind the complement receptors (e.g. CD21/35) highly expressed on the FDC surface.

Because we detected paternal-derived OVA Ag in maternal SLTs during pregnancy, to address our hypothesis, we assessed whether fetoplacental sEVs released to the maternal peripheral blood represent a cell-free mechanism by which paternal Ags are delivered intact to maternal SLTs. We used genetically-engineered MT124 B6 male mice to impregnate CMV-Cre B6 female mice in which following Cre-mediated recombination, the fetoplacental unit releases green sEVs tagged with CD81-mNeoGreen. With this approach we detected CD81-mNeonGreen^{Pos} content in maternal leukocytes and FDCs in the mother's spleen, as well as in the mother's kidney, liver, and heart. This supports the notion, at least in mice, that feto-maternal sEVs target maternal cells in SLTs and in non-lymphoid organs. The pattern of localization of CD81-mNeonGreen sEVs in maternal leukocytes and FDCs (FDCs are not leukocytes) was similar to that of paternal OVA Ag. Quantification was not necessary because no CD81-mNeoGreen signal was detected in WT tissues. To further test our hypothesis, in the next chapter we analyzed whether sEVs released by

the mouse trophoblasts to maternal peripheral blood carry paternal Ags. Our findings are in agreement with recent transplantation studies in mice, in which sEVs released by vascularized cardiac allografts are captured by marginal zone and red pulp macrophages, cDCs. FDCs and B cells in the recipient's spleen [107].

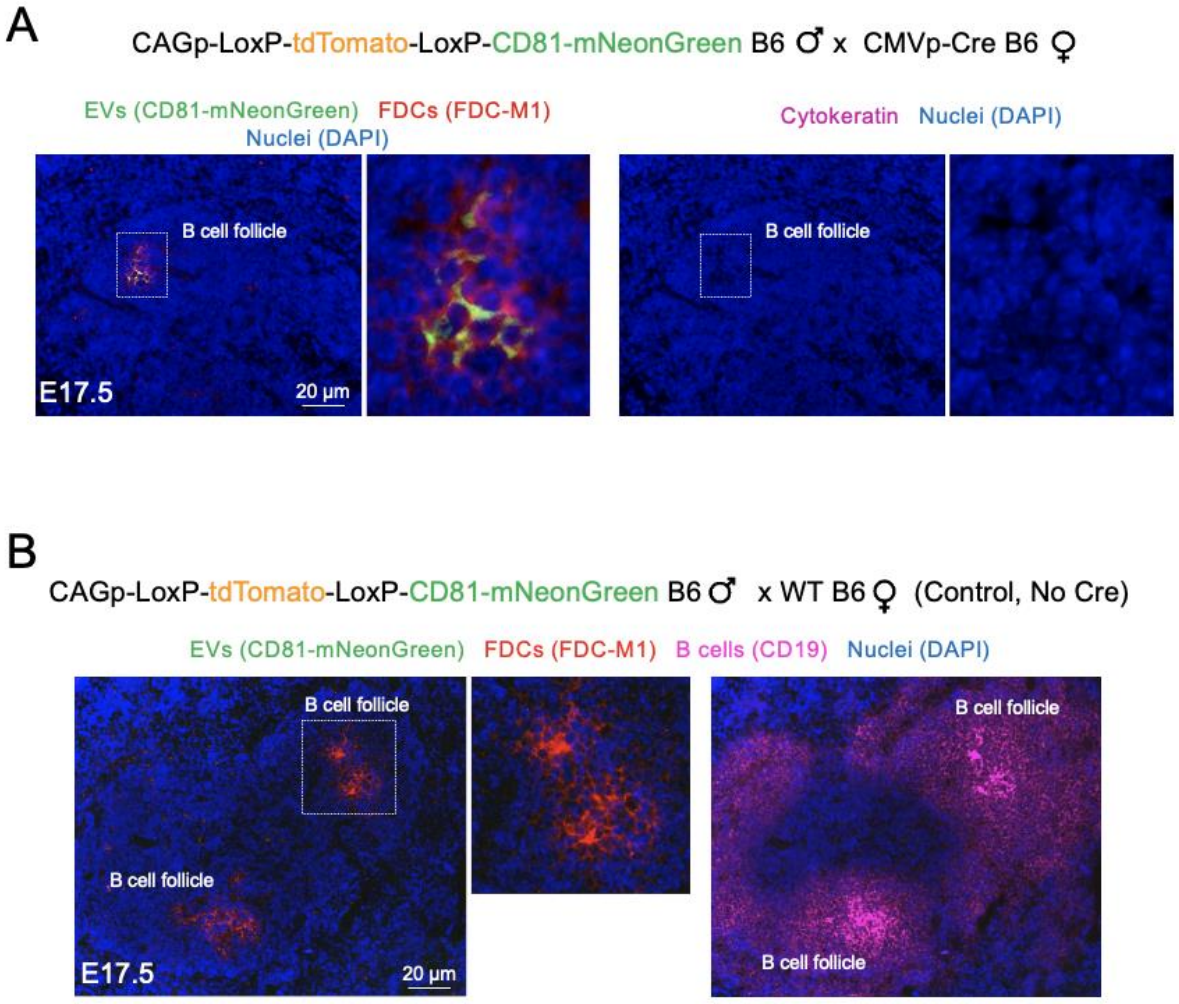

Figure 13: No trophoblast-derived fragments in maternal SLTs or CD81-mNeonGreen in control samples.

A) Tissue sections of maternal spleen from CMV-Cre B6 females mated with MT124 B6 males did not contain cytokeratin^{Pos} trophoblast-derived fragments detectable by fluorescence microscopy. **B)** CD81-mNeonGreen^{Pos} material was undetectable in spleens of control WT B6 females (No-Cre) impregnated with MT124 B6 males.

3.4 Materials and Methods

3.4.1 Mice

WT C57Bl/6 ($H2^b$, B6), WT BALB/c ($H2^d$), Act-mOVA C57Bl/6, and B6.C-Tg (CMV-Cre)1Cgn/J (CMV-Cre) mice were purchased from the Jackson Laboratory. MT124 B6 mice were developed by Dr. Steve Gould at Johns Hopkins University and generously shared with us. Mice were bred and maintained in the pathogen-free animal facility of the University of Pittsburgh School of Medicine. Animal care and handling were performed in accordance with institutional guidelines and procedures approved by Institutional Animal Care and Use Committee (IACUC) protocol numbers 19106062 and 20098112.

3.4.2 Immunofluorescence microscopy

Mouse tissue fragments were embedded in Optimal Cutting Temperature Compound (OCT), snap-frozen in 2 methyl-butane pre-chilled in liquid nitrogen and stored at -80°C until use. Frozen tissues were sectioned (10 μm) with a cryostat and mounted on slides pre-treated with Vectabond (Vector Laboratories).

For detection of OVA in BALB/c samples, tissue sections were fixed with 4% paraformaldehyde (PF) in PBS (15 min, RT), washed in PBS and blocked with 5% goat serum. Cryosections of BALB/c spleen, uterus-draining and non-draining lymph nodes, and placentas

were incubated with anti-OVA antibody (Ab), anti-mouse CD19 Ab, anti-mouse FDC-M1 Ab, or anti-mouse Pan-keratin Ab (all at a dilution of 1:100) in 5% goat serum (overnight, 4°C), followed by AF488-goat anti-rabbit IgG, AF647-goat anti-rat IgG, or AF555-goat anti-rat IgG (1:400) in 5% goat serum (45 min, RT).

To analyze CD81-mNeonGreen^{Pos} content in different cell types, tissue sections were fixed with 96% ethanol in PBS (15 min, RT), washed in PBS and blocked with 5% goat serum. Cryosections of uterus-draining and non-draining lymph nodes, placenta, kidney, liver, heart, and lungs of pregnant CMV-Cre B6 females impregnated with MT124 B6 males were incubated with anti-mouse CD163 Ab, anti-mouse CD169 Ab, anti-mouse pan-keratin Ab, anti-mouse CD31 Ab, anti-mouse FDC-M1 Ab, anti-mouse F4/80 Ab, hamster anti-mouse CD11c Ab, anti-mouse CD19 Ab, or Anti-mouse CD3 Ab (all at a dilution of 1:100) in 5% goat serum (overnight, 4°C), followed by AF488-goat anti-mouse IgG, AF647-goat anti-rat IgG, or AF555-goat anti-rat IgG (1:400) in 5% goat serum (45 min, RT).

Cell nuclei were counterstained with DAPI, and tissue sections were fixed post-labelling in 4% PF / PBS (15 min, RT). Coverslips were mounted with Vector® TrueVIEW® Autofluorescence Quenching Kit. The tissues were imaged using a Nikon E800 microscope with Zeiss Axiocam 506 camera.

4.0 Trophoblast extracellular vesicles deliver paternal antigens that are presented to T cells in secondary lymphoid tissues.

4.1 Introduction

Multiple biological functions have been attributed to EVs, in particular as a mechanism of cell-to-cell transfer of Ags, proteins, mRNAs, non-coding RNAs, small DNA fragments, and lipids [11]. Thus, continuous release of fetoplacental EVs to the maternal systemic blood may be a mechanism by which paternal Ags and placenta-specific Ags are delivered to immune cells located in the mother's SLTs, in which the conceptus EV-derived Ags are presented to T lymphocytes in a pro-tolerogenic manner. Previous studies in non-pregnancy models have shown that sEVs are rapidly internalized by Ag-presenting cells (APCs), in which the EV-derived Ags are processed into peptides that are loaded in MHC class-I and –II molecules for presentation to CD8 T and CD4 T cells, respectively [108]. Therefore, in this section, we wanted to assess the delivery of paternal antigens by fetoplacental sEVs to maternal SLT and their presentation to maternal T cells.

4.2 Results

4.2.1 Extracellular vesicles with paternal Ags are present in blood of pregnant mice.

Upon observation of localization of the surrogate paternal Ag OVA and fetoplacental CD81-mNeonGreen^{Pos} sEVs in immune cells of the mother SLTs in pregnant mice, we next

analyzed in pregnant mice, whether fetoplacental sEVs released to maternal blood carry the surrogate paternal Ag OVA. We collected plasma from WT BALB/c pregnant females (E17.5) impregnated with OVA B6 mice, or control WT B6 males. To specifically isolate fetoplacental-derived OVA^{Pos} MVs, OVA^{Pos} sEVs, and soluble OVA, plasma MVs and sEVs, pre-purified by 10,000*g* and 100,000*g* ultracentrifugation respectively, and its corresponding supernatants, were immunoprecipitated with magnetic beads coated with a polyclonal rabbit anti-OVA Ab. Following immunoprecipitation, the presence of EVs on the surface of the OVA Ab-coated beads was confirmed by electron microscopy (Figure 14C). Analysis by western blot of the immunoprecipitated material using a mouse monoclonal Ab against OVA demonstrated the presence of OVA in the trophoblast-derived MVs and sEVs, and as soluble Ag in the EV-free fraction (Figure 14A). Treatment of the samples with peptide: N-glycosidase F (PNGase) prior to western blot analysis indicated that the higher M.W. of the OVA detected in the plasma MVs, sEVs and their supernatants, compared to soluble OVA used as control, was due to OVA N-linked glycosylation (Figure 14B). The purity of the sEVs was confirmed by their positivity for the sEV-associated markers CD81 and CD63 and absence of gp96, the latter an endoplasmic reticulum-associated marker (Figure 14A). As a control, OVA was undetectable in immuno-precipitates of EVs, and EV supernatants collected from plasma of control WT B6 female mice impregnated with WT B6 males (Figure 14A).

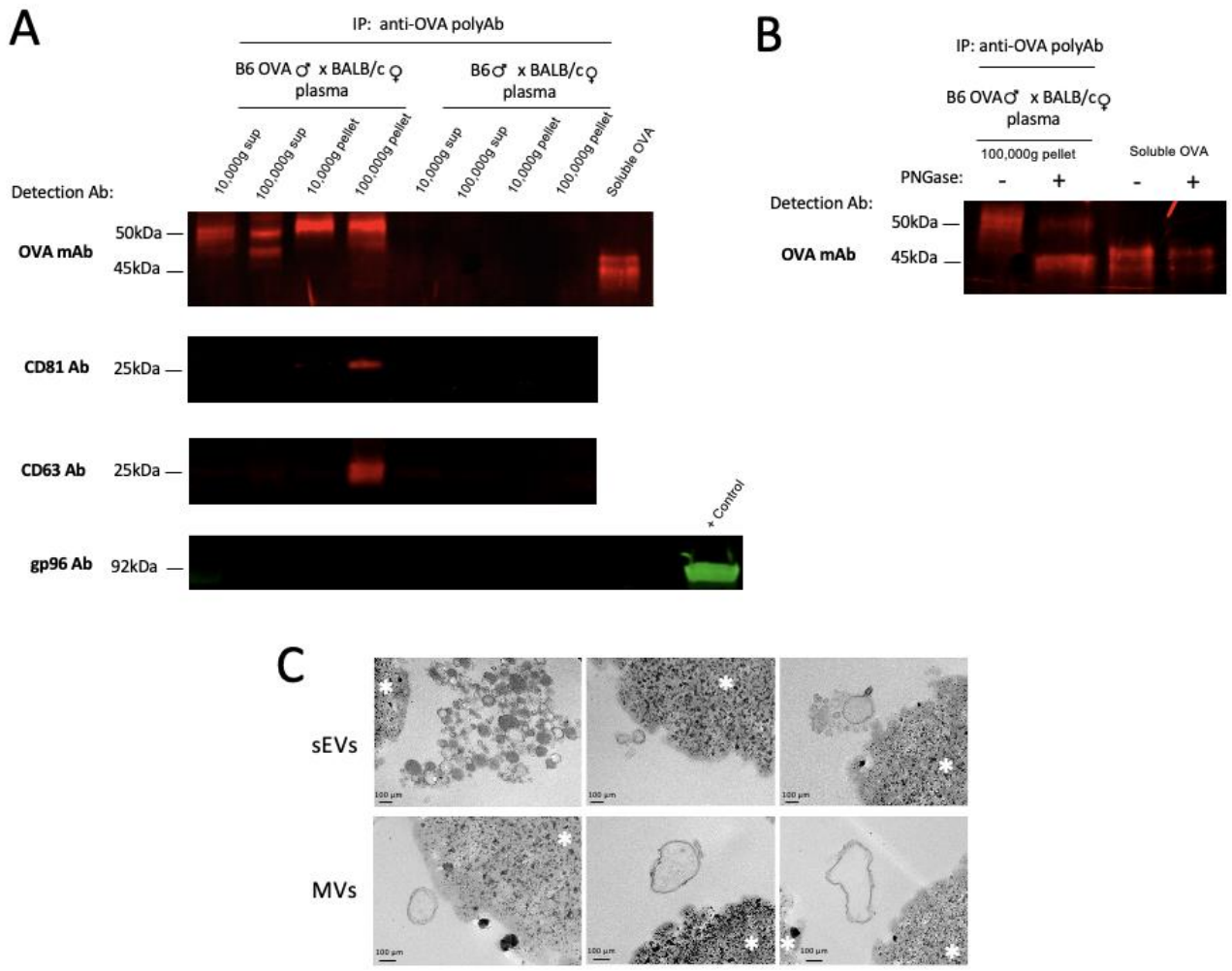

Figure 14: Maternal peripheral blood EVs carry paternal Ags in mice.

A) Immunoprecipitation and western blot detection of OVA, the sEV-associated markers CD81 and CD63, and the ER-marker gp96 in MVs and sEVs purified from plasma of BALB/c female mice impregnated with mOVA B6 males or control WT B6 males (E12.5-E17.5), and in 10,000*g* and 100,000*g* cleared plasma form the same females. **B)** PNGase digestion of the immunooprecipitate restored the OVA MW to the size of the positve control, which indicates that the OVA released by the conceptus is N-glycosylated. **C)** Transmission electron microscope analysis confirmed that the sEVs and MVs bound the OVA-Ab coated beads used for the immunoprecipitation.

4.2.2 Mouse trophoblast cells release extracellular vesicles carrying paternal antigens

In the above experiments, the EVs carrying the parental Ag OVA isolated from peripheral blood of pregnant mice could have been released by the placenta, the fetus, or both. To

conclusively demonstrate that the trophoblast secretes EVs carrying paternal Ags, we generated primary trophoblast cell cultures from placentas (E12.5 – E17.5) of pregnant WT BALB/c females mated with OVA B6 males, or with control WT B6 males (Figure 15A). Immunofluorescence microscopy of cytospins of the mouse primary trophoblast cell cultures demonstrated predominance of trophoblast cell clusters, detected with an anti-pan-cytokeratin Ab, and minimal contamination with desmin^{Pos} decidual cells (Figure 15B). Consistent with the results obtained in EVs isolated from plasma of pregnant mice, OVA Ag was detectable by western blot analysis in trophoblast-derived MVs and sEVs, the latter positive for the sEV-associated marker CD63 and negative for the endoplasmic reticulum protein gp96 (Figure 16A). By contrast, OVA was undetectable in vesicles isolated from trophoblast cultures of control pregnant WT BALB/c females mated with WT B6 males (Figure 16A). Immuno-electron microscopy of mouse primary trophoblast cell cultures confirmed the expression of OVA Ag on intraluminal vesicles inside multivesicular bodies of trophoblast cells (Figure 15C). The presence of OVA Ag on mouse trophoblast sEVs was confirmed with an *in vivo* assay of proliferation of CFSE-labelled T cell receptor (TCR) transgenic CD8 T cells (OT-I T cells), which recognize the OVA-derived peptide SIINFEKEL presented by the B6 MHC class-I molecule H2-K^{b} and express the TCRα chain V2 [109]. Administration of sEVs isolated from primary cultures of OVA B6 male x WT BALB/c female trophoblast cells, in the footpad of virgin female B6 mice (Thy1.2 congenic) reconstituted (i.v.) 24 hours prior with CFSE-labelled Thy1.1^{Pos} OT-I T cells (5 x 10^{6} / mouse) triggered proliferation of the CFSE-labelled OT-I CD8 T cells, the latter assessed in the draining popliteal lymph node, based on CFSE-dilution (the CFSE content halves each time OT-I T cells divide) (Figure 15B). In this model, the i.v. injected OT-I CD8 T cells are distinguished from endogenous (Thy1.2^{Pos}) T cells by the expression of Thy1.1. By contrast administration of an equivalent

volume (30 µl) of the primary culture of 100,000*g* cleared supernatant did not have a detectable effect on the OT-I T cells (Figure 16B). In the same model, footpad injection of control (OVA^{Neg}) sEVs or 100,000*g* cleared supernatant from primary cultures of control WT B6 male x WT BALB/c female trophoblast cells, did not trigger proliferation of OT-I T cells *in vivo*.

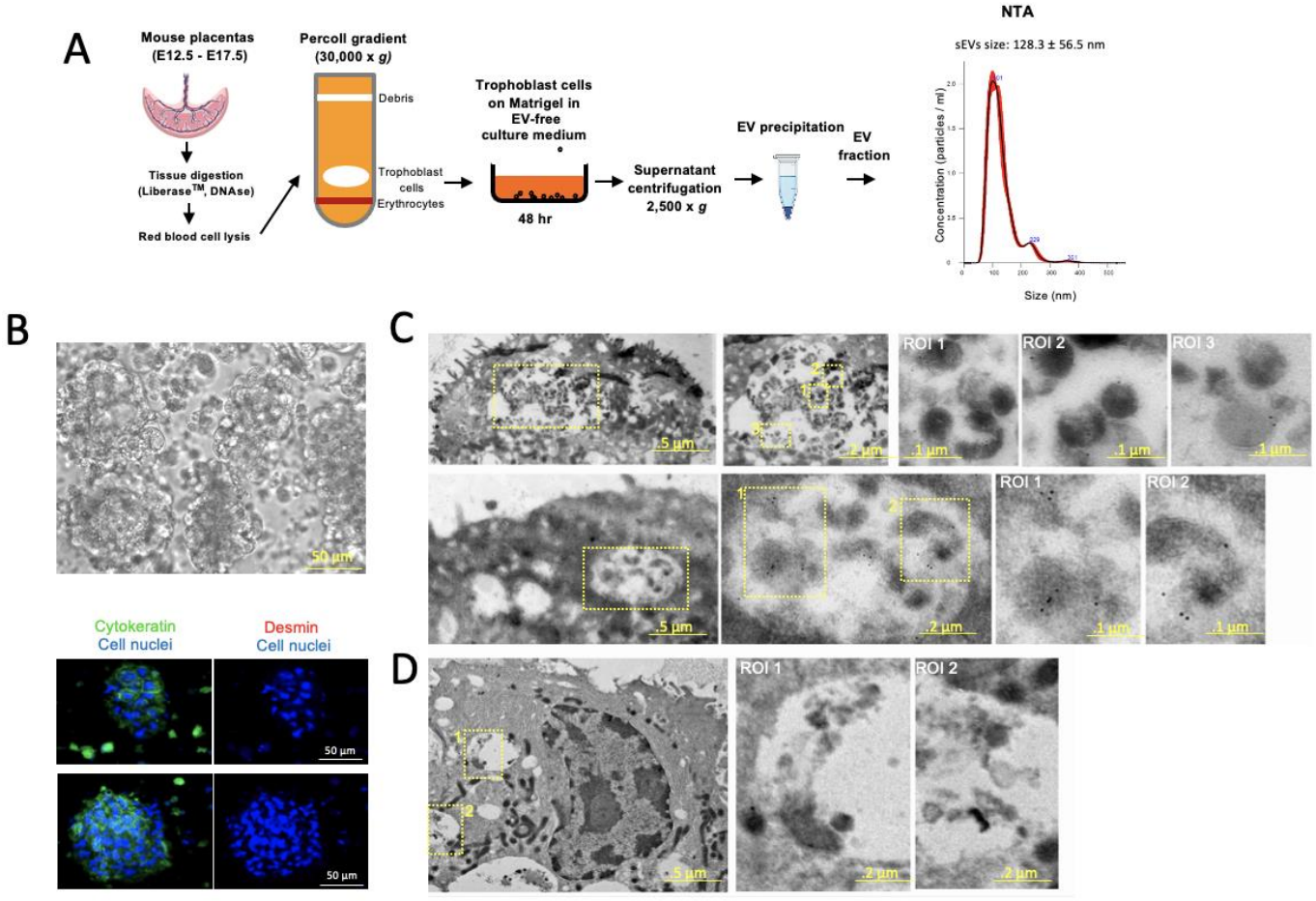

Figure 15: Isolation of primary mouse trophoblasts.

A) Diagram of the methodology used to purify EVs from supernatants of primary cultures of mouse trophoblast cells. NTA: nanoparticle tracking analysis. **B)** Top: bright field microscopy image showing clusters of mouse trophoblast cells after 48 hours of culture. Bottom: immunofluorescence microscopy of cytospins of primary cultures of mouse trophoblast cells, composed mainly by $cytokeratin^{Pos}$ trophoblast cells with minimal contamination with $desmin^{Pos}$ decidual cells. **C)** Immuno-electron microscopy analysis of primary cultures of trophoblast cells from placentas (E12.5-E17.5) of BALB/c female mice impregnated with mOVA B6 males. Images show multivesicular bodies with

content of intraluminal vesicles expressing OVA Ag (6 nm gold) on the surface. ROI: region of interest. **D)** Immuno-electron microscopy images of primary cultures of trophoblast cells isolated from placentas of BALB/c female mice impregnated with control WT B6 males (E12.5-E17.5) showing multivesicular bodies with content of intraluminal vesicles on which OVA Ag was not detected.

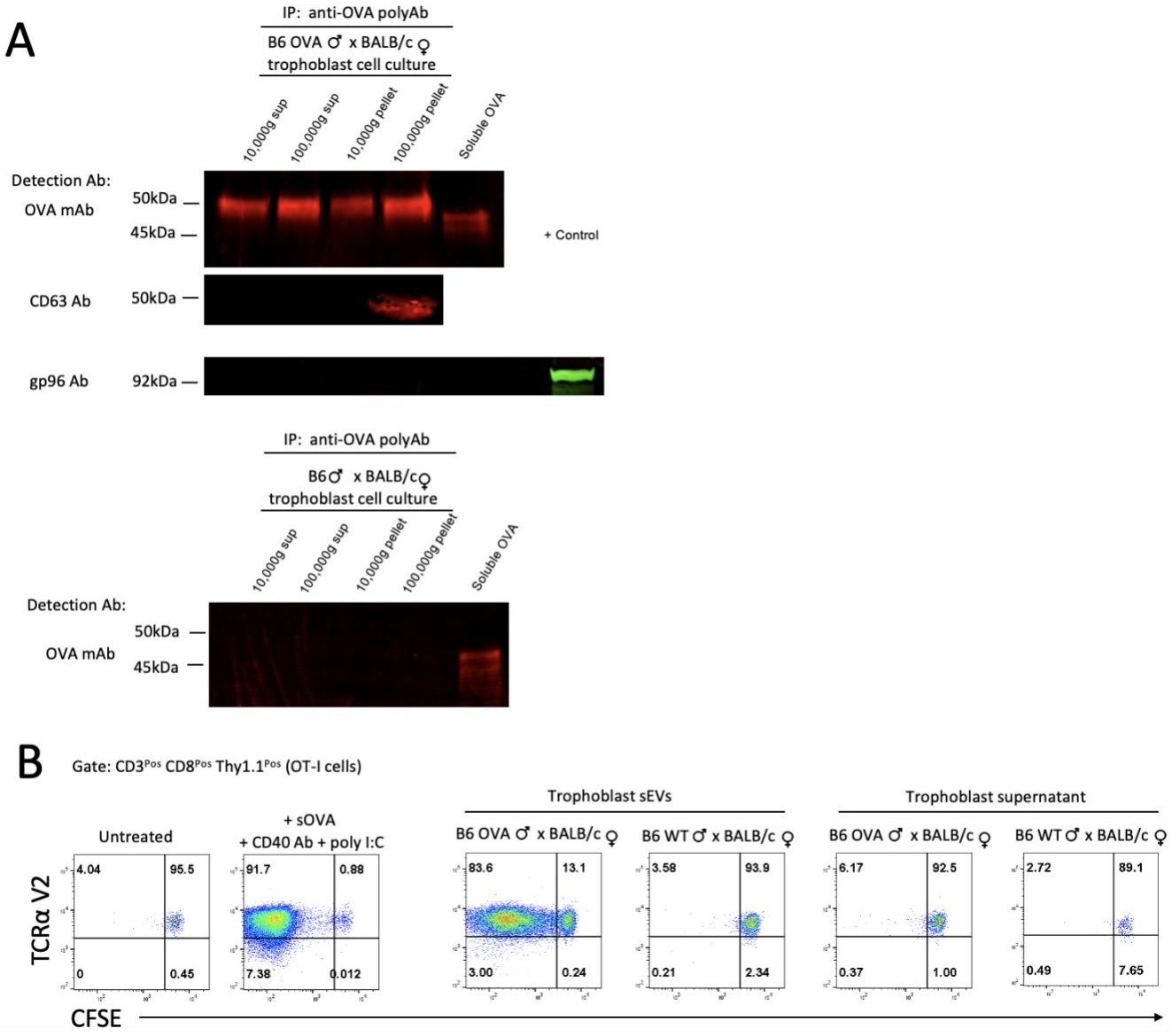

Figure 16: Mouse trophoblast EVs carry OVA paternal Ag.

A) Immunoprecipitation and western blot of EVs isolated from mouse primary trophoblast cultures for detection of OVA Ag, the sEV-associated marker CD63, and the ER-marker gp96. **B)** WT B6 female virgin mice (Thy1.2 congenic) were i.v. injected with CFSE-labeled Thy1.1 congenic OT-I CD8 T cells followed by footpad injection of sEVs or 100,000g cleared supernatants from primary cultures (48 hours) of trophoblast cells from BALB/c females impregnated with mOVA B6 males or control B6 males. As a positive control to elicit optimal OT-I T cell activation, a group of mice was injected i.p. with soluble OVA + agonistic CD40 Ab + Poly I:C, 24 hours after OT-I T cell transfer.

4.2.3 Presentation of parental antigen OVA carried by trophoblast extracellular vesicles promotes deficient activation and cell death of maternal CD4 T cells in SLTs

To assess the maternal CD4 T cell response to OVA Ag delivered to the mother's spleen by trophoblast-derived sEVs *in vivo*, we used an adoptive transfer model of Thy1.1 congenic, TCR transgenic, OT-II CD4 T cells specific for the $OVA_{323-339}$ peptide presented in IA^b MHC class-II molecules. These OT-II mice also encode monomeric red fluorescent protein (mRFP) downstream of the endogenous Foxp3 gene (FoxP3 is a marker of regulatory CD4 T cells or CD4 FoxP3 Tregs) under control of the endogenous Foxp3 promoter (B6 FIR-mRFP OT-II mice, Thy1.1 congenic) (Figure 17B).

Untouched CD4 T cells, purified by negative selection with magnetic beads from the spleen of Thy1.1 congenic B6 FIR OT-II mice, depleted of endogenous CD4 CD25 Tregs by negative selection with a CD25 mAb, were labeled with the green dye CFSE, and injected i.v. into WT B6 virgin females congenic for Thy1.2. The following two days, sEVs purified from primary cultures of OVA B6 male x WT BALB/c female trophoblast cells, or from control WT B6 male x WT BALB/c female trophoblast cultures, were injected i.v. (tail vein). As a positive control of

optimal CD4 T cell activation, B6 mice were injected i.p. with soluble OVA Ag + the Toll-like receptor 3 agonist poly I:C + agonistic CD40 Ab (Figure 17B).

Four days after the first sEV injection, splenocytes from the host B6 female mice were harvested and the following parameters were analyzed on the Thy1.1 congenic OT-II CD4 T cells: (i) T-cell proliferation based on CFSE dilution and absolute number of OT-II T cells in the spleen; (ii) T-cell activation based on down-regulation of CD62 ligand (L), and increase of CD69 (marker of early T cell activation) and CD44 (marker of late T cell activation) ; (iii) differentiation of CD4 FoxP3 Tregs based on de novo expression of FoxP3-mRFP, (iv) T-cell death based on uptake of fixable viability dye (FVD), and T-cell apoptosis based on generation of a fluorogenic substrate by caspase 3, (v) T-cell exhaustion based on expression of PD-1, Lag-3 and TIM3, and (vi) T-cell polarization based on the intracellular content of interferon (IFN)-γ, interleukin (IL)-4 and IL-10 (Figures 18 and 19).

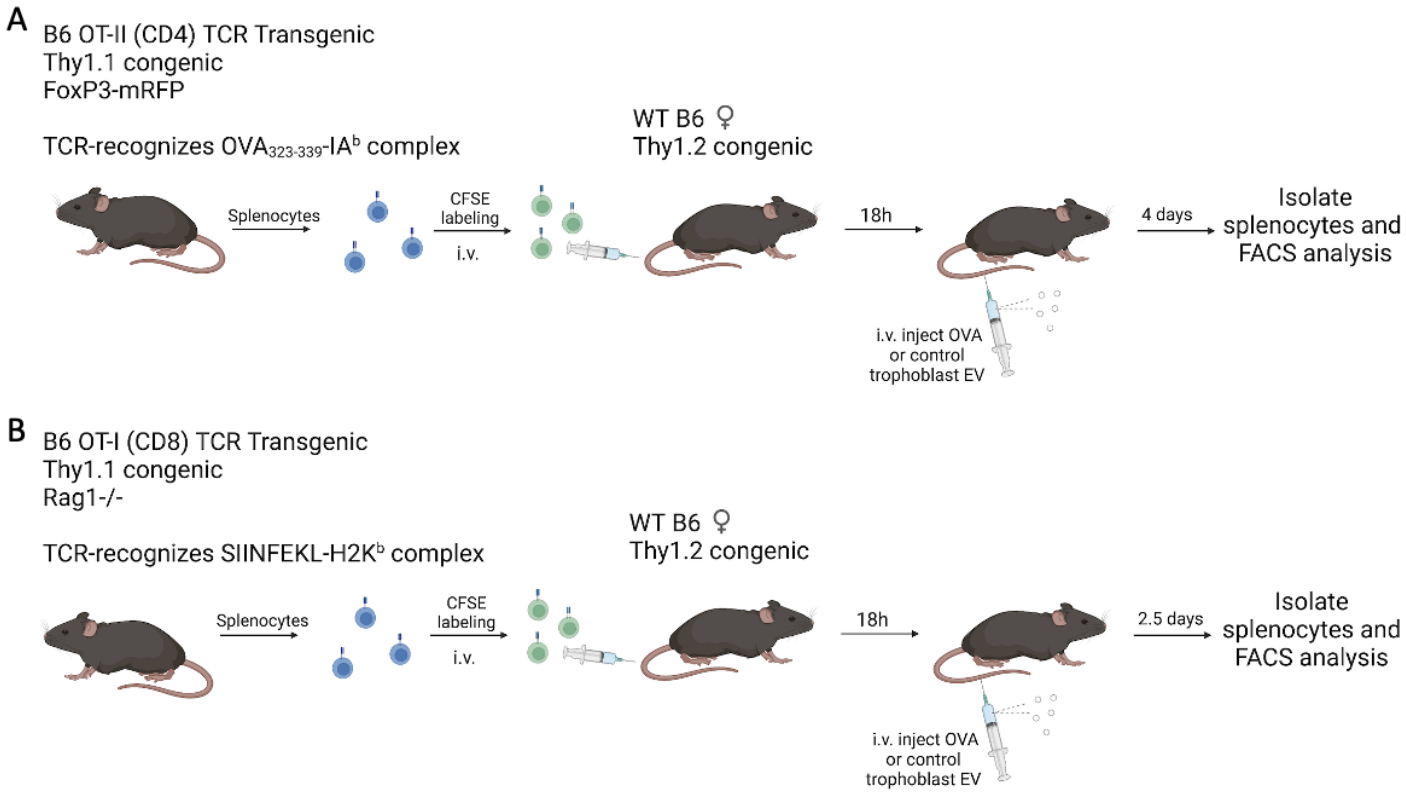

Figure 17. Experimental design of the experiments with OT-I and OT-II T cells.

A) OT-II TCR transgenic mouse. CD4 T cell receptor is programmed to only recognize OVA peptide, $_{OVA323-339}$-IAb complex. OT-II mice have red fluorescent protein-tagged FoxP3 for tracking formation of regulatory T cells. OT-II donor T cells have Thy1.1 T cell surface protein to distinguish from host T cells which have Thy1.2 T cell surface protein. OT-II CD4 T cells are harvested from mouse spleens, labeled with CFSE, and i.v. injected into host WT B6 female mice. Eighteen hours later, OVA or WT trophoblast sEVs are i.v. injected into host mice. Four days later, splenocytes are isolated for FACS. **B)** OT-I TCR transgenic mouse. CD8 T cell receptor is programmed to only recognize the OVA peptide, SIINFEKL-H2K^b complex. OT-I mice are Rag1$^{-/-}$, they do not develop mature T and B cells. OT-I donor T cells have Thy1.1 T cell surface protein to distinguish from host T cells which have Thy1.2 T cell surface protein. OT-I CD8 T cells are harvested from mouse spleens, labeled with CFSE, and i.v. injected into host WT B6 female mice. Eighteen hours later, OVA or WT trophoblast sEVs are i.v. injected into host mice. Two and a half days later, splenocytes are isolated for FACS. Made with BioRender.

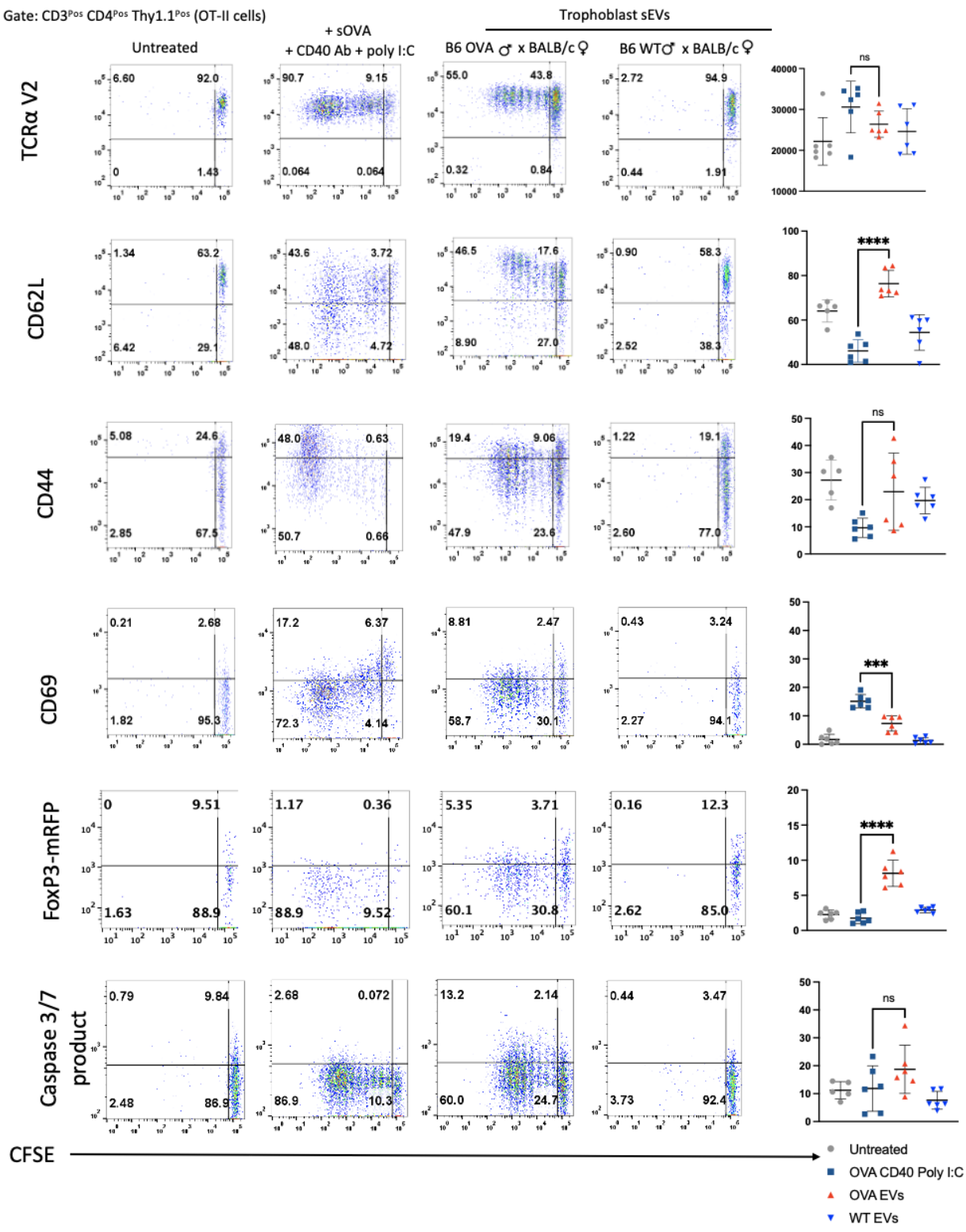

Figure 18: *In vivo* analysis of CD4 T cell activation in the spleen in response to trophoblast sEVs carrying the paternal Ag OVA.

Flow cytometry analysis of splenocytes of B6 female virgin mice (Thy1.2 congenic) that received i.v. CFSE-labelled Thy1.1-congenic FIR-mRFP OT-II CD4 T cells (CD25-depleted), and that were injected 24 hours later with sEVs purified from primary trophoblast culture supernatants from BALB/c females impregnated with mOVA B6 males or control WT B6 males. As a positive control, to elicit optimal OT-II T cell activation, a group of mice was injected i.p. with soluble OVA + agonistic CD40 Ab + poly I:C, 24 hours after the OT-II T cell transfer. On the dot diagrams, each dot represents a mouse. Flow cytometry analysis was done 4 days after sEV injection. For the analysis, OT-II CD4 T cells were gated based on their positivity for CD3, CD4 and Thy1.1. *** $P < 0.001$, **** $P < 0.0001$, ns: not significant.

We found that i.v. administration of trophoblast sEVs carrying OVA promote proliferation but induced deficient activation of the OT-II CD4 T cells, based on the lack of downregulation of CD62L and significantly reduced increase in the activation marker CD69, when compared to positive controls in which optimal OT-II T cell activation was induced by injection of soluble OVA + poly I:C + agonistic CD40 Ab (Figure 18). In accordance with the induction of OT-II CD4 T cells unfitted for survival, the percentage of apoptotic OT-II T cells increased in response to systemic administration of trophoblast EVs carrying OVA. No difference in surface expression of the TCRαV2 was detected between the experimental and control groups, indicating that down-regulation or internalization of the TCR is not a mechanism by which the conceptus-specific CD4 T cell response in down-regulated by the trophoblasts sEVs. Administration of the trophoblast sEVs carrying OVA associated to a small increment in the percentage of the OVA-specific CD4 FoxP3 Tregs compared to the positive control (Figure 18). Importantly, unlike the positive controls, intracellular IFN-γ was undetectable in OT-II CD4 T cells that proliferated in response to i.v. injected trophoblast sEVs carrying OVA (Figure 19). As negative controls, CFSE-labelled OT-II CD4 T cells did not proliferate in mice that did not receive trophoblast EVs or in animals

injected i.v. with sEVs purified from control WT B6 male x WT BALB/c female trophoblast cultures.

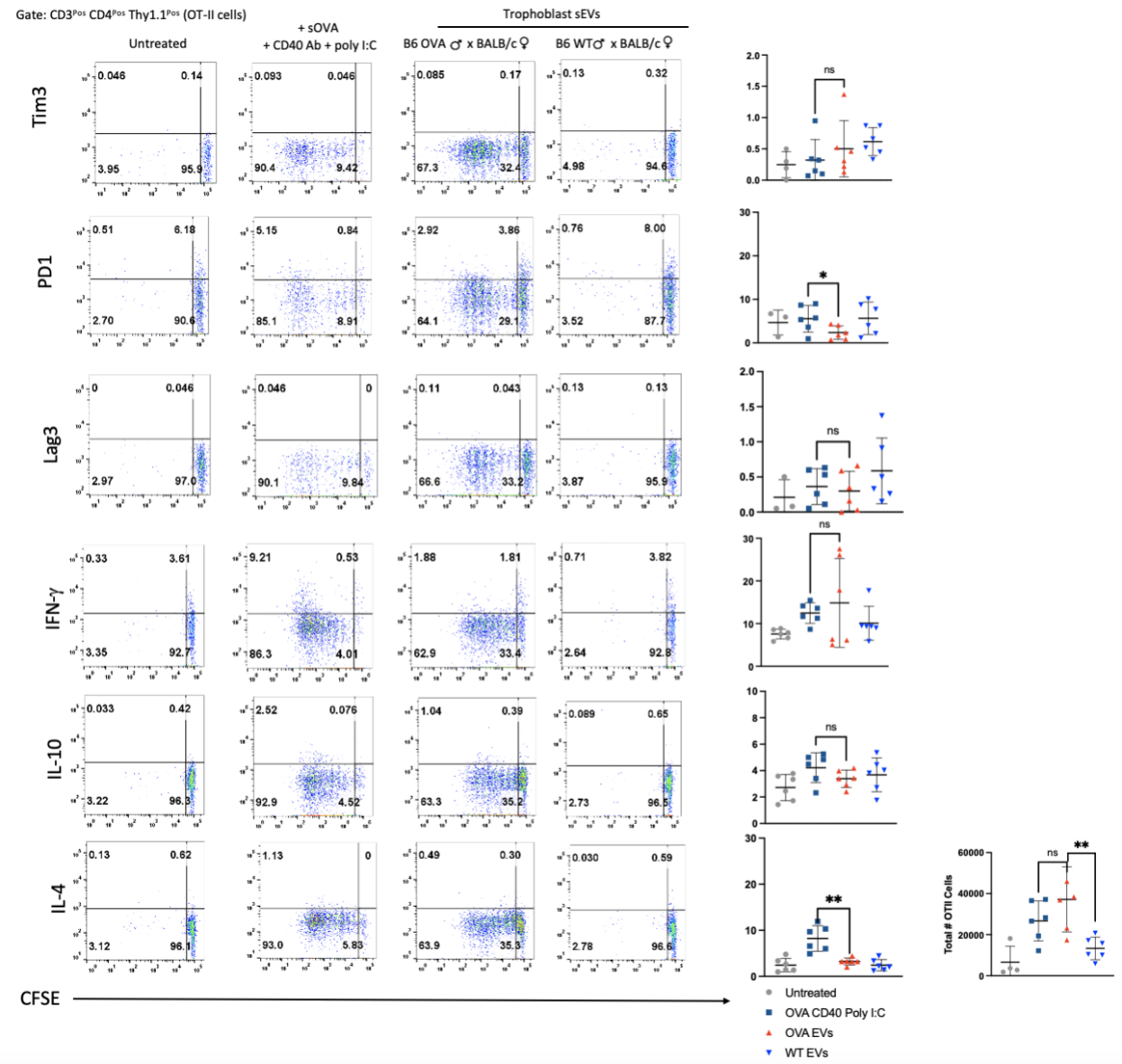

Figure 19: Analysis *in vivo* of CD4 T cell exhaustion and polarization in the spleen in response to trophoblast sEVs carrying the paternal antigen OVA.

Flow cytometry analysis of splenocytes of B6 female virgin mice (Thy1.2 congenic) that received i.v. CFSE-labelled Thy1.1-congenic OT-II FIR-mRFP CD4 T cells (CD25-depleted), and that were injected 24 hours later with sEVs purified from primary trophoblast culture supernatants from BALB/c females impregnated with mOVA B6 males or control WT B6 males. As a positive control to elicit optimal OT-II T cell activation, a group of mice were injected i.p.

with soluble OVA + agonistic CD40 Ab + poly I:C, 24 hours after the OT-II T cell transfer. Flow cytometry analysis was done 4 days after sEV injection. On the dot diagrams, each dot represents a mouse. For the analysis, OT-II CD4 T cells were gated based on their positivity for CD3, CD4 and Thy1.1. * $P < 0.05$, ** $P < 0.01$, ns: not significant.

4.2.4 Presentation of parental Ag OVA carried by trophoblast sEVs promotes deficient activation and cell death of maternal CD8 T cells in SLTs

Next, we investigated if OVA Ag carried by trophoblast EVs is recognized by maternal CD8 T cells in the mother's spleen in a pro-tolerogenic fashion. We used an *in vivo* adoptive transfer model of Thy1.1 congenic, TCR transgenic, OT-I CD8 T cells that specifically recognize the OVA-derived peptide SIINFEKL presented by the B6 MHC class-I molecule $H2K^b$. The OT-I mice are deficient in the Rag1 gene and therefore do not develop mature CD4 T or B cells (Figure 17A). Thus, purification of untouched OT-I CD8 T cells from the spleen by negative selection by magnetic bead sorting is not required.

Splenic OT-I CD8 T cells were labeled with the green dye CFSE, and injected i.v. in WT B6 virgin females, congenic for Thy1.2. The following day, sEVs purified from primary cultures of OVA B6 male x WT BALB/c female trophoblast cells, or from control WT B6 male x WT BALB/c female trophoblast cultures, were injected i.v. (tail vein) (Figure 17A). As a positive control of optimal CD8 T cell activation, B6 mice were injected i.p. with soluble OVA Ag + the Toll-like receptor 3 agonist poly I:C + agonistic CD40 Ab.

Two days after the sEV injection, splenocytes from the host B6 female mice were harvested and the following parameters were analyzed on the Thy1.1 congenic OT-I CD8 T cells : (i) T-cell proliferation based on CFSE dilution and absolute number of OT-I T cells in the spleen; (ii) T-cell

activation based on down-regulation of CD62 ligand (L), and increase of CD69 (marker of early activation) and CD44 (late activation marker); (iii) T-cell death based on uptake of fixable viability dye (FVD), and T-cell apoptosis based on generation of a fluorogenic substrate by caspase 3, (v) T-cell exhaustion based on expression of PD-1, Lag-3 and TIM3, and (vi) T-cell bias based on the intracellular content of interferon (IFN)-γ and intracellular granzyme B, a serine protease released by activated / effector CD8 T cells that triggers apoptotic-cell death on target cells (Figures 20-21).

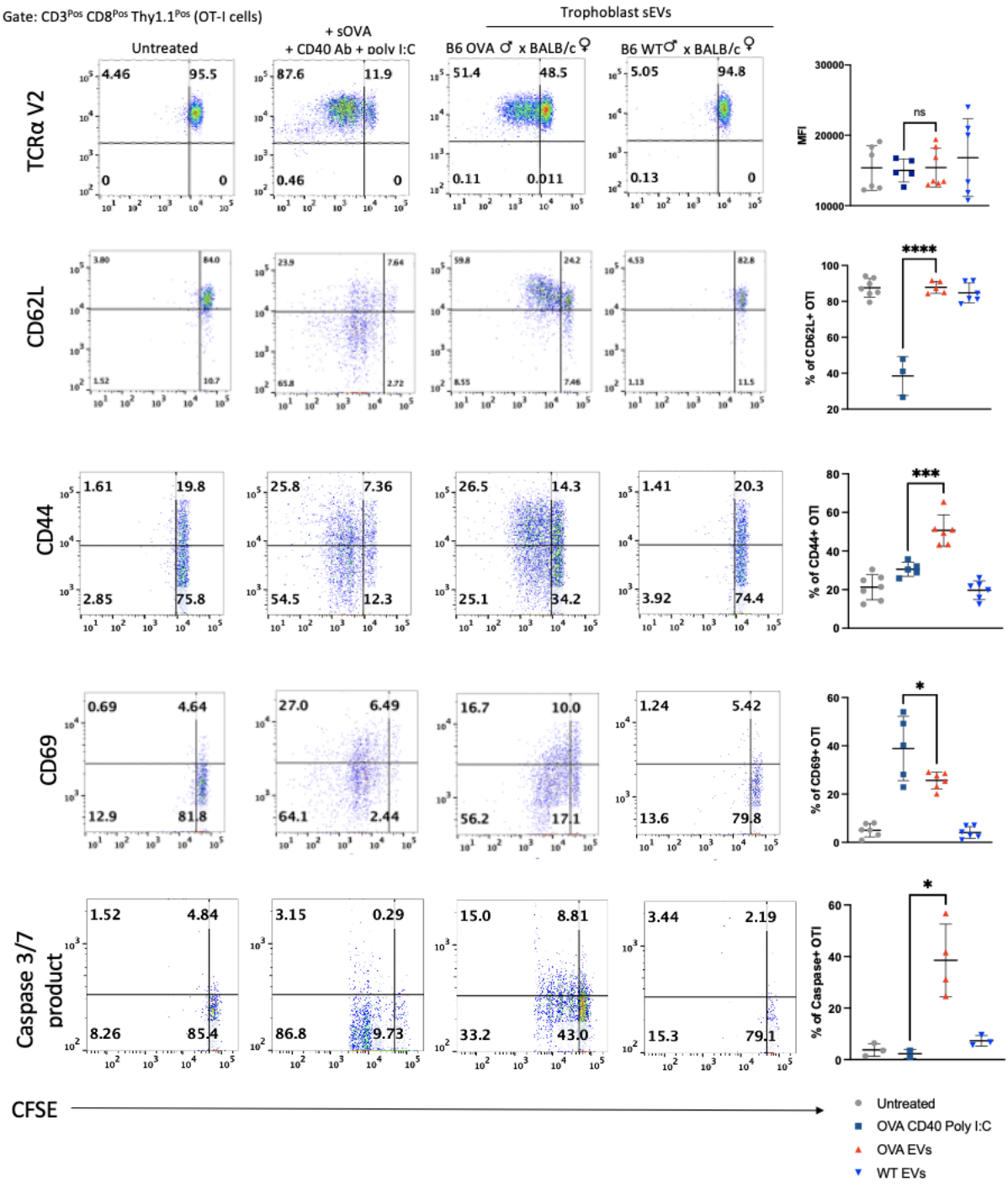

Figure 20: Analysis *in vivo* of CD8 T cell activation in the spleen in response to trophoblast sEVs carrying the paternal Ag OVA.

Flow cytometry analysis of splenocytes of B6 female virgin mice (Thy1.2 congenic) that received i.v. CFSE-labelled Thy1.1-congenic OT-I CD8 T cells, and that were injected 24 hours later with sEVs purified from primary trophoblast

culture supernatants from BALB/c females impregnated with mOVA B6 males or control WT B6 males. As a positive control to elicit optimal OT-I T cell activation, a group of mice were injected i.p. with soluble OVA + agonistic CD40 Ab + poly I:C, 24 hours after the OT-I T cell transfer. Flow cytometry analysis was done 2 days after sEV injection. On the dot diagrams, each dot represents a mouse. For the analysis, OT-I CD8 T cells were gated based on their positivity for CD3, CD8 and Thy1.1. * $P < 0.05$, *** $P < 0.001$, **** $P < 0.001$, ns: not significant.

Overall, we determined that i.v. administration of trophoblast sEVs carrying OVA promote proliferation but induced deficient activation of the OT-I CD8 T cells, based on the lack of downregulation of CD62L and reduced increase in the activation marker CD69, when compared to positive controls in which optimal OT-I T cell activation was induced by injection of soluble OVA + poly I:C + agonistic CD40 Ab. In keeping with the induction of OT-I CD8 T cells unfitted for survival, the percentage of apoptotic OT-I T cells increased in response to systemic administration of the trophoblast EVs carrying OVA (Figure 20). No difference on the surface expression of the TCRαV2 was detected between the experimental and control groups, indicating that down-regulation or internalization of the TCR is not a mechanism by which the conceptus-specific CD8 T cell response is down-regulated by the trophoblast sEVs. Notably, unlike the positive controls, the content of intracellular IFN-γ was undetectable in OT-I CD8 T cells that proliferated in response to i.v. injected trophoblast sEVs carrying OVA (Figure 21). Granzyme B was not detectable in OT-I CD8 T cells that were injected with OVA sEVs compared to positive control injected (Figure 21). As negative controls, CFSE-labelled OT-I CD8 T cells did not proliferate in mice that did not receive trophoblast EVs or in animals injected i.v. with sEVs purified from control WT B6 male x WT BALB/c female trophoblast cultures.

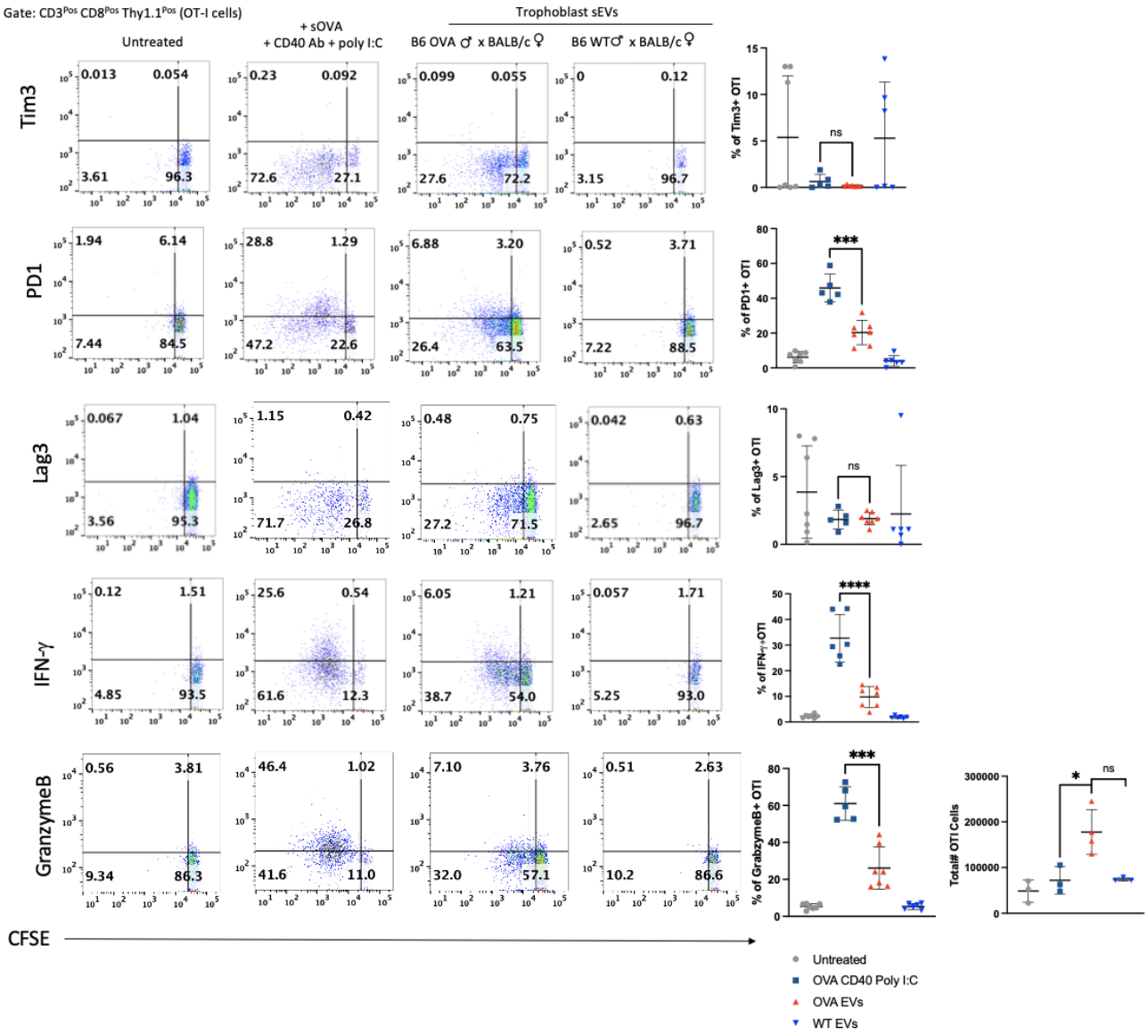

Figure 21: Analysis *in vivo* of CD8 T cell exhaustion and polarization in the spleen in response to trophoblast sEVs carrying the paternal Ag OVA.

Flow cytometry analysis of splenocytes of B6 female virgin mice (Thy1.2 congenic) that received i.v. CFSE-labelled Thy1.1-congenic OT-I CD8 T cells, and that were injected 24 hours later with sEVs purified from primary trophoblast culture supernatants from BALB/c females impregnated with mOVA B6 males or control WT B6 males. As a positive control to elicit optimal OT-I T cell activation, a group of mice was injected i.p. with soluble OVA + agonistic CD40 Ab + poly I:C, 24 hours after the OT-I T cell transfer. Flow cytometry analysis was done 2 days after sEV injection.

On the dot diagrams, each dot represents a mouse. For the analysis, OT-I CD8 T cells were gated based on their positivity for CD3, CD8 and Thy1.1. *** $P < 0.001$, **** $P < 0.0001$, ns: not significant.

4.3 Discussion

The Act-mOVA B6 male x WT BALB/c female mice pregnancy model provided an ideal system for isolation of fetoplacental-derived EVs carrying the model Ag OVA as a surrogate paternal Ag. It enabled us to track paternal Ags in the maternal tissues, confirming that they can be detected in those tissues and allowing us to confirm the EVs in fact carry the OVA Ag. The Act-mOVA model was a useful system in detection of surrogate paternal Ag both *in vivo* from maternal plasma and *ex vivo* from primary cultures of trophoblast cells, and for further analysis of the EVs *in vitro* and in immunological assays of T-cell activation *in vivo*.

We confirmed the presence of highly pure sEVs in our preparations based on their relatively high content of the sEVs-associated markers CD63 and CD81, and lack of the endoplasmic reticulum protein gp96. We noticed that the molecular weight of the OVA detected in the EV samples isolated from maternal plasma or primary cultures of trophoblasts was higher than that of soluble OVA used as control. By digesting the EVs with PNGase, an enzyme that removes N-linked glycans, we demonstrated that the molecular weight discrepancy was due to N-glycosylation of the EV samples.

These findings indicate that the trophoblast sEVs released into maternal circulation transport paternal Ag to maternal SLTs. By using OVA-specific TCR transgenic CD4 or CD8 T cells as surrogate maternal responding T cells, we demonstrated that the paternal Ag delivered through the sEVs are processed and presented to maternal T cells in the spleen. Importantly,

analysis of the maternal T cell response *in vivo* was Ag-specific since the OT-II CD4 T cells and the OT-I CD8 T cells are TCR transgenic T cells that specifically recognize the OVA-derived peptides $OVA_{323-339}$ and SIINFEKL presented in the context of $H2^b$ MHC class-II and class-I molecules, respectively.

We found that systemic administration of trophoblast-derived sEVs carrying the surrogate paternal Ag OVA triggers a CD4 and CD8 T cell response that closely recapitulates the maternal T cell response previously described in the spleen of pregnant mice [53]. Presentation of the OVA-derived peptides carried by the trophoblast sEVs was associated to cell proliferation and deficient activation of the OVA peptide specific OT-II CD4 and OT-I CD8 T cells, when compared to controls in which the T cells were optimally activated. They also underwent increased apoptotic cell death and a minor increase in the percentage of CD4 FoxP3 Tregs. In our setting, the percentage of proliferating T cells undergoing apoptosis following injection of trophoblast sEVs carrying OVA and detected by FACS *ex vivo* could have been underestimated, because *in vivo* apoptotic T cells are rapidly removed by splenic phagocytes. Importantly, after administration of trophoblast sEVs expressing OVA the content of the type-1 response cytokine IFN-γ and granzyme B decreased significantly in those proliferating CD8 T cells that survived. We did not detect differences in the expression of T-cell exhaustion markers PD1, Tim3 and Lag3, or surface levels of TCRs between the experimental and the positive control groups. Taken together, these changes are in line with the cell proliferation induced by deficient activation and consequent deletion, and deficient type-1 polarization reported by previous studies in conceptus-specific maternal T cells in the mother's spleen. There are important technical differences between previous studies in pregnant mice and our *in vivo* model that could have affected the outcome of the OVA-specific T cell response in our study. We administered the trophoblast-derived sEVs in bolus in a single dose

for the 2-day OT-I experiment, or in two consecutive daily doses for the 4-day OT-II studies, whereas during pregnancy the trophoblast sEVs are released continuously to the maternal blood once the placenta is developed. This could be addressed in future experiments by injecting mice with EVs periodically over the course of 15-17 days. Another important consideration is the potential role that hormones present during pregnancy may exert on the T cell response.

4.4 Materials and Methods

4.4.1 Mice

WT C57BI/6 (B6), Act-mOVA C57Bl/6, and C57BL/6-Tg(TcraTcrb)1100Mjb/Crl (OT-I) knockout for Rag1 mice were purchased from Charles River. Thy1.1 congenic C57Bl/6 FIR-mRFP OT-II mice were generated by Dr. Geoffrey Camirand at the Thomas E. Starzl Transplantation Institute and generously shared with us. Mice were bred and maintained in the pathogen-free animal facility of the University of Pittsburgh School of Medicine. Animal care and handling were performed in accordance with institutional guidelines and procedures approved by Institutional Animal Care and Use Committee (IACUC) protocol numbers 19106062 and 20098112.

4.4.2 Isolation of mouse trophoblast cells

Placentas were removed from pregnant mice between E12.5 and E17.5. Ten to twenty-five placentas were minced and digested with Medium-199 supplemented with sodium bicarbonate (0.01M), HEPES, Liberase^{TM} (0.25WU/mL), and DNase (0.2mg/mL), for 1 h at 37ºC. Cells were

passed through 100 µm strainer and centrifuged at 500*g* for 5 min. Supernatant was removed and pellet was resuspended in 5mL red blood cell lysis buffer (Sigma) for 10 min. Cells were washed with PBS and centrifuged (500*g*, 5 min). Pellet was resuspended in 10 mL cold PBS supplemented with 0.01M EDTA and centrifuged (500*g*, 5 min). Percoll gradient was used to separate trophoblast cells. Primary mouse trophoblast cells were cultured in NCTC-109 medium supplemented with 5% EV-free FBS, for 2 days, in 6-well plates covered with Matrigel.

4.4.3 Isolation of EVs from mouse plasma and trophoblast media, IP, and western blot

Mouse blood and placentas were collected at E17.5 from BALB/c female mice mated with OVA B6 or control WT B6 males. Placental trophoblast cells were isolated and cultured as described above, and culture supernatants were collected after 48 h. Blood was drawn via cardiac puncture with a 3 ml syringe with a 27G ½ needle, pre-treated with heparin. Blood was collected in BD Microtainer® tubes with K_2EDTA (Becton Dickinson).

Blood was centrifuged at 2,000*g* for 10 min at 4°C, and plasma was collected and diluted to 2 ml final volume with 5mM EDTA / PBS containing 1x Halt protease / phosphatase inhibitor cocktail (Thermo Fisher). Next, mouse plasma and the supernatants of primary trophoblast cell cultures were centrifuged at 10,000*g* (30 min, 4°C), and the 10,000*g* pellets containing the MVs were resuspended in 500 µl 5mM EDTA / PBS with 1x Halt protease / phosphatase inhibitor cocktail. Five hundred µl of the 10,000*g* supernatant was reserved for the immunoprecipitation, and the remaining supernatant was ultracentrifuged at 100,000*g* to pellet sEVs. The supernatant was collected and the 100,000*g* pellet containing the sEVs was resuspended in 500 µl 5mM EDTA / PBS with 1x Halt protease/phosphatase inhibitor cocktail. Immunoprecipitation of OVA was

conducted using 50ul of sheep anti-rabbit IgG Dynabeads (Invitrogen) coupled with 2 ug of anti-OVA polyclonal rabbit antibody (ab181688), per the Invitrogen instructions. Five hundred µl of plasma supernatant and EV pellet samples were incubated with 50 ul of the Ab-coupled beads (overnight, at 4°C, orbital rotation). The sample was then placed on a PureProteome™ magnetic stand (Millipore Sigma), the supernatant was removed, and 100 µl of 0.1M glycine (pH 2.5) was added to the beads to elute the OVA Ag from the beads. The amount of protein in the eluate was measured with a NanoDrop 2000c. For immunoblotting, 12 µg of each sample (resuspended in glycine) was diluted to 50 µl with PBS and 4x laemmli sample buffer (BioRad) supplemented with β-mercaptoethanol reducing agent. Samples were heated at 95°C for 10 min and loaded into 10% poly-acrylamide mini-PREOTEAN®TGX™ precast gels (BioRad). Gels were electroblotted on polyvinylidine difluoride membranes (BioRad). For detection of OVA, membranes were probed with a mouse anti-OVA monoclonal Ab (ab17293) diluted 1:500 in Intercept® Blocking Buffer / 0.1% Tween 20. Membranes were incubated with an IRDye 680-conjugated donkey anti-mouse Igg (Li-Cor) diluted 1:10,000 in Intercept® Blocking Buffer / 0.1% Tween 20. Membranes were imaged with a Licor Odyssey infrared imaging system.

4.4.4 Isolation of trophoblast sEVs

A ExoDiscovery™ Lab Spinner centrifuge fitted with ExoDiscovery™-D20 disc was used to isolate mouse trophoblast sEVs. Supernatants of the mouse trophoblast cell cultures were centrifuged at 2000*g* for 10 min at 4°C, to remove cells and debris. The cleared supernatants were then centrifuged at 10,000*g* for 30 min at 4°C to pellet the MVs, and then filtered through 0.22µm filters (Millipore). The filtered supernatants were then run though the ExoDiscovery™-D20 disc according to the manufacturer's protocol. Final elution volume of the trophoblast sEVs was 600µl

in PBS. The amount of protein in the sEV preparations was assessed with a NanoDrop 2000c. The average size of the sEVs was measured with a LM10 NanoSight's instrument equipped with a high-sensitivity electron-multiplying charge-coupled device camera and the NTA 2.0 software (NanoSight), as previously described [46]. Samples were measured by NTA at room temperature, at concentrations ranging from 1.09×10^8 to 10.68×10^8 particles/ml after 1:100 to 1:1000 dilutions in batches of PBS BioPerformance certified for molecular biology (MilliporeSigma) that were previously validated in our LM10 NanoSight's instrument to be particle-free. Samples were run at 12.5 frames/s, with five repeats of 60 s each, within a range of 20 to 60 particles per frame, with more than 350 completed tracks per video, camera shutter speed at 65 ms, pump speed set at 50, and blur and minimum track length set at automatic. NTA parameters were kept identical throughout the whole capture and analysis when comparing different samples. Results were analyzed with the NTA 2.3 software with default settings.

4.4.5 Adoptive transfer of OT cells

OT-II CD4 T cells were isolated from spleens of B6 FIR-mRFP OT-II mice. Negative selection for OT-II cells was done using the Dynabeads™ Untouched™ mouse CD4 cell kit (Invitrogen). B6 FIR-mRFP OT-II cells were depleted of endogenous CD4 FoxP3 CD25 Treg cells by addition of a CD25 monoclonal Ab (PC61.5) to the cocktail for depleting Ab of the Dynabeads™ Untouched™ mouse CD4 cell kit. Purified OT-II T cells and splenocytes from $Rag1^{KO}$ OT-I mice were labeled with 0.1 µg/µl CellTrace™ CFSE cell proliferation dye (Invitrogen), for 30min at 37ºC. CFSE-labeled OT cells were injected i.v. into naïve virgin B6 female mice (3-5 x 10^6 cells / mouse). sEVs (100µg in 200 µl of PBS, per dose, per mouse) purified from the OVA^{Pos} or control (OVA^{Neg}) trophoblast cell culture supernatants were injected in the tail

vein of the host B6 females. For the 4-day OT-II experiments, the sEVs were administered twice, on days 1 and 2 after OT-II T cell administration. For the 2-day OT-I experiments (OT-I CD8 T cells respond more rapidly *in vivo* than OT-II CD4 T cells), the sEVs were injected in a single dose, the day after OT-I T cell transfer. As a positive control of OT-I and OT-II T cell activation, mice were injected i.p. with a single dose of soluble OVA (100 µg) + poly I:C (50 µg) and agonistic CD40 Ab (clone FGK45.5, 100 µg). Splenocytes were harvested for flow cytometry analysis of OT-I and OT-II T cells, 2 and 4 days respectively, after administration of the sEVs.

4.4.6 Analysis by flow cytometry

Following adoptive transfer of TCR transgenic OTI and OTII T cells and subsequent OVA trophoblast sEV injected, WT trophoblast sEV injected, no EV control, or positive control soluble OVA + poly I:C + agonistic CD40 Ab injected, spleens were harvested two (OT-I) or four (OT-II) days post EV injection. Spleens were flushed using a 27g syringe with PBS and teased apart using fine forceps, then muddled through a 70 µM cell strainer. RBCs were lysed using RBC lysis buffer at RT for 3 min. Cells were labeled with anti-CD16/CD32 Ab (to block FcR), and then labeled with the following Ab combinations for 30 min at 4°C: (i) BUV395-CD3, BV605-CD8, APC-Thy1.1, PerCP-Cy5.5-CD69, PE-Cy7-CD62L, BUV737-CD44, BV421-TCRV2, eF780-FVD (ii) BUV395-CD3, BV605-CD4, APC-Thy1.1, PerCP-Cy5.5-CD69, PE-Cy7-CD62L, BUV737-CD44, BV421-TCRV2, eF780-FVD (iii) BUV395-CD3, BV605-CD8, APC-Thy1.1, PerCP-Cy5.5-CD366, PE-Cy7-CD279, BUV737-CD223, BV421-Caspase3 (iv) BUV395-CD3, BV605-CD4, APC-Thy1.1, PerCP-Cy5.5-CD366, PE-Cy7-CD279, BUV737-CD223, BV421-Caspase3. All combinations were fixed in paraformaldehyde. For intracellular cytokine staining, $2x10^7$ cells per spleen were plated in each well of a 6 well plate. Cells were incubated 18h with

cell stimulation cocktail (eBioscience). Cells were harvested and surface labeling was done first using combinations: (i) BUV395-CD3, BV605-CD8, APC-Thy1.1 or (ii) BUV395-CD3, BV605-CD4, APC-Thy1.1 for 30 min at 4°C. Cells were then fixed for 20 min at RT with 4%PFA. Then intracellular labeling was done by resuspending cells in permeabilization buffer and labeling with combinations (i) PerCP-Cy5.5-IFN-γ, Pacific blue-GranzymeB or (ii) PerCP-Cy5.5-IFN-γ, PE-Cy7-IL-10, BV421-IL-4 for 30 min at 4°C. Cells were washed with permeabilization buffer, centrifuged, and resuspended in staining buffer prior to analysis. All samples were analyzed using BD® LSR II flow cytometer and analyzed using FlowJo v10 software.

5.0 Interaction of human placental small extracellular vesicles with human antigen-presenting cells in secondary lymphoid tissues *in vivo.*

5.1 Introduction

Thus far, our work demonstrated in mouse models that trophoblast-derived EVs released to the maternal peripheral blood are captured by Ag-presenting cells in the mother's spleen, and that the paternal surrogate Ag OVA carried by the trophoblast sEVs is processed and presented to OVA-specific CD4 T and CD8 T cells in a suboptimal manner, meaning the T cells were deficiently activated ($CD62L^{High}$ $CD69^{Low}$) and therefore undergo apoptotic cell death after a few cycles of cell divisions and with lower content of the Th1 / Tc1 cytokine IFN-γ, as opposed to optimal T cell activation which generates proliferating T cell fit for survival and elicits a robust immune response. Because the structure of the mouse and human placentas differ, next, we analyzed if some of those findings could be recapitulated in a translational model using humanized mice.

CD34+ humanized mouse models, or huMice, are a useful *in vivo* model commonly used to study human immune system responses to drugs, molecules, or compounds. HuMice are generated by an adoptive transfer of human CD34+ stem cells isolated from cord blood. Utilization of this model allowed us to inject sEVs isolated from primary human trophoblast cells (PHT) into huMice to assess localization and interaction with human leukocytes. This system is particularly beneficial to us because of inability to study EV trafficking in humans. It allowed us to analyze PHT sEVs in mice while avoiding a xenograft.

5.2 Results

5.2.1 Generation of humanized mice (huMice)

To evaluate if the interaction between trophoblast-derived sEVs and Ag-presenting cells in the mother's SLTs as we described in mouse models, also takes place between human trophoblast EVs and human Ag-presenting cells *in vivo* in the spleen, we used a translational model, humanized mice (huMice). To generate huMice, $CD34^{Pos}$ human hematopoietic stem cells (HSCs) were purified from cord blood and injected i.v. (10^5 $CD34^{Pos}$ cells per mouse) in 3-week-old NSG (NOD Scid Gamma)-SGM3™ mice, γ-irradiated (100 rads) prior to injection to kill any remaining endogenous lymphocytes. The NOD background of the NSG- SGM3™ mice promotes human hematopoietic stem cell engraftment due to (i) absence of hemolytic complement, (ii) decreased cDC function, (iii) defective macrophage function, and (iv) expression of the Sirpα allele that recognizes its ligand human CD47 as self. Since the NSG-SGM3™ mice are also Scid, they lack endogenous (mouse) T, B and NK cells, which prevents rejection of the human chimeric leukocytes by the mouse innate and adaptive immune systems. Expression of transgenic human Stem Cell Factor, human granulocyte-macrophage colony-stimulating factor (GM-CSF), and human interleukin (IL)-3 (SGM3) by the NSG-SGM3™ mice improves human hematopoietic stem cell engraftment and human myeloid cell development.

Between 12 and 15 weeks after hematopoietic stem cell injection, when human leukocyte chimerism is expected to be fully developed, the huMice used in the experiments had a minimum of 70 % of human chimeric leukocytes. Flow cytometry analysis of huMice spleens at the time of the experiments contained the following populations of human leukocytes: B cells, CD4 T and

CD8 T cells (mostly CD45RA^{Pos} naïve T cells), cells of myeloid lineage (CD33^{Pos}), monocytes (CD14^{Pos}) and NK cells (CD56^{Pos}) (Figure 22A-B).

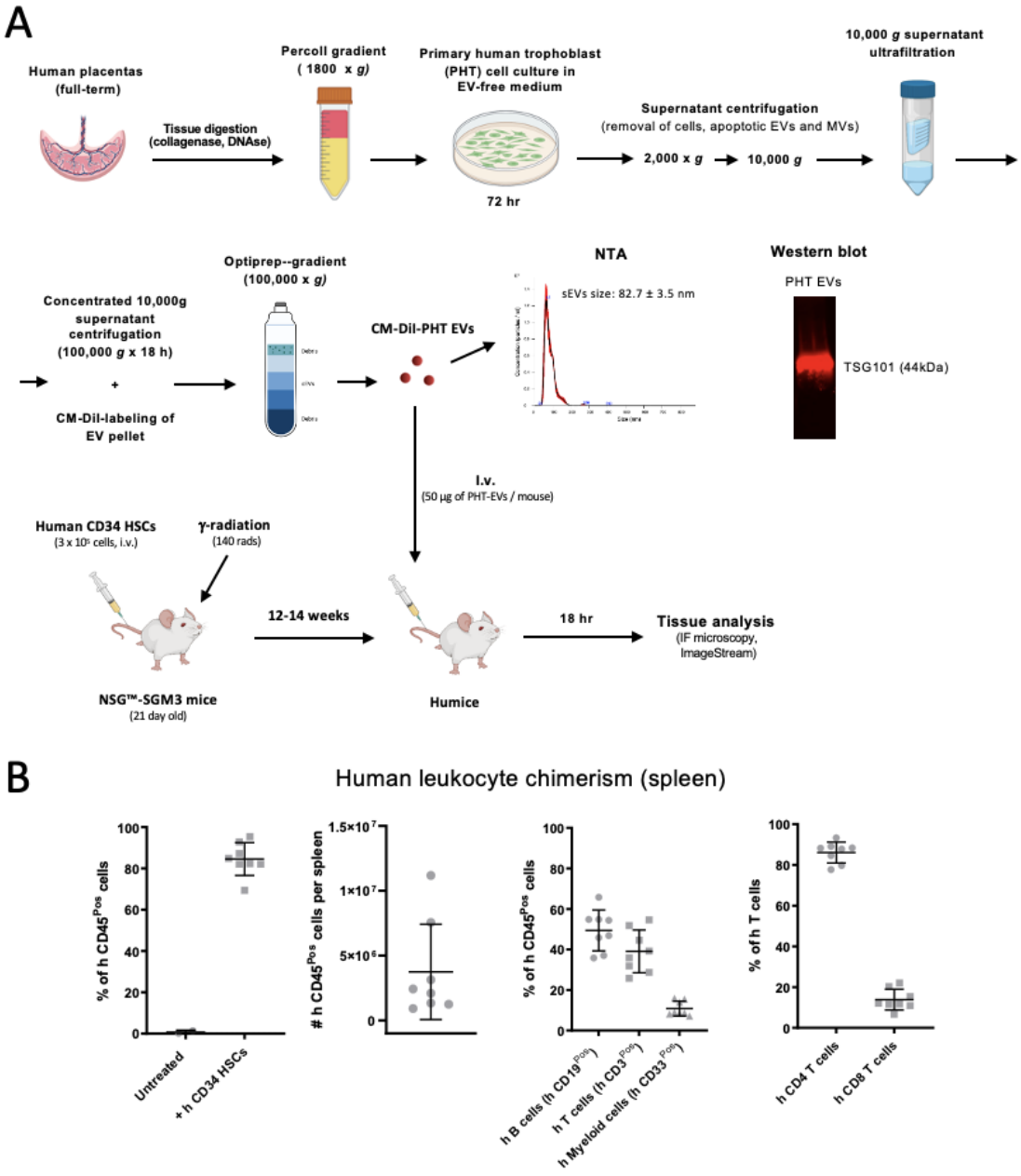

Figure 22: Purification of sEVs from human primary trophoblast cultures and generation of huMice.

A) Diagram with the methodology used to isolate sEVs from cultures of primary human trophoblasts and for generation of huMice, and the experimental design. **B)** Flow cytometry analysis for the assessment of percentage of

human leukocyte chimerism in huMice spleens, 12-15 weeks after transfer of $CD34^{Pos}$ human hematopoietic stem cells. Each dot represents a huMouse.

5.2.2 Human trophoblast extracellular vesicles target human immune cells in the spleen *in vivo*

To test if blood-borne human trophoblast (PHT)-derived sEVs are captured by human leukocytes in huMice tissues, sEVs purified from culture supernatants of PHT cells were labelled red with the lipophilic dye CM-Dil and injected i.v. in huMice (Figure 17A). Untreated huMice were used as controls. Eighteen hours after sEV injection, analysis by microscopy on tissue sections revealed the presence of CM-DiI^{Pos} content in human marginal zone metallophilic $CD169^{Pos}$ macrophages and red pulp $CD163^{Pos}$ macrophages of the huMice spleens (Figure 22A). CM-Dil^{Pos} content was also detected in human $CD163^{Pos}$ macrophages in the huMice bone marrow and liver (Supplemental Figure 3A) and was absent in human chimeric leukocytes in thymus and lung. Importantly, the antibodies against human CD169 and CD163 used did not cross-react with their mouse orthologues, which validates that the human PHT-derived EVs were indeed captured by human leukocytes and not by residual macrophages of mouse origin (Supplemental Figure 3B). ImageStream analysis of single cell suspensions of spleens of huMice injected systemically 18 hours prior with PHT-derived sEVs labelled with CM-DiI showed the presence of CM-DiI on dotted areas on human B cells, human conventional (c) DC1 (HLA-DR^{Pos} $CD141^{Pos}$ $CD1d^{Neg}$) and human cDC2 (HLA-DR^{Pos} $CD141^{Neg}$ $CD1c^{Pos}$) and was undetectable on human $CD3^{Pos}$ T cells (Figure 23C-E). HuMice do not generate fully developed peripheral lymph nodes under steady state conditions and lack human FDCs in the spleen [110]. Thus, the human trophoblasts release

sEVs that through peripheral blood reach human Ag-presenting cells and macrophage subsets in the spleen, and human macrophages in liver and bone marrow.

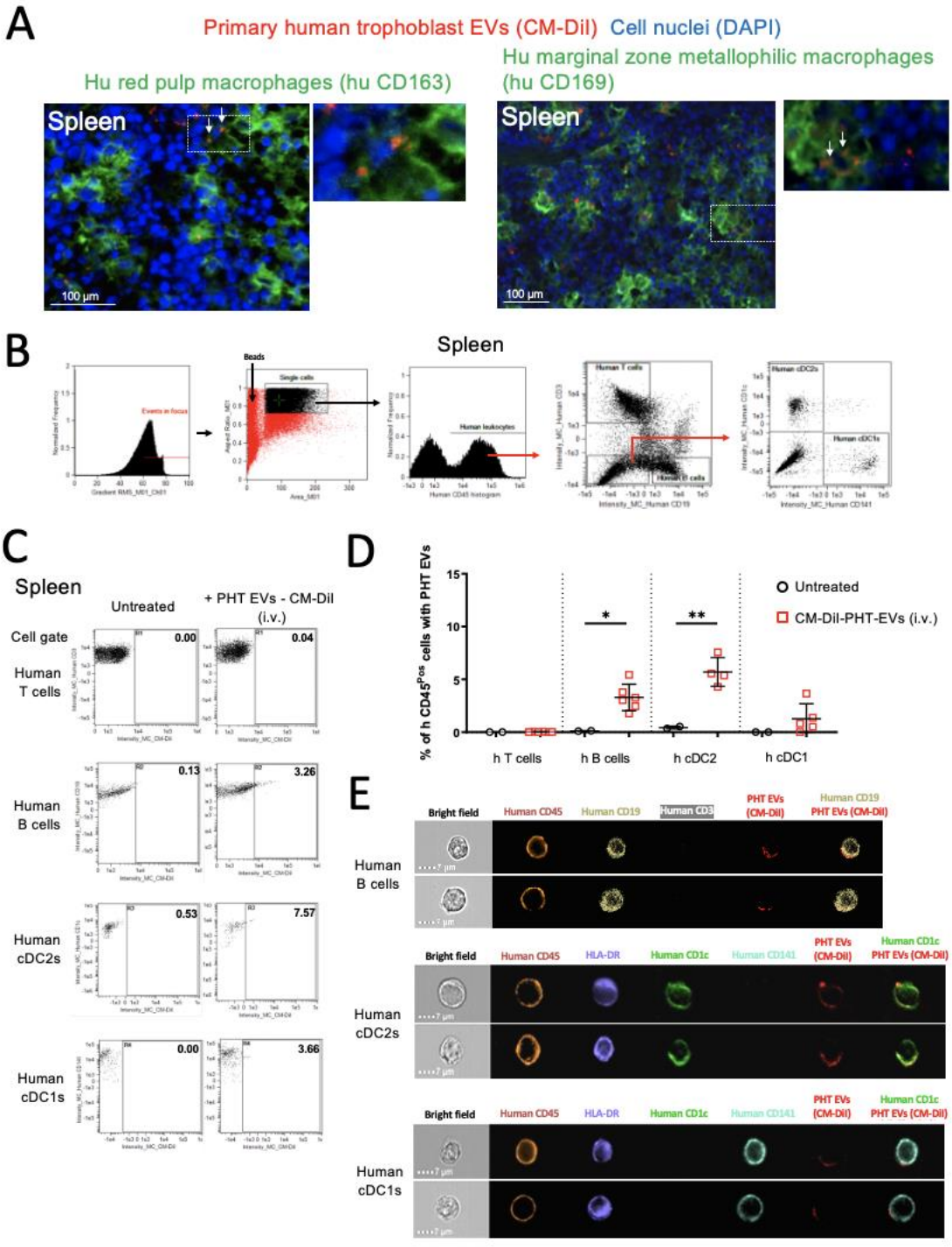

Figure 23: Human trophoblast sEVs target different subsets of human leukocytes in spleen *in vivo*.

A) Analysis by immunofluorescence microscopy on tissue sections of human $CD163^{Pos}$ and human $CD169^{Pos}$ macrophages (green) in huMice spleens, both with CM-DiI^{Pos} content (red, indicated by arrows), analyzed 24 hours after i.v. injection of CM-DiI-labeled PHT sEVs. Cell nuclei were counterstained with DAPI (blue). Images are representative of 6 huMice. **B)** Strategy used during the Amnis Imagestream analysis to gate different populations of human leukocytes in huMice splenocytes. **C)** Representative Imagestream dot plots indicating percentages of human T and B cells, human cDC1s and human cDC2s with CM-DiI^{Pos} content. **D)** Quantification by Imagestream analysis of percentages of human T and B cells, human cDC1s and human cDC2s with CM-DiI^{Pos} content. Each dot represents a huMice. (E) Imagestream pictures of individual human B cells, human cDC1s and cDC2a with small areas of CM-DiI^{Pos} material, the latter compatible with clusters of sEVs attached or internalized by the acceptor cells. Imagestream analysis was done 24 hours after i.v. injection of the CM-DiI-labelled PHT sEVs. * $P < 0.05$, ** $P < 0.01$, ns: not significant.

5.3 Discussion

To validate our findings from experimental mouse models in a translational model, we systemically administered sEVs purified from culture supernatants of PHT cells in huMice with established chimerism for multiple lineages of human leukocytes. To track the vesicles *in vivo*, the PHT sEVs were labelled with the red dye CM-DiI, and the analysis was done on tissue cryosections fixed in paraformaldehyde to preserve the signal of the lipophilic fluoroprobe used to label the sEVs. Interestingly, the PHT sEVs were detected in human cDCs and B lymphocytes, both Ag-presenting cells that have been proved to present conceptus-derived Ags to T cells in mouse pregnancy models [20]. We expected that the number of sEVs captured by the human leukocytes *in vivo*, in particular by those that are non-professional phagocytes, be relatively low since in our model the trophoblast sEVs were injected in one bolus, instead of being released continuously and in higher quantities by the human placenta. ImageStream is an image flow cytometry technology

that is particularly suitable for detection of small foci of fluroroprobe^{Pos} material within or on the surface of acceptor cells. Unlike traditional flow cytometry that measures the total amount of fluorescence per cell, ImageStream images each cell on which the tiny foci containing the attached or internalized CM-DiI-labelled sEVs can be clearly detected.

Interestingly, the PHT sEVs were detected in human metallophilic (CD169^{Pos}) macrophages located in the splenic marginal zone. Previous studies in mice have shown that blood born EVs are rapidly internalized by CD169^{Pos} macrophages in the splenic marginal zone [111]. In huMice, a recent study demonstrated that sEVs released by human skin grafts are captured and concentrated by human CD169 macrophages in subcapsular sinus of the graft-draining lymph nodes, which is an analogue structure to the splenic marginal zone [107]. As shown in mice and huMice models, our results suggest that the sEVs released by the trophoblast to peripheral blood are rapidly trapped by the CD169^{Pos} macrophages of the splenic marginal zone. Unlike the highly phagocytic CD163^{Pos} macrophages of the splenic red pulp, the contents internalized by CD169^{Pos} macrophages are transported by transcytosis, without being degraded, to the opposite site of the cells where the follicular B cells and T cells are located. Whether those human splenic CD169^{Pos} macrophages that capture trophoblast sEVs from blood present conceptus Ags carried on the EVs to B cells or transfer the sEVs to Ag-presenting cells for Ag-processing and presentation to maternal T cells, and if this process leads to suppression of the T cell response against the fetoplacental unit in humans (and differences in Ag presentation in mouse vs human), remains unknown.

5.4 Materials and Methods

5.4.1 Mice

NSG-SGM3 mice were purchased from the Jackson Laboratory. Mice were bred and maintained in the pathogen-free animal facility of the University of Pittsburgh School of Medicine. Animal care and handling were performed in accordance with institutional guidelines and procedures approved by Institutional Animal Care and Use Committee (IACUC) protocol numbers 19106062 and 20098112.

5.4.2 Generation of huMice

CD34 hematopoietic stem cells (HSCs) were isolated from cord blood from the placenta of healthy pregnant women according to the guidelines of the Institutional Review Board (IRB) of the University of Pittsburgh. Heparinized cord blood was diluted (1:1) with phosphate-buffered saline (PBS), and peripheral blood mononuclear cells (PBMCs) were purified with two consecutive discontinuous Ficoll-Paque (1.077 g/ml) density gradients (900g for 30 min at 18° to 20°C). Human HSCs were purified from PBMCs by magnetic sorting with CD34 Ab microbeads (Miltenyi Biotec) and cryopreserved in liquid nitrogen until use. CD34 HSC purity by flow cytometry analysis was ≥ 90% with less than 1% of CD3 T cells. To reconstitute NSG-SGM3 mice, CD34 HSCs were thawed, washed in PBS, and cultured in RPMI 1640 supplemented with 10% fetal bovine serum (FBS) for 1 hour at 37°C. A minimum of 3 x 10^5 HSCs in 300 µl of PBS were i.v. injected in 3 wk-old NSG-SGM3 mice, γ-irradiated (140 cGy) 2 hours prior. huMice were treated with Neomycin and Polymyxin B in the drinking water during the first week after

irradiation. Percentages of human leukocyte chimerism were determined by flow cytometry analysis in peripheral blood 12-15 weeks after HSC injection, and in the spleen at the end of the experiments (14 to 16 weeks). huMice were left untreated or injected i.v. with CM-DiI-labeled human PHT-derived sEVs (50 µg / huMice). Eighteen hours later, mice were euthanized for analysis of traffic of the injected EVs in spleen, bone marrow, liver, thymus and lung. Studies on huMice were approved by the IACUC (protocol no. 20067566) and the IRB (no. PRO13120232) of the University of Pittsburgh.

5.4.3 Placentas and dispersed primary human trophoblasts

All placentas used in our studies were obtained from uncomplicated pregnancies and term deliveries at Magee-Women's Hospital in Pittsburgh, under a protocol that was approved by the Institutional Review Board at the University of Pittsburgh. PHT cells were isolated using the trypsin-DNase-dispase/Percollx method as described by Kliman et al. [112], with modifications as we previously published [113, 114].

5.4.4 Generation and purification of EVs from primary human trophoblasts

EVs were purified from culture supernatants of PHT cells cultured in DMEM containing 10% EV-free bovine growth serum, and penicillin / streptomycin at 37◦ C in a 5% CO2 air atmosphere. Supernatants were centrifuged at 200g (10 min, 4°C), 1800g (20 min, 4°C) followed by passage through a 0.22µm filter and then centrifuged 10,000g (30 min, 4°C). The 10,000g supernatants were concentrated by ultrafiltration on sterile Vivacell 100 (Sartorius) filters (2800g, 35 min, 4°C). The filtered supernatants were adjusted to a volume of 11 ml with PBS and

centrifuged at 110,000g for 22h at 4°C. The 110,000g pellets with the EVs were incubated with CM-DiI–PBS (0.1 μg/μl, 300 μl final volume), at 37°C for 5 min, and then on ice for 20 min. The CM-DiI–labeled EVs were purified from the free dye using iodixanol (OptiPrep) gradients, as previously described [75], with minor modifications. Briefly, 300 μl of CM-DiI– labeled EVs were mixed with 6 ml of 30% (w/v) OptiPrep solution in sucrose buffer [0.25 M sucrose, 10 mM tris (pH 8.0), and 1 mM EDTA, pH 7.4], allowed 30-min mixing on a rocker to equilibrate the solution, and then transferred into Ultra-Clear (Beckman Coulter) sterile 11-ml tubes. Next, 3 ml of 20% (w/v) OptiPrep solution in sucrose buffer, followed by 2.5 ml of 10% (w/v) OptiPrep solution in sucrose buffer, was successively layered on top on the 30% OptiPrep solution containing the EVs. The tubes with the OptiPrep gradients were centrifuged at 110,000g (16 hours, 4°C). The fractions containing the EVs were harvested, washed in PBS, and centrifuged at 110,000g for 90 min, and the EV pellets were collected in 300 μl of PBS. The amount of protein in the EV preparations was assessed with a NanoDrop 2000c. The average size of the EVs was measured with a LM10 NanoSight's instrument equipped with a high-sensitivity electron-multiplying charge-coupled device camera and the NTA 2.0 software (NanoSight), as previously described [76]. Samples were measured by NTA at room temperature, at concentrations ranging from 1.09 × 108 to 10.68 × 108 particles/ml after 1:100 to 1:1000 dilutions in batches of PBS BioPerformance certified for molecular biology (Millipore Sigma) that were previously validated in our LM10 NanoSight's instrument to be particle-free. Samples were run at 12.5 frames/s, with five repeats of 60 s each, within a range of 20 to 60 particles per frame, with more than 350 completed tracks per video, camera shutter speed at 65 ms, pump speed set at 50, and blur and minimum track length set at automatic. NTA parameters were kept identical throughout the whole capture and analysis when

comparing different samples. Results were analyzed with the NTA 2.3 software with default settings.

5.4.5 Amnis ImageStream analysis

Single cell suspensions of splenocytes from huMice i.v. injected with CM-DiI-labeled human PHT-derived sEVs, were Fc receptor (FcR)– blocked with anti-human and anti-mouse CD16/CD32 Abs, and incubated (30 min at 4°C) with the following Ab: FITC-human CD1c, PerCP-human CD19, Pacific Blue-HLA-DR, BV605-human CD45, APC-human CD141, and APC-Cy7-human CD3. Fluorochrome-conjugated Ab were used between 1:100 and 1:200 final concentration, diluted in PBS/1% FBS/0.1% sodium azide solution (pH 7.4 to 7.6). Cells were fixed in 4% paraformaldehyde-PBS immediately after labeling. Cells (2×10^5 per group) were analyzed with a two-laser Amnis ImageStream analyzer at a magnification of ×60. Cell images were analyzed with the software IDEAS v6.2. Events in focus were gated by plotting the gradient root mean square (RMS) feature of the bright field of camera 1 (channel 1) against the gradient RMS feature of the bright field of camera 2 (channel 9). From the events in focus, single cells were identified as events with low area and high aspect ratio intensity (bright field of camera 1, channel 1). Single cells were selected for further analysis based on the following phenotypes: $CD45^{Pos}$ $CD3^{Pos}$ $CD19^{Neg}$ (human T cells), $CD45^{Pos}$ $CD3^{Neg}$ $CD19^{Pos}$ (human B cells), $CD45^{Pos}$ $CD3^{Neg}$ $CD19^{Neg}$ HLA-DR^{Pos} $CD141^{Pos}$ $CD1d^{Neg}$ (human cDC1) and $CD45^{Pos}$ $CD3^{Neg}$ $CD19^{Neg}$ HLA-DR^{Pos} $CD141^{Neg}$ $CD1c^{Pos}$ (human cDC2).

5.4.6 Flow Cytometry

For flow cytometry assessment of human leukocyte chimerism in huMice, peripheral blood was collected in BD Microtainer tubes with K_2EDTA (Becton Dickinson) and erythrocytes were lysed with Red Blood Cell Lysing Buffer Hybri-Max™ (Sigma) (15 min, RT). Peripheral leukocytes were then incubated with anti-human CD16/32 Ab and anti-mouse CD16/32 Ab to block mouse and human FcR, following by incubation with PE-Cy7 anti-mouse CD45 and BUV737 anti-human CD45. For evaluation of human leukocyte chimerism in spleen, splenocytes of huMice were treated with Red Blood Cell Lysing Buffer Hybri-Max™ (15 min, RT), rinsed in PBS, incubated with anti-human CD16/32 Ab and anti-mouse CD16/32 Ab. Next, splenocytes were incubated with the following combination of Abs: PE-Cy7 anti-mouse CD45, BUV737 anti-human CD45, FITC anti-human CD3, APC-Cy7 anti-human CD4, BV421 anti-human CD8 and APC anti-human CD19; or PE anti-human CD45 and BV605 anti-human CD33.

In all experiments, appropriate irrelevant Ab were used as controls, and cells were fixed in 4 % PF / PBS. Data were acquired with a BD LSR II flow cytometer and analyzed using FlowJo v10 software.

5.4.7 Immunofluorescence microscopy

Mouse and huMice tissue fragments were embedded in Optimal Cutting Temperature Compound (OCT), snap-frozen in 2 methyl-butane pre-chilled in liquid nitrogen, and stored at -80°C until use. Frozen tissues were sectioned (10 μm) with a cryostat and mounted on slides pre-treated with Vectabond (Vector Laboratories).

For detection of CM-DiI-labelled EVs in huMice, tissue sections were fixed with 4% paraformaldehyde (PF) in PBS (15 min, RT), washed in PBS and blocked with 5% goat serum. Cryosections of huMice spleen, bone marrow, thymus, liver and lungs were incubated with anti-human CD163 Ab or anti-human CD169 Ab (both at 1:100) in 5% goat serum (overnight, 4°C), followed by AF488-goat anti-mouse IgG (1:400) in 5% goat serum (45 min, RT).

Cell nuclei were counterstained with DAPI and tissue sections were fixed post-labelling in 4% PF / PBS (15 min, RT). Coverslips were mounted with Vector® TrueVIEW® Autofluorescence Quenching Kit. The tissues were imaged using a Nikon E800 microscope with Zeiss Axiocam 506 camera.

6.0 General Discussion

Pregnancy is associated with highly complex changes in a woman's physiology requiring multiple developmental, metabolic, endocrine, and immunological pathways to function in a synchronized and highly regulated manner in order to achieve successful birth. It is an "immunological paradox" in which the semi-allogeneic fetus survives and evades the maternal immune system for 40 weeks. Defense mechanisms must be deployed to prevent diseases of pregnancy, such as PE, stillbirth, IUGR, and preterm birth.

EVs are released from all eukaryotic cell types studied thus far. EVs function as a mechanism of cell-to-cell communication through exchange of proteins (e.g., Ags, enzymes, cytokines, surface receptors, etc.), lipids, carbohydrates, coding, and non-coding RNAs, and small DNA fragments between donor and acceptor cells. Increasing evidence indicates that EVs play key roles during steady-state conditions and in the pathogenesis of autoimmune disorders, microbial infections, cancer metastasis, and transplant rejection.

Fetoplacental-derived EVs are released by the fetoplacental unit into the maternal circulation during pregnancy. Previous work by us and others has demonstrated that human trophoblast-derived EVs transport placenta-specific microRNAs that confer viral resistance to the EV-acceptor cells, and that fetoplacental EVs play multiple roles in the pathogenesis of PE [11, 33]. However, the full scope of fetoplacental EVs functions remains to be explored. Here, we examined the role of these EVs in the pathogenesis of PE and in feto-maternal tolerance during pregnancy. We found that EVs from the plasma of pregnant women with PE cause an increase in arterial constriction in mouse mesenteric arteries, suggesting that they may contribute to the characteristic high blood pressure observed in PE patients. Additionally, we found that

fetoplacental EVs carry paternal Ags to maternal SLTs where they are presented to and recognized by T cells.

6.1 sEVs from the plasma of women with PE cause an increase in arterial constriction

Using pressurized arteriography, we found that sEVs from the plasma of women with PE cause an increase in arterial constriction in mouse mesenteric arteries in an endothelial cell-mediated fashion, suggesting that these sEVs may contribute to high blood pressure found in patients with PE. In support of this finding, the vascular contractile effects of PE sEVs was decreased when we exposed mouse mesenteric arteries to EV-depleted plasma from pregnant women with PE, suggesting that sEVs are involved in the vasoconstrictive effect of plasma from women with PE. Importantly, these vascular effects were specific to sEVs and not recapitulated in experiments with the larger MVs. This may be related to differences in the ability of sEVs to enter and interact with vascular endothelial cells [78, 79] or could also be related to variation in EV content. Therefore, future studies will involve examination of the specific cargo of these EVs to help determine specific mechanisms of action that lead to the observed EV-induced vasoconstriction.

6.2 Paternal antigens and fetoplacental small extracellular vesicles traffic to maternal secondary lymphoid tissues

Our results in mouse semi-allogeneic pregnancy models revealed the presence of the surrogate paternal Ag OVA associated to trophoblast-derived sEVs, which traffic systemically and are captured by maternal leukocytes in the mother's spleen and LN. These findings partially address our hypothesis that fetoplacental EVs carry paternal Ag to maternal SLT during pregnancy. To test this concept, we mated WT BALB/c females with C57Bl/6 (B6) Act-mOVA or control WT males. By immunofluorescence microscopy analysis of tissue sections of maternal spleen and LN on E17.5, we detected the paternal surrogate Ag OVA in B cell follicles of the maternal spleen, in a punctate pattern, in close apposition to FDCs that reside within the follicles. These findings suggest that the paternal Ag OVA is captured by FDCs for possible presentation to B cells, as an intact / native (non-processed) paternal Ag. We also observed colocalization of OVA Ag with FDCs in the maternal uterine draining and non-draining lymph nodes (LN). Previous studies in non-pregnancy models in mice, have shown that FDCs avidly capture, concentrate and retain soluble Ags for weeks or months in the form of immuno-complexes, or soluble Ags coated with complement factors, which bind the complement receptors (e.g. CD21/35) highly expressed on the FDC surface [115].

Because we detected the surrogate paternal Ag OVA in maternal SLTs during pregnancy by immunofluorescence microscopy, we next tested whether fetoplacental sEVs released into the maternal peripheral blood represent a cell-free mechanism by which fetoplacental Ags are transported to the maternal SLTs. To test this, we used a novel mouse model, in which genetically engineered MT124 B6 males, encoding CD81-mNeonGreen cDNA flanked by LoxP sites, were used to impregnate CMV-Cre B6 females, the latter encoding Cre under the ubiquitous CMV

promoter. In this system, following Cre-recombination, the fetoplacental unit secretes sEVs tagged with the sEV-associated marker CD81 linked to the green fluoroprobe mNeonGreen. Using this approach, we detected endogenously released fetoplacental CD81-mNeonGreen^{Pos} material in the maternal leukocytes and FDCs in the mother's spleen and LN, as well as in the maternal heart, liver, and kidney. This finding supports the idea, at least in mice, that fetoplacental sEVs target systemically maternal cells in SLTs and non-lymphoid organs. Immuno-labelling of the mother's spleen sections with an antibody against cytokeratin demonstrated that the CD81^{Pos} material corresponded likely to fetoplacental sEVs, instead of small fragments of trophoblast released into peripheral circulation. Therefore, we conclude that fetoplacental sEVs travel to maternal SLT where they are captured by maternal APCs. The pattern of localization of CD81-mNeoGreen sEVs in maternal leukocytes and FDCs (FDCs are not leukocytes) was similar to that of paternal OVA Ag. To further validate our hypothesis, we confirmed in the Act-OVA B6 male → WT BALB/c female mouse pregnancy model that sEVs released by the mouse trophoblasts to maternal peripheral blood carry the surrogate paternal Ag OVA. Our findings are in agreement with recent studies by our laboratory in the field of transplantation in mouse models, in which donor-derived sEVs released by vascularized cardiac allografts are captured by marginal zone and red pulp macrophages, cDCs, FDCs and B cells in the recipient's spleen [107]. Future directions include quantifying the amount of CD81^{pos} material in maternal tissues to identify the tissue and cell type with the highest amount of localization of CD81-mNeoGreen sEVs.

6.3 Trophoblast extracellular vesicles deliver paternal antigens that are presented to T cells in secondary lymphoid tissues

To assess EV delivery of paternal Ag to maternal lymphoid and non-lymphoid tissues, we used the mOVA mouse pregnancy model. On E17.5, we collected maternal plasma and placentas from BALB/c females impregnated by Act-mOVA or control WT B6 males. MVs and sEVs carrying the surrogate paternal Ag OVA on the vesicle surface were purified by immuno-precipitation using magnetic beads pre-coated with an antibody against OVA, from maternal plasma and 48 hour-supernatants of primary cultures of mouse trophoblast cells. Purity of sEV populations was confirmed by detection of the sEV-associated markers CD63 and CD81, and absence of the endoplasmic reticulum marker gp96. Digestion of the sEVs with PNGase revealed that the OVA Ag associated to the maternal plasma and trophoblast-derived sEVs was N-linked glycosylated. This explains why the OVA protein band detected by Western blot in the EVs exhibits a higher molecular weight than that of soluble OVA used as a positive control. These findings indicate that, in support of our hypothesis, paternal Ags (i.e., OVA) are carried by trophoblast-derived EVs that have been released into maternal blood.

To test whether peptides derived from the surrogate paternal Ag OVA, delivered systemically through placental sEVs, is recognized by maternal T cells in the spleen, we used OVA-specific TCR-transgenic CD4 or CD8 T cells as surrogate maternal responding T cells. By using this approach, we demonstrated that the paternal Ag OVA delivered through sEVs is processed and presented to maternal T cells in the mother's spleen. The adaptive immune response was paternal Ag-specific because the OT-I CD8 and OT-II CD4 T cells recognize the OVA-derived peptides SIINFEKL and $OVA_{323-339}$ presented in the context of $H2K^b$ ($H2^b$ MHC class-I) and IA^b ($H2^b$ MHC class-II) molecules, respectively.

Interestingly, following i.v. administration of trophoblast-derived sEVs carrying OVA Ag, we found that the sEV-associated OVA Ag triggers a maternal CD4 and CD8 T cell response similar to the previously described in the spleen of pregnant mice [53]. In our experiments, presentation of the OVA-derived peptides resulting from the capture and processing of the trophoblast sEVs by the maternal APCs in the spleen was associated with cell proliferation and deficient activation of the OVA peptide specific OT-II CD4 and OT-I CD8 T cells, when compared to controls in which the T cells were optimally activated by intraperitoneal administration of soluble OVA plus adjuvants. Indeed, we detected deficient T-cell activation ($CD62L^{High}$ $CD69^{Low}$) and increased percentages of proliferating CD4 OT-II and CD8 OT-I T cells undergoing apoptotic cell death, in the spleens of virgin female mice injected with trophoblast sEVs carrying OVA, as compared to controls injected with soluble OVA plus adjuvants. In mice injected with sEVs from primary cultures of trophoblasts expressing OVA, a minor increase in the percentage of CD4 OT-II FoxP3 Tregs was also evident, and the content of the type-I response cytokine IFN-γ in the OT cells was significantly lower. By contrast, we did not detect significant differences in the expression of the T-cell exhaustion markers PD1, Tim3 and Lag3, or in the surface levels of TCRs between the experimental and the positive control groups, suggesting that T cell exhaustion or internalization of the surface TCR are not mechanisms by which trophoblast sEVs down-regulate the maternal T cell response during pregnancy. Taken together, these data are in line with the T cell proliferation induced by deficient activation and likely consequent deletion, and deficient type-1 polarization, as reported by previous studies in fetoplacental-specific maternal T cells in the mother's spleen [53].

It is important to note that there are technical differences between our *in vivo* model and previous studies in pregnant mice that could have affected the outcome of the OVA-specific T cell

response in our study. We administered the trophoblast-derived sEVs in a single bolus for the 2-day OT-I T cell experiment, or in two consecutive daily doses for the 4-day OT-II T cell studies, whereas during pregnancy the trophoblast sEVs are released continuously to the maternal blood once the placenta is developed. To address this in future studies, multiple injections of EVs may be administered over a period of 15-17 days. Another important consideration is the potential effect of gestational hormones on the T cell response. This could be addressed by measuring the response of T cells following exposure to gestational hormones including progesterone and human gonadotropic hormone *in vitro*.

6.4 Interaction of human placental small extracellular vesicles with human antigen-presenting cells in secondary lymphoid tissues *in vivo*

To verify our findings from *in vivo* mouse systems in a translational humanized mouse model, we systemically administered sEVs harvested from tissue culture supernatant of primary human trophoblasts in huMice. Prior to human sEV administration, huMice chimerism for multiple lineages of human leukocytes was confirmed by FACS analysis. sEVs were labeled red with the CM-DiI dye for *in vivo* tracking. Tissue cryosections were fixed in paraformaldehyde to preserve the signal of the lipophilic fluoroprobe used to label the sEVs. The PHT sEVs were detected in human cDCs and B lymphocytes, both Ag-presenting cells that have been proved to present conceptus-derived Ags to T cells in mouse pregnancy models [20]. We did not detect PHT sEVs in human chimeric leukocytes in thymus and lung. We expected that the number of sEVs captured by the human leukocytes *in vivo*, in particular by those that are non-professional phagocytes, be relatively low since in our model the trophoblast sEVs were injected in one bolus, instead of being

released continuously and in higher quantities by the human placenta. ImageStream is an image flow cytometry technology that is particularly suitable for detection of small foci of fluroroprobe^{Pos} material within or on the surface of acceptor cells. Unlike traditional flow cytometry that measures the total amount of fluorescence per cell, ImageStream images each cell on which the tiny foci containing the attached or internalized CM-DiI-labelled sEVs can be clearly detected.

Interestingly, the PHT sEVs were detected in human metallophilic (CD169^{Pos}) macrophages located in the splenic marginal zone. Previous studies in mice have shown that blood-borne EVs are rapidly internalized by CD169^{Pos} macrophages in the splenic marginal zone [111]. In this regard, our group demonstrated that sEVs released by human skin grafts transplanted in huMice are captured and concentrated by human CD169 macrophages located in the sub-capsular sinus of the graft-draining lymph nodes, an area structurally analogue to the marginal zone of the spleen. In line with previous findings in mouse and huMice models, our results suggest that the sEVs released by the human trophoblasts to maternal peripheral blood are captured by the human CD169^{Pos} marginal zone macrophages of the spleen. Opposing the highly phagocytic CD163^{Pos} red pulp macrophages of the spleen, the contents internalized by CD169^{Pos} macrophages are transported via transcytosis and without being degraded, to the opposite site of the specialized phagocyte whether the follicular B cells and T cells reside. It is unknown whether those human splenic CD169^{Pos} macrophages that capture trophoblast sEVs from blood present fetoplacental Ags delivered by the trophoblast sEVs directly to B cells or transfer the sEVs to Ag-presenting cells including DCs and B cells for Ag-processing and presentation to maternal T cells. Whether this process leads to down-regulation of the T cell response against the fetoplacental unit in humans, remains unknown. Future directions include assessment of the effect of primary trophoblast EVs on different subsets of APCs (human and mouse) *in vivo* and *in vitro*.

In conclusion, our findings indicate that fetoplacental sEVs perform critical roles during both normal and pathological pregnancy. Overall, we found that (i) human plasma sEVs from women with PE cause an increase in constriction of mouse mesenteric arteries, (ii) fetoplacental sEVs are a cell-free mechanism to deliver trophoblast / paternal Ags to maternal immune cells resident in the mother's SLT in mice and huMice, and (iii) presentation of paternal Ag delivered through trophoblast sEVs to maternal immune cells in the spleen leads to deficient activation of the Ag-specific CD4 and CD8 T cells in mice. Our results provide novel insight on the role of fetoplacental sEVs in regulation of the maternal vascular tone and feto-maternal immunological tolerance in the mother's SLTs during pregnancy.

7.0 Other Contributions

My interests in the involvement of fetoplacental EVs in PE and feto-maternal tolerance impelled my curiosity of the wider roles of fetoplacental EVs in pregnancy. Therefore, I contributed to other projects in our laboratory that focused on the effects of hypoxia on placental EVs. Recently, our laboratory demonstrated that membrane viscosity of placental extracellular vesicles can reveal the extent of hypoxic damage to human placental trophoblast cells. We found that the membrane of microvesicles released by PHT cells grown under hypoxic conditions is less viscous than that of microvesicles released by PHT cells grown in normal conditions. I helped to culture PHT cells in normal and hypoxic conditions, isolate EVs from PHT media supernatants in both conditions, and analysis of lipidomics data. These data were published in the journal Placenta in April 2022:

Huang C, Li H, Powell JS, Ouyang Y, Wendell SG, Suresh S, Hsia KJ, Sadovsky Y, Quinn D. Assessing hypoxic damage to placental trophoblasts by measuring membrane viscosity of extracellular vesicles. Placenta. 2022 Apr;121:14-22. doi: 10.1016/j.placenta.2022.02.019. Epub 2022 Feb 24. PMID: 35245720; PMCID: PMC9010367.

Appendix A.1 Supplemental Figures

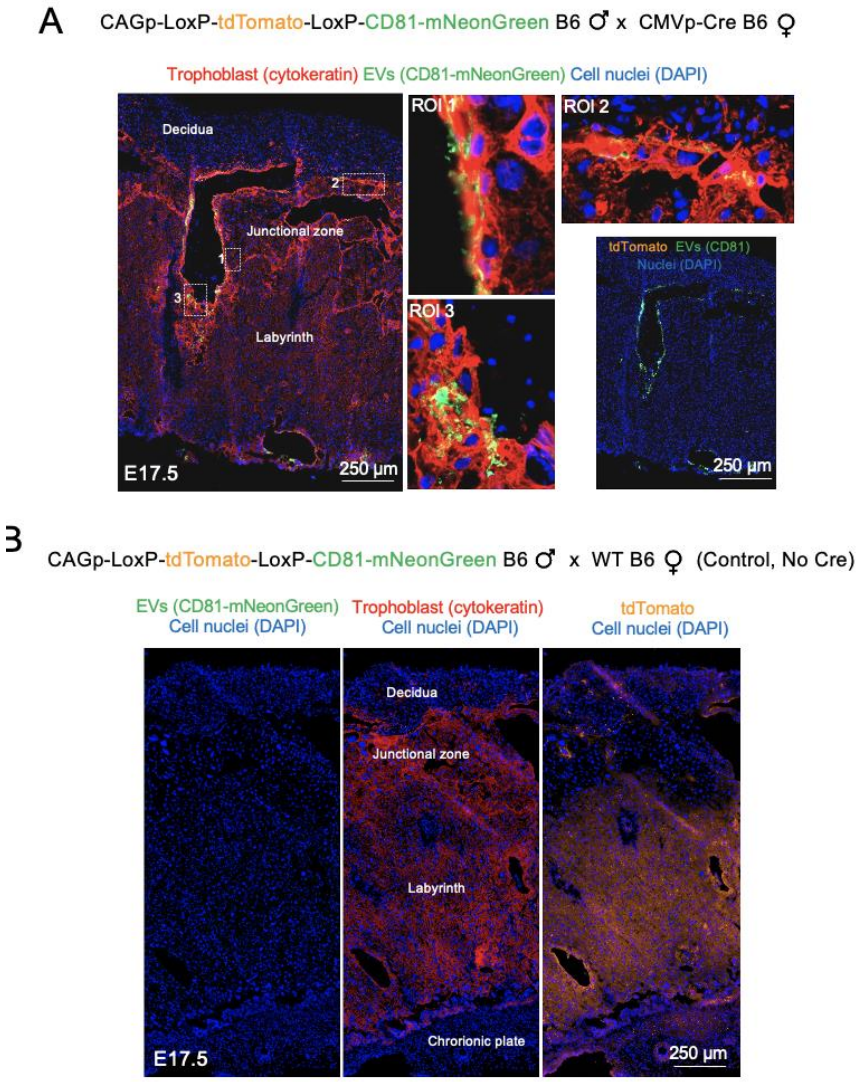

Supplemental Figure 1: Validation of the MT124 B6 mouse pregnancy model.

A) Detection by immunofluorescence microscopy of tissue cryosections of CD81-mNeonGreen, and absence of tdTomato signal in E17.5 placentas, from CMVp-Cre B6 female mice mated with MT124 B6 male mice. **B)** As a

negative control, absence of CD81-mNeonGreen and expression of tdTomato in E17.5 placentas from WT B6 females mated with WT B6 males.

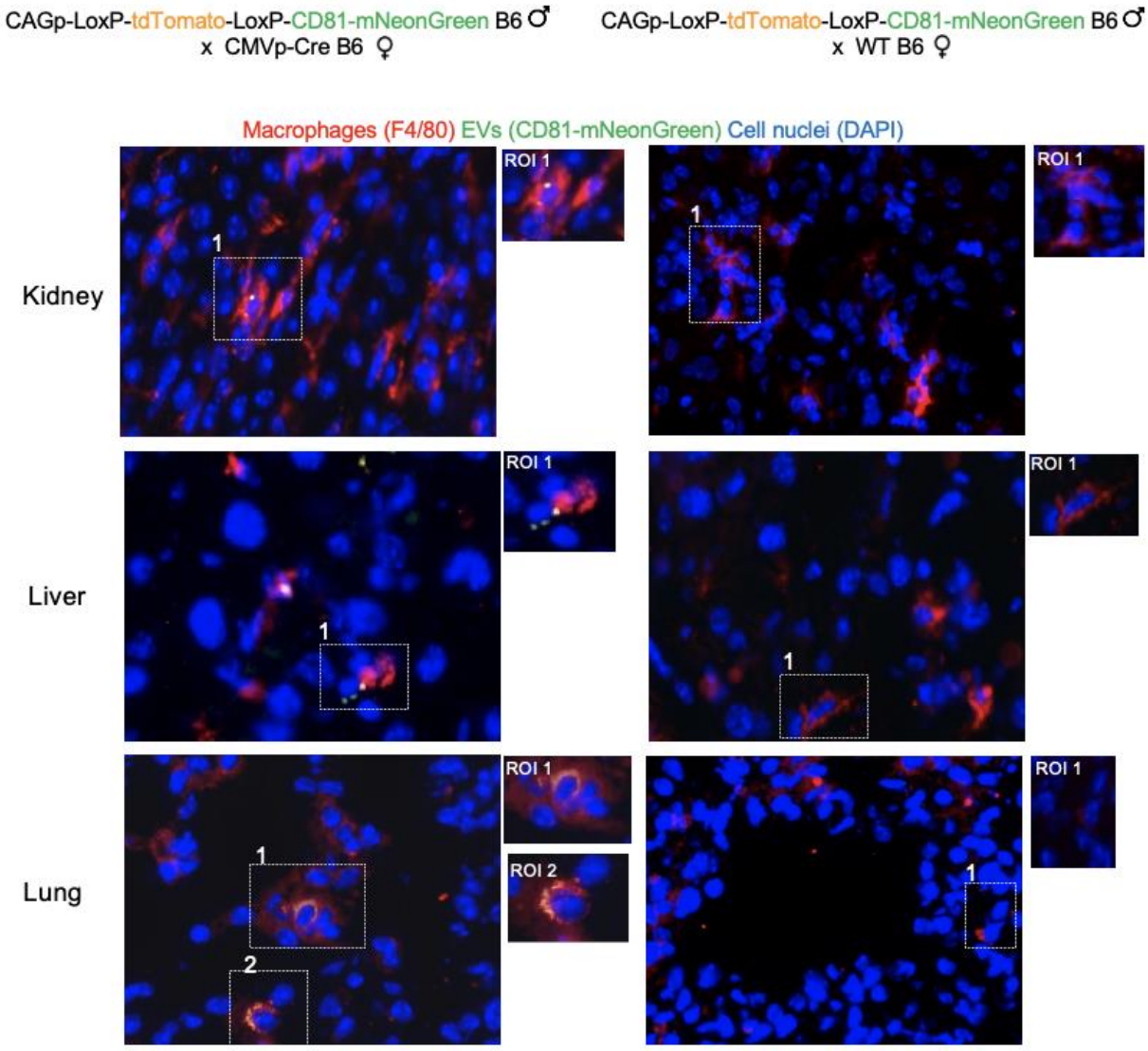

Supplemental Figure 2: Detection of mNeonGreen-CD81^{pos} content in maternal tissues.

Detection by immunofluorescence microscopy on tissue cryosections of CD81-mNeonGreen^{Pos} content in the mother's kidney, liver, and lung (E17.5) of CMVp-Cre B6 female mice impregnated by MT124 B6 or control WT B6 males.

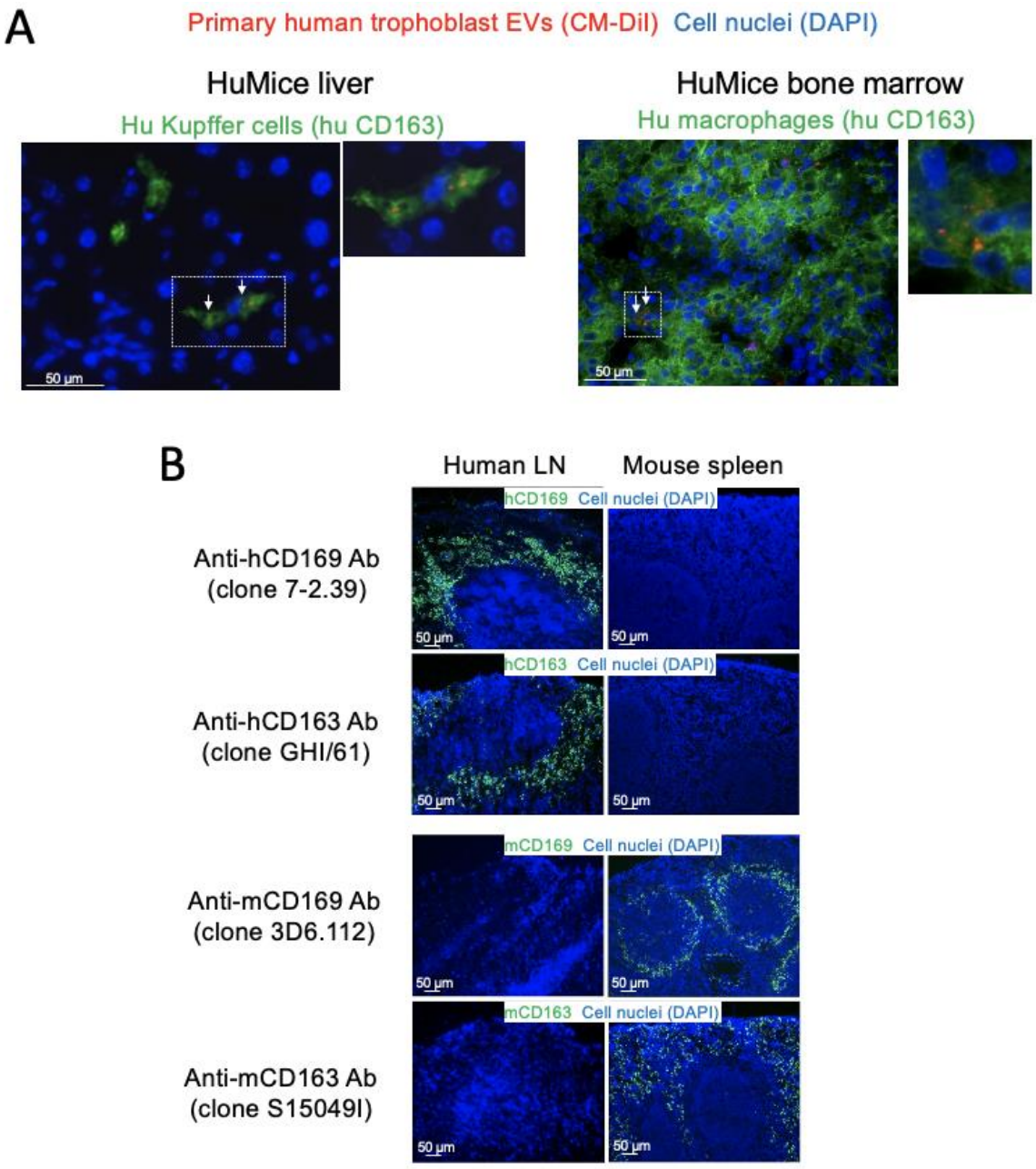

Supplemental Figure 3: PHT detection in other huMice tissues, no cross-reactivity of Abs.

A) CM-DiI-labelled (red) PHT sEVs injected i.v. in huMice were detected by fluorescence microscopy on tissue sections in human CD163 macrophages in the huMice liver and bone marrow. **B)** Analysis by immunofluorescence microscopy on tissue sections of species cross-reactivity between human and mouse of the antibodies against human CD169 and CD163 used for the huMice experiments.

Bibliography

1. Burton, G.J., et al., *Pre-eclampsia: pathophysiology and clinical implications.* BMJ, 2019. **366**: p. l2381.
2. Sutton, A.L.M., L.M. Harper, and A.T.N. Tita, *Hypertensive disorders in pregnancy.* Obstet Gynecol Clin North Am, 2018. **45**(2): p. 333-347.
3. Melchiorre, K., V. Giorgione, and B. Thilaganathan, *The placenta and preeclampsia: villain or victim?* Am J Obstet Gynecol, 2022. **226**(2S): p. S954-S962.
4. Fisher, S.J., *Why is placentation abnormal in preeclampsia?* Am J Obstet Gynecol, 2015. **213**(4 Suppl): p. S115-22.
5. Karumanchi, S.A. and J.P. Granger, *Preeclampsia and Pregnancy-Related Hypertensive Disorders.* Hypertension, 2016. **67**(2): p. 238-42.
6. Rana, S., et al., *Preeclampsia: Pathophysiology, Challenges, and Perspectives.* Circ Res, 2019. **124**(7): p. 1094-1112.
7. Morelli, A.E. and Y. Sadovsky, *Extracellular vesicles and immune response during pregnancy: A balancing act.* Immunol Rev, 2022. **308**(1): p. 105-122.
8. Desrochers, L.M., et al., *Microvesicles provide a mechanism for intercellular communication by embryonic stem cells during embryo implantation.* Nat Commun, 2016. **7**: p. 11958.
9. Mitchell, M.D., et al., *Placental exosomes in normal and complicated pregnancy.* Am J Obstet Gynecol, 2015. **213**(4 Suppl): p. S173-81.
10. Mong, E.F., et al., *Chromosome 19 microRNA cluster enhances cell reprogramming by inhibiting epithelial-to-mesenchymal transition.* Sci Rep, 2020. **10**(1): p. 3029.
11. Delorme-Axford, E., et al., *Human placental trophoblasts confer viral resistance to recipient cells.* Proc Natl Acad Sci U S A, 2013. **110**(29): p. 12048-53.
12. Ouyang, Y., et al., *Trophoblastic extracellular vesicles and viruses: Friends or foes?* Am J Reprod Immunol, 2021. **85**(2): p. e13345.
13. Sadovsky, Y., et al., *Placental small extracellular vesicles: Current questions and investigative opportunities.* Placenta, 2020. **102**: p. 34-38.
14. Bai, K., et al., *Placenta-Derived Exosomes as a Modulator in Maternal Immune Tolerance During Pregnancy.* Front Immunol, 2021. **12**: p. 671093.
15. Tong, M. and L.W. Chamley, *Placental extracellular vesicles and feto-maternal communication.* Cold Spring Harb Perspect Med, 2015. **5**(3): p. a023028.
16. Nair, S. and C. Salomon, *Extracellular vesicles and their immunomodulatory functions in pregnancy.* Semin Immunopathol, 2018. **40**(5): p. 425-437.
17. Yadava, S.M., et al., *miR-15b-5p promotes expression of proinflammatory cytokines in human placenta by inhibiting Apelin signaling pathway.* Placenta, 2021. **104**: p. 8-15.
18. Dutta, S., et al., *Hypoxia-induced small extracellular vesicle proteins regulate proinflammatory cytokines and systemic blood pressure in pregnant rats.* Clin Sci (Lond), 2020. **134**(6): p. 593-607.
19. Rendell, V., N.M. Bath, and T.V. Brennan, *Medawar's Paradox and Immune Mechanisms of Fetomaternal Tolerance.* OBM Transplant, 2020. **4**(1).

20. Rizzuto, G., et al., *Establishment of fetomaternal tolerance through glycan-mediated B cell suppression.* Nature, 2022. **603**(7901): p. 497-502.
21. Parasar, P., N. Guru, and N.R. Nayak, *Contribution of macrophages to fetomaternal immunological tolerance.* Hum Immunol, 2021. **82**(5): p. 325-331.
22. Al-Khunaizi, N.R., K.S. Tabbara, and E.M. Farid, *Is there a role for HLA-G in the induction of regulatory T cells during the maintenance of a healthy pregnancy?* Am J Reprod Immunol, 2020. **84**(2): p. e13259.
23. Elizabeth C.W. Gregory, M.P.H., Claudia P. Valenzuela, M.P.H., and Donna L. Hoyert, Ph.D., *Fetal Mortality: United States, 2020*, in *National Vital Statistics Reports*. 2022, U.S. Department of Health and Human Services: Online. p. 1-20.
24. Lima, P.D., et al., *Leukocyte driven-decidual angiogenesis in early pregnancy.* Cell Mol Immunol, 2014. **11**(6): p. 522-37.
25. Turco, M.Y. and A. Moffett, *Development of the human placenta.* Development, 2019. **146**(22).
26. Hertig, A.T., J. Rock, and E.C. Adams, *A description of 34 human ova within the first 17 days of development.* Am J Anat, 1956. **98**(3): p. 435-93.
27. Frankel, E.B., et al., *Ist1 regulates ESCRT-III assembly and function during multivesicular endosome biogenesis in Caenorhabditis elegans embryos.* Nat Commun, 2017. **8**(1): p. 1439.
28. Knofler, M., et al., *Human placenta and trophoblast development: key molecular mechanisms and model systems.* Cell Mol Life Sci, 2019. **76**(18): p. 3479-3496.
29. Herrick EJ, B., B., *Embryology, Placenta.* StatPearls, 2022.
30. Hemberger, M., C.W. Hanna, and W. Dean, *Mechanisms of early placental development in mouse and humans.* Nat Rev Genet, 2020. **21**(1): p. 27-43.
31. Chappell, L.C., et al., *Pre-eclampsia.* Lancet, 2021. **398**(10297): p. 341-354.
32. Phipps, E.A., et al., *Pre-eclampsia: pathogenesis, novel diagnostics and therapies.* Nat Rev Nephrol, 2019. **15**(5): p. 275-289.
33. Salomon, C. and G.E. Rice, *Role of Exosomes in placental homeostasis and pregnancy disorders.* Prog Mol Biol Transl Sci, 2017. **145**: p. 163-179.
34. Palma, C., et al., *Extracellular Vesicles and Preeclampsia: Current Knowledge and Future Research Directions.* Subcell Biochem, 2021. **97**: p. 455-482.
35. Jeppesen, D.K., et al., *Reassessment of Exosome Composition.* Cell, 2019. **177**(2): p. 428-445 e18.
36. Zhang, H., et al., *Identification of distinct nanoparticles and subsets of extracellular vesicles by asymmetric flow field-flow fractionation.* Nat Cell Biol, 2018. **20**(3): p. 332-343.
37. Mathieu, M., et al., *Specificities of exosome versus small ectosome secretion revealed by live intracellular tracking of CD63 and CD9.* Nat Commun, 2021. **12**(1): p. 4389.
38. van Niel, G., G. D'Angelo, and G. Raposo, *Shedding light on the cell biology of extracellular vesicles.* Nat Rev Mol Cell Biol, 2018. **19**(4): p. 213-228.
39. Phuong H.D. Nguyen, A.H.L., Jonetta Shi Qi Pek, Thach Tuan Pham, Migara Kavishka Jayasinghe, Dang Vinh Do, Cao Dai Phung, Minh T.N. Le, *Extracellular vesicles and lipoproteins—Smart messengers of blood cells in the circulation.* Journal of Extracellular Biology, 2022. **1**(7).
40. Wortzel, I., et al., *Exosome-Mediated Metastasis: Communication from a Distance.* Dev Cell, 2019. **49**(3): p. 347-360.

41. Hoshino, A., et al., *Tumour exosome integrins determine organotropic metastasis.* Nature, 2015. **527**(7578): p. 329-35.
42. Zhang, Z.G. and M. Chopp, *Exosomes in stroke pathogenesis and therapy.* J Clin Invest, 2016. **126**(4): p. 1190-7.
43. Hill, A.F., *Extracellular Vesicles and Neurodegenerative Diseases.* J Neurosci, 2019. **39**(47): p. 9269-9273.
44. Salomon, C., et al., *Placental Exosomes as Early Biomarker of Preeclampsia: Potential Role of Exosomal MicroRNAs Across Gestation.* J Clin Endocrinol Metab, 2017. **102**(9): p. 3182-3194.
45. Mouillet, J.F., et al., *The role of trophoblastic microRNAs in placental viral infection.* Int J Dev Biol, 2014. **58**(2-4): p. 281-9.
46. Li, H., et al., *Unique microRNA Signals in Plasma Exosomes from Pregnancies Complicated by Preeclampsia.* Hypertension, 2020. **75**(3): p. 762-771.
47. Tahlia I. Smith, A.E.R., *Extracellular vesicles in reproduction and pregnancy.* Extracellular Vesicles and Circulating Nucleic Acids, 2022. **3**: p. 292-317.
48. Herrera-Van Oostdam, A.S., et al., *Placental exosomes isolated from urine of patients with gestational diabetes exhibit a differential profile expression of microRNAs across gestation.* Int J Mol Med, 2020. **46**(2): p. 546-560.
49. Radnaa, E., et al., *Extracellular vesicle mediated feto-maternal HMGB1 signaling induces preterm birth.* Lab Chip, 2021. **21**(10): p. 1956-1973.
50. Hadley, E.E., et al., *Amnion epithelial cell-derived exosomes induce inflammatory changes in uterine cells.* Am J Obstet Gynecol, 2018. **219**(5): p. 478 e1-478 e21.
51. Ariyakumar, G., et al., *NF-kappaB regulation in maternal immunity during normal and IUGR pregnancies.* Sci Rep, 2021. **11**(1): p. 20971.
52. Billingham, R.E., L. Brent, and P.B. Medawar, *Actively acquired tolerance of foreign cells.* Nature, 1953. **172**(4379): p. 603-6.
53. Erlebacher, A., et al., *Constraints in antigen presentation severely restrict T cell recognition of the allogeneic fetus.* J Clin Invest, 2007. **117**(5): p. 1399-411.
54. Perchellet, A.L., S. Jasti, and M.G. Petroff, *Maternal CD4(+) and CD8(+) T cell tolerance towards a fetal minor histocompatibility antigen in T cell receptor transgenic mice.* Biol Reprod, 2013. **89**(4): p. 102.
55. Polanczyk, M.J., et al., *Enhanced FoxP3 expression and Treg cell function in pregnant and estrogen-treated mice.* J Neuroimmunol, 2005. **170**(1-2): p. 85-92.
56. Ouyang, Y., et al., *Isolation of human trophoblastic extracellular vesicles and characterization of their cargo and antiviral activity.* Placenta, 2016. **47**: p. 86-95.
57. Gutierrez-Vazquez, C., et al., *Transfer of extracellular vesicles during immune cell-cell interactions.* Immunol Rev, 2013. **251**(1): p. 125-42.
58. Herzenberg, L.A., et al., *Fetal cells in the blood of pregnant women: detection and enrichment by fluorescence-activated cell sorting.* Proc Natl Acad Sci U S A, 1979. **76**(3): p. 1453-5.
59. Bonney, E.A. and P. Matzinger, *The maternal immune system's interaction with circulating fetal cells.* J Immunol, 1997. **158**(1): p. 40-7.
60. Dakic, A., et al., *Development of the dendritic cell system during mouse ontogeny.* J Immunol, 2004. **172**(2): p. 1018-27.

61. Holland, O.J., et al., *Minor histocompatibility antigens are expressed in syncytiotrophoblast and trophoblast debris: implications for maternal alloreactivity to the fetus.* Am J Pathol, 2012. **180**(1): p. 256-66.
62. *Hypertension in pregnancy. Report of the American College of Obstetricians and Gynecologists' Task Force on Hypertension in Pregnancy.* Obstet Gynecol, 2013. **122**(5): p. 1122-1131.
63. Staff, A.C., *The two-stage placental model of preeclampsia: An update.* J Reprod Immunol, 2019. **134-135**: p. 1-10.
64. Myatt, L. and J.M. Roberts, *Preeclampsia: Syndrome or disease?* Curr Hypertens Rep, 2015. **17**(11): p. 83.
65. Otani, K., et al., *Plasma exosomes regulate systemic blood pressure in rats.* Biochem Biophys Res Commun, 2018. **503**(2): p. 776-783.
66. Tong, M., et al., *Placental Nano-vesicles Target to Specific Organs and Modulate Vascular Tone In Vivo.* Hum Reprod, 2017. **32**(11): p. 2188-2198.
67. Pillay, P., et al., *Placental exosomes and pre-eclampsia: Maternal circulating levels in normal pregnancies and, early and late onset pre-eclamptic pregnancies.* Placenta, 2016. **46**: p. 18-25.
68. Gao, X., et al., *The potential role of serum exosomes in preeclampsia.* Curr Drug Metab, 2020. **21**(5): p. 352-356.
69. Biro, O., et al., *Circulating exosomal and Argonaute-bound microRNAs in preeclampsia.* Gene, 2019. **692**: p. 138-144.
70. Wu, M., et al., *Exosomal microRNA302a promotes trophoblast migration and proliferation, and represses angiogenesis by regulating the expression levels of VEGFA in preeclampsia.* Mol Med Rep, 2021. **24**(6).
71. Wang, Z., et al., *Overview of extracellular vesicles in the pathogenesis of preeclampsiadagger.* Biol Reprod, 2021. **105**(1): p. 32-39.
72. Gilani, S.I., et al., *Preeclampsia and Extracellular Vesicles.* Curr Hypertens Rep, 2016. **18**(9): p. 68.
73. Czernek, L. and M. Duchler, *Exosomes as Messengers Between Mother and Fetus in Pregnancy.* Int J Mol Sci, 2020. **21**(12).
74. Simon, C., et al., *Extracellular Vesicles in Human Reproduction in Health and Disease.* Endocr Rev, 2018. **39**(3): p. 292-332.
75. Hashimoto, A., K. Sugiura, and A. Hoshino, *Impact of exosome-mediated feto-maternal interactions on pregnancy maintenance and development of obstetric complications.* J Biochem, 2021. **169**(2): p. 163-171.
76. Tannetta, D., et al., *Syncytiotrophoblast extracellular vesicles - Circulating biopsies reflecting placental health.* Placenta, 2017. **52**: p. 134-138.
77. Ashworth, J.R., et al., *Plasma from pre-eclamptic women and functional change in myometrial resistance arteries.* Br J Obstet Gynaecol, 1998. **105**(4): p. 459-61.
78. Baruah, J. and K.K. Wary, *Exosomes in the Regulation of Vascular Endothelial Cell Regeneration.* Front Cell Dev Biol, 2019. **7**: p. 353.
79. Li, H., et al., *Internalization of trophoblastic small extracellular vesicles and detection of their miRNA cargo in P-bodies.* J Extracell Vesicles, 2020. **9**(1): p. 1812261.
80. Wang, Y., X. Du, and J. Wang, *Transfer of miR-15a-5p by placental exosomes promotes pre-eclampsia progression by regulating PI3K/AKT signaling pathway via CDK1.* Mol Immunol, 2020. **128**: p. 277-286.

81. Konecna, B., L. Tothova, and G. Repiska, *Exosomes-associated DNA—New marker in pregnancy complications?* Int J Mol Sci, 2019. **20**(12).
82. Tong, M., V.M. Abrahams, and L.W. Chamley, *Immunological effects of placental extracellular vesicles.* Immunol Cell Biol, 2018.
83. Ayala-Ramirez, P., et al., *Assessment of placental extracellular vesicles-associated Fas Ligand and TNF-related apoptosis-inducing ligand in pregnancies complicated by early and late onset preeclampsia.* Front Physiol, 2021. **12**: p. 708824.
84. Gong, R.Q., et al., *Roles of exosomes-derived lncRNAs in preeclampsia.* Eur J Obstet Gynecol Reprod Biol, 2021. **263**: p. 132-138.
85. Pillay, P., et al., *Exosomal Th1/Th2 cytokines in preeclampsia and HIV-positive preeclamptic women on highly active anti-retroviral therapy.* Cytokine, 2020. **125**: p. 154795.
86. Ellis, R., et al., *Increased expression and phosphorylation of 6-phosphofructo-2-kinase/fructose-2,6-bisphosphatase isoforms in urinary exosomes in pre-eclampsia.* J Transl Med, 2019. **17**(1): p. 60.
87. Chang, X., et al., *Exosomes from women with preeclampsia induced vascular dysfunction by delivering sFlt (soluble fms-like tyrosine kinase)-1 and sEng (soluble endoglin) to endothelial cells.* Hypertension, 2018. **72**(6): p. 1381-1390.
88. Hu, C.C., et al., *Pre-eclampsia is associated with altered expression of the renal sodium transporters NKCC2, NCC and ENaC in urinary extracellular vesicles.* PLoS One, 2018. **13**(9): p. e0204514.
89. Biro, O., et al., *Various levels of circulating exosomal total-miRNA and miR-210 hypoxamiR in different forms of pregnancy hypertension.* Pregnancy Hypertens, 2017. **10**: p. 207-212.
90. Tong, M., et al., *Micro- and nano-vesicles from first trimester human placentae carry Flt-1 and levels are increased in severe preeclampsia.* Front Endocrinol (Lausanne), 2017. **8**: p. 174.
91. Motta-Mejia, C., et al., *Placental vesicles carry active endothelial nitric oxide synthase and their activity is reduced in preeclampsia.* Hypertension, 2017. **70**(2): p. 372-381.
92. Escudero, C.A., et al., *Role of extracellular vesicles and microRNAs on dysfunctional angiogenesis during preeclamptic pregnancies.* Front Physiol, 2016. **7**: p. 98.
93. Tan, P.P.S., et al., *Exosomal microRNAs in the development of essential hypertension and its potential as biomarkers.* Am J Physiol Heart Circ Physiol, 2021. **320**(4): p. H1486-H1497.
94. Perez-Hernandez, J., et al., *Urinary- and plasma-derived exosomes reveal a distinct microRNA signature associated with albuminuria in hypertension.* Hypertension, 2021. **77**(3): p. 960-971.
95. Myers, J., et al., *In preeclampsia, the circulating factors capable of altering in vitro endothelial function precede clinical disease.* Hypertension, 2005. **45**(2): p. 258-63.
96. Hayman, R., et al., *Plasma from women with pre-eclampsia induces an in vitro alteration in the endothelium-dependent behaviour of myometrial resistance arteries.* BJOG, 2000. **107**(1): p. 108-15.
97. Hayman, R., et al., *The preliminary characterization of a vasoactive circulating factor(s) in preeclampsia.* Am J Obstet Gynecol, 2001. **184**(6): p. 1196-203.
98. Cronqvist, T., et al., *Syncytiotrophoblast derived extracellular vesicles transfer functional placental miRNAs to primary human endothelial cells.* Sci Rep, 2017. **7**(1): p. 4558.

99. Sween, L.K., A.D. Althouse, and J.M. Roberts, *Early-pregnancy percent body fat in relation to preeclampsia risk in obese women.* Am J Obstet Gynecol, 2015. **212**(1): p. 84 e1-7.
100. American College of Obstetrics and Gynecology (ACOG), *ACOG Practice Bulletin No. 33: Diagnosis and Management of Preeclampsia and Eclampsia.* Obstet Gynecol, 2002. **99**(1): p. 159-167.
101. Crandall, M.E., T.M. Keve, and M.K. McLaughlin, *Characterization of norepinephrine sensitivity in the maternal splanchnic circulation during pregnancy.* Am J Obstet Gynecol, 1990. **162**(5): p. 1296-301.
102. Halpern, W., G. Osol, and G.S. Coy, *Mechanical behavior of pressurized in vitro prearteriolar vessels determined with a video system.* Ann Biomed Eng, 1984. **12**(5): p. 463-79.
103. Pearce, L.L., et al., *Role of metallothionein in nitric oxide signaling as revealed by a green fluorescent fusion protein.* Proc Natl Acad Sci U S A, 2000. **97**(1): p. 477-82.
104. Gandley, R.E., K.P. Conrad, and M.K. McLaughlin, *Endothelin and nitric oxide mediate reduced myogenic reactivity of small renal arteries from pregnant rats.* Am J Physiol Regul Integr Comp Physiol, 2001. **280**(1): p. R1-7.
105. MacPherson, R.D., L.J. McLeod, and R.L. Rasiah, *Myogenic response of isolated pressurized rabbit ear artery is independent of endothelium.* Am J Physiol, 1991. **260**(3 Pt 2): p. H779-84.
106. Lewis, S.M., A. Williams, and S.C. Eisenbarth, *Structure and function of the immune system in the spleen.* Sci Immunol, 2019. **4**(33).
107. Zeng, F., et al., *Graft-derived extracellular vesicles transported across subcapsular sinus macrophages elicit B cell alloimmunity after transplantation.* Sci Transl Med, 2021. **13**(585).
108. Mantegazza, A.R., et al., *Presentation of phagocytosed antigens by MHC class I and II.* Traffic, 2013. **14**(2): p. 135-52.
109. Dersh, D., J.W. Yewdell, and J. Wei, *A SIINFEKL-Based System to Measure MHC Class I Antigen Presentation Efficiency and Kinetics.* Methods Mol Biol, 2019. **1988**: p. 109-122.
110. Shultz, L.D., et al., *Humanized mice for immune system investigation: progress, promise and challenges.* Nat Rev Immunol, 2012. **12**(11): p. 786-98.
111. Aichele, P., et al., *Macrophages of the splenic marginal zone are essential for trapping of blood-borne particulate antigen but dispensable for induction of specific T cell responses.* J Immunol, 2003. **171**(3): p. 1148-55.
112. Kliman, H.J., et al., *Purification, characterization, and in vitro differentiation of cytotrophoblasts from human term placentae.* Endocrinology, 1986. **118**(4): p. 1567-82.
113. Nelson, D.M., et al., *Hypoxia limits differentiation and up-regulates expression and activity of prostaglandin H synthase 2 in cultured trophoblast from term human placenta.* Am J Obstet Gynecol, 1999. **180**(4): p. 896-902.
114. Mouillet, J.F., et al., *MiR-205 silences MED1 in hypoxic primary human trophoblasts.* FASEB J, 2010. **24**(6): p. 2030-9.
115. Heesters, B.A., et al., *Endocytosis and recycling of immune complexes by follicular dendritic cells enhances B cell antigen binding and activation.* Immunity, 2013. **38**(6): p. 1164-75.